

Future Air Force Close Air Support Aircraft

a project presented to
The Faculty of the Department of Aerospace Engineering
San José State University

in partial fulfillment of the requirements for the degree
Master of Science in Aerospace Engineering

by

Oscar Ho

December 2018

approved by

Dr. Nikos J. Mourtos
Faculty Advisor



Table of Contents

List of Symbols	5
1.1. Introduction	7
1.2. Literature Review	8
1.3. Motivation.....	10
2.1. Mission Specification and Comparative Study.....	11
2.1.1. Comparative Study of Similar Planes	11
2.1.2. Mission Specification	13
2.1.3. Mission Profile	13
2.2. Configuration Selection.....	14
2.2.1. Performance and Configuration Comparison of Similar Aircrafts	14
2.2.2. Overall Configuration	17
2.2.3. Wing Configuration	17
2.2.4. Empennage Configuration	18
2.2.5. Integration of the Propulsion System	18
2.2.6. Landing Gear Disposition	19
2.3. Weight Sizing and Weight Specifications.....	19
2.3.1. Mission Weight Estimates.....	19
2.3.2. Calculation of Mission Weights.....	21
2.3.3. Discussion of Mission Weight Analysis	23
2.3.4. Takeoff Weight Sensitivities.....	24
2.3.5. Trade Studies	26
2.3.6: Discussion of Weight Sensitivities and Trade Studies.....	27
2.4. Performance Constraint.....	28
2.4.1. Manual Calculation of Performance Constraints.....	28
2.4.1.1 Stall Speed: Manual Calculation.....	29
2.4.1.2 Takeoff Distance: Manual Calculation	29
2.4.1.3 Landing Distance: Manual Calculation.....	29
2.4.1.4 Drag Polar Estimation: Manual Calculation	29
2.4.1.5 Climb Constraints: Manual Calculation.....	29
2.4.1.6 Maneuvering Constraints: Manual Calculation	30
2.4.1.7 Speed Constraints: Manual Calculation	30

2.4.2. Calculation of Performance Constraints with AAA Program	30
2.4.2.1. Stall Speed: AAA.....	30
2.4.2.2. Takeoff Distance: AAA.....	31
2.4.2.3. Landing Distance: AAA	32
2.4.2.4. Drag Polar Estimation	33
2.4.2.5. Climb Constraints	34
2.4.2.6. Maneuvering Constraints: AAA.....	35
2.4.2.7. Speed Constraints	35
2.4.3. Summary of Performance Constraints.....	36
2.4.4. Discussion of Performance Constraints	37
2.5. Fuselage Design.....	39
2.5.1. Cockpit Design.....	39
2.5.2. Fuselage Design.....	40
2.6. Wing, High-Lift System, and Lateral Control Design	43
2.6.1. Wing Planform Design.....	43
2.6.1.1. Sweep Angle- Thickness Ratio Combination	44
2.6.2. Airfoil Selection	44
2.6.3. Wing Design Evaluation	45
2.6.4. Design of the High-Lift Devices	46
2.6.5. Design of the Lateral Control Services	47
2.6.6. Preliminary Sketch of Wing.....	47
2.6.7. Discussion of Wing Design	48
2.7. Empennage Design.....	49
2.7.1. Overall Empennage Design	49
2.7.2. Design of the Horizontal Stabilizer.....	49
2.7.3. Design of the Vertical Stabilizer	51
2.7.4. Empennage Design Evaluation.....	52
2.7.5. Design of the Longitudinal and Directional Controls	53
2.7.6. Discussion of Empennage Design.....	55
2.8. Landing Gear Design and Weight Balance	55
2.8.1. Estimation for the Center of Gravity Location for the FAFCAS	56
2.8.2. Landing Gear Design	58

2.8.3. Updated Estimation of the Center of Gravity Location for the FAFCAS.....	63
2.8.4. CG Locations for Various Loading Scenarios	64
2.8.5. Discussion of Landing Gear Design and Weight Balance	65
2.9. Stability & Control Analysis/ Weight & Balance-Stability & Control Check	66
2.9.1. Static Longitudinal Stability.....	66
2.9.2. Static Directional Stability	67
2.9.3. Minimum Control Speed with One Engine Inoperative	68
2.9.4. Discussion of Stability and Control Analysis.....	69
2.10. Drag Polar Estimation	70
2.10.1. Airplane Zero Lift Drag	70
2.10.2. Low Speed Drag Increments	70
2.10.3. Compressibility Drag	71
2.10.4. Area Ruling.....	71
2.10.5 Airplane Drag Polars.....	72
2.10.6. Discussion of Drag Polar	73
2.11. Class I Design Method Conclusion	74
3.1. Summary of Class I FAFCAS Design	75
3.1.1. Introduction of Class II Design Method.....	77
3.2. Class II Landing Gear Design.....	78
3.2.1. Landing Gear Tire Sizing	78
3.2.2. Strut Design.....	80
3.2.3. Discussion of Class II Landing Gear Sizing	80
3.3. V-N Diagram.....	81
3.4. Class II Weight Estimation.....	83
3.4.1. Class II Structure Weight Estimation.....	84
3.4.2. Class II Power Plant Weight Estimation	84
3.4.3. Class II Fixed Equipment Weight Estimation.....	85
3.4.4. Discussion of Class II Weight Estimations	85
4.1 Summary of Class I and Class II Component Weight Estimation.....	87
4.2. Class II Weight and Balance Analysis	89
4.2.1 Class II Aircraft Component Center of Gravity Location	89
4.2.1.1 Structural Component C.G. Location	90

4.2.1.2. Power Plant Component C.G. Location.....	91
4.2.1.3. Fixed Equipment C.G. Location	91
4.2.2. Effect of Moving Components on Overall C.G.	92
4.2.3. Class II Weight & Balance- Stability and Control Check	93
4.2.4. Estimating Airplane Inertias.....	95
4.3. Discussion of Class II Weight and Balance Analysis	96
5.1 Class II Stability and Control.....	96
5.2 Development of Trim Diagram.....	96
5.2.1 MIL-F-8785C Flight Conditions.....	97
5.2.2 Airplane Lift vs. α Curve	99
5.2.3 Airplane Pitching Moment Coefficient vs. Airplane Lift Coefficient Curve	100
5.3. Airplane Trim Diagram and Longitudinal Controllability and Trim	103
5.4 Results of Class II Longitudinal Control and Trim Analysis.....	106
6.1 Cost Estimation of the FAFCAS.....	107
6.1.1 Research, Development, Test and Evaluation Cost	107
6.1.2 Acquisition Cost	108
6.1.3 Operation Cost	109
6.2 Life Cycle Cost of the FAFCAS Program	109
References	113

List of Symbols

Symbol	Definition	Units
AAA	Advanced Aircraft Analysis	
ac	Aerodynamic center	
AR	Aspect Ratio	
B	Wing span	ft
CAS	Close Air Support	
Cd	Drag Coefficient	
Cdo	Zero lift drag coefficient	
Cf	Skin friction coefficient	
cf	Flap Chord	ft
CG	Center of Gravity	
Cj	Specific Fuel Consumption	Lb/hr/lb
Cl	Lift Coefficient	
Clmax	Max Lift Coefficient	
Clmaxto	Max Lift Coefficient for takeoff	

Cl _{maxl}	Max Lift Coefficient for landing	
C _t	Tip Chord	ft
C _r	Root Chord	ft
C _{nδ_r}	Rudder control derivative	
CL _α	Total airplane lift curve slope	
C _{mδ_e}	Elevator control power derivative	
D _s	Diameter of the shock absorber strut	ft
e	Oswald factor	
E	Endurance	hr
F	Equivalent parasite area	Ft ²
G _w	Gross Weight	lb
L/D	Lift to Drag Ratio	
LCN	Load Classification Number	
L _m	Distance from center of gravity to main landing gear	ft
L _n	Distance from center of gravity to nose landing gear	ft
MAC	Mean Aerodynamic Chord	ft
MEC	Mean Geometric Chord	ft
M.G.	Main Landing Gear	
N _d	Drag induced yawing moment due to the inoperative engine	
N.G.	Nose Landing Gear	
N _{lim}	Limit Load Factor	
N _s	Number of wheels	
N _{crit}	Critical engine-out yawing moment	
P _m	Main Landing Gear Strut Load	Lbs
P _n	Nose Landing Gear Strut Load	lbs
R	Range	Nautical mile
S	Wing Area	Ft ²
S _e	Elevator Area	Ft ²
S _h	Horizontal Stabilizer Area	Ft ²
S _r	Rudder Area	Ft ²
S _s	Stroke of the shock absorber	ft
S _t	Allowable tire deflection	ft
S _v	Vertical Stabilizer Area	Ft ²
S _w	Wing Area	Ft ²
S _{wetted}	Wetted Area	Ft ²
T	Thrust	lbf
T/W	Thrust to weight ratio	
V _A	Design Maneuvering speed	knots
V _H	Max level speed	knots
V _h	Horizontal volume coefficient	
V _L	Max dive speed	knots
V _I	Landing speed	knots
V _s	Stall speed	knots
VTOL	Vertical Takeoff/ Landing	
V _{to}	Takeoff speed	knots
V _v	Vertical volume coefficient	
W/S	Wing loading	
W/Sto	Wing loading for take off	

WE	Empty Weight	Lbs
WF	Fuel Weight	lbs
Woe	Aircraft Operating Weight Empty	lbs
Wto	Takeoff Weight	lbs
Xh	Horizontal Stabilizer Aerodynamic center position	ft
Xv	Vertical Stabilizer Aerodynamic center position	ft
Yt	Lateral thrust moment arm	
ΔSM	Incremental static margin	
δ_f	Flap Angle	degree
δ_r	Rudder deflection required to hold the engine out condition	degree
Γ_w	Dihedral Angle	degree
Λ	Taper Ratio	
μg	Ground friction constant	

1.1. Introduction

Close air support (CAS) has had a vital role of the Air Force since the introduction of aircraft into the military. The physical and psychological impact a military aircraft can bring into the battlefield can turn the tides of battle. This is made even more apparent in recent theaters of war in the Middle East, where dogfights have taken the backstage and air to ground strikes are relied upon more. The A-10 Thunderbolt II has been the USAF's primary close air support aircraft for the last 40 years, but much of the fleet is nearing the end of their service lives. The A-10 was designed specifically for close air support role and thus has multiple attributes that assist with this mission such as; armored airframe to protect from ground fire, ability to use unguided and guided munitions, short take off and landing distance, and minimal maintenance requirements. The original service life of the A-10 was to be at 2028, but a wing replacement program is being looked at to extend the service life. The planned replacement for the A-10, the F-35 Lightning II, has been given criticism as being a step back in CAS ability. The F-35 has relies heavily on guided munitions and has a higher sortie cost than the A-10. The Embraer A-29 Super Tucano, Beechcraft AT-6 Wolverine, and Textron Scorpion were also considered by the Air Force as a cheaper replacement for the A-10 in low threat environments. But these light aircrafts do not have the speed or the protection to provide close air support in a higher intensity conflict as the A-10. Thus a new, more focused design is needed in order to properly replace the fleet of A-10's.

The Future Air Force Close Air Support Aircraft (FAFCAS) is designed as a replacement for the aging fleet of A-10's. To replace the A-10, the aircraft will need to have low operating costs, limited logistical needs on the ground, good maneuverability at low speeds, and protection from ground fire. The initial step to achieve such a requirement is to determine the aircraft configuration and testing if it's a feasible design. Performance wise, the FAFCAS will need to improve upon the A-10 with respect to landing/take off distance, range, and turn rate. A step by step design process laid out by Roskam will be used to design the FAFCAS.

1.2. Literature Review

The FAFCAS design goal is to create an aircraft that has similar or greater performance than the A-10 in low speed flight. Table 1 lists the FAFCAS performance parameter that the design has to meet. The list of sources that are listed in §Appendix 3A are used for the preliminary and final configuration design of the FAFCAS. Roskam Part I instructs how to do a preliminary sizing of the aircraft components. The author states that the design aircraft's mission specification must first be chosen before the design process can start. After the mission specification was chosen, the author provides a rapid method to do a preliminary sizing of the design parameters by comparing multiple aircrafts with similar mission specifications. Sources [6]-[11], [13]-[14], and [19] list the specifications and performance parameters of multiple military aircraft with similar mission specifications as the FAFCAS. The aircraft used in this step are as follow; A-10, Su-25, F-35A/B/C, Su-34/32, AV-8B Harrier, F-15E Strike Eagle, and the Tornado. The parameters from the various aircrafts are tabulated and an average is obtained to size the components of the FAFCAS. The parameters that will be estimated from the preliminary sizing are as presented:

- Takeoff Weight (W_{to})
- Empty Weight (W_E)
- Payload Weight (W_{PL})
- Takeoff Thrust
- Fuel Weight (W_F)
- Wing Area
- Wing Aspect Ratio
- Lift Coefficient for clean, take off, and landing configuration

Roskam Part II contains a step by step process to do a Class I and Class II design of an aircraft. The process for the Class I design process are as follow:

- Preliminary configuration layout and propulsion system configuration.
- Initial layout of wing and fuselage.
- Class I tail sizing, weight and balance, and determining the drag polar.
- Initial landing gear disposition.
- Sizing iteration and reconfiguration.

In the Class II design process, the author describes how to refine the design resulting from the Class I process. The process of refining the design for Class II is as follow:

- Layout of wing, fuselage, and empennage.
- Class II weight, balance, drag polar, flap effects, stability and control.
- Performance verification.
- Preliminary structural layout.

- Landing gear disposition and retraction check.
- Cost calculations.

Roskam Part III, V, and VI are used as in depth references for specific steps during the design process in Part II. In Roskam Part III the author focuses on how to create a realistic layout for the aircraft's cockpit, fuselage, wing, empennage, and where to install the propulsion system. The author provides reference pilot and canopy dimensions in order for the cockpit to have enough visibility. Examples of structural arrangements for military aircrafts are presented:

- Seat and payload arrangement in the fuselage.
- Wing layout design and its effects on drag.
- Empennage layout design and its effects on drag and stability.
- Propulsion system layout design and its effects on propulsion efficiency.

Roskam Part V is used in the steps involving the weight estimation of the FAFCAS components. The author provides a Class I and a Class II method for the weight estimation. In Class I method, the average component weights of aircrafts with similar mission specifications are used to get a first estimate. In the Class II method, V-n diagrams and preliminary structure arrangements are used to get more realistic weight estimation. Roskam Part VI is used in steps involved in the calculation of the design aircraft's drag, power, thrust, lift, and other stability and control data. The author provides a systematic approach to predict the forces and stability. The data predicted are used in the Class II design method from Part II. The author also provides example data for the parameters above for different aircrafts. Additional references are used in conjunction with the instructions provided by Roskam to fill in gaps not covered by the author. In Struett's paper, *Empennage Sizing and Aircraft Stability using MATLAB*, the author discusses how to size the empennage of a low speed aircraft for a desired stability. The design process is given with the required variables needed for calculations. The author states how some variables can be estimated from similar aircrafts to get rid of some unknowns in the equations. A MATLAB code is then provided with instructions to be used to size the empennage. This is an important component when designing the FAFCAS as the fighter aircraft cannot be too stable. Close air support aircraft needs to be able to perform high G maneuvers quickly at low altitudes, which means some instability is needed. Engine parameters are needed in the steps involving the calculation of thrust. The FAFCAS will be designed to two Pratt & Whitney F100 engines. Source [16] provides the specifications of the engines. Military aircraft have certifications that have to be met in order to be considered a safe design. Sources [17] and [18] lists the minimum takeoff and landing distance that military aircraft needs to meet in order to pass certification. It also lists the minimum altitude it must be able to pass by takeoff/ landing to avoid the flight control towers. In the preliminary wing design of the FAFCAS, a NACA 6715 and NACA 4416 airfoil will be chosen for the wing. Source [20] will be used to obtain the airfoils lift and pitching coefficients. This reference is used during the calculation of the aircrafts lift and drag.

Table 1: FAFCAS Design Parameters

Payload	13,000 lbs
Takeoff/ Landing Field Length	1 km
Cruise Speed	480 knots
Stall Speed	120 knots
Range	1000 km
Takeoff Weight	94,000 lbs

1.3. Motivation

The A-10 will be approaching their service life at 2028 and a replacement aircraft will be needed to take up the CAS role in the air force. Most missions that are taken up by the Air Force are ground strikes against insurgent targets with limited radar capabilities, where ground troops are already engaged in combat with. Thus expensive stealth aircrafts such as the F-35 will be exceeding what is needed for a replacement CAS aircraft. With no foreseeable end to the anti-insurgency missions in the Middle East, there will always be a need for a capable CAS aircraft to support the ground troops.

As can be seen back in §Chapter 1.1, the USAF currently has no replacement for the A-10 that can conduct close air support in the same capacity. The F-35 has high operating costs due to its stealth that has to be constantly maintained and its armaments are also limited as compared to the A-10. The F-35 has internal weapon bays that limit the size of the payload. In addition the F-35's GAU-22/A is a 25mm cannon, which is less effective than the A-10's 30mm cannon. The Embraer A-29 Super Tucano, Beechcraft AT-6 Wolverine, and Textron Scorpion are light attack aircrafts that were considered as a cheaper alternative for the A-10 in low intensity conflicts. But each of the aircraft listed have less protection for the pilot and redundant systems to survive hits from the ground. Although the light aircrafts have similar combat radius range and speed as the A-10, their payload capacity is lacking. The payload capacity of the F-35, A-10, A-29, AT-6, and the Scorpion is listed on Table 2.

Table 2: Payload Capacity of Different Close Air Support Aircraft

Aircraft	Payload (Lbs)
A-10	16,000
F-35	15,000
A-29	3,300
AT-6	4,110
Scorpion	6,200

As can be seen in Table 2, the light attack aircrafts have much lower payload capacity than the A-10, which limits how much close air support the aircraft can provide. Thus the FAFCAS will attempt to address the issues of the low payload capacity of the light attack aircrafts and the high operating cost of the F-35. The design aircraft will be focusing on creating an aircraft that performs equal to or better than the A-10 so the fleet can be properly replaced.

Thus no significant new technology needs to be researched to complete this design. The weight of the aircraft will be a potential design concern due to the increased armor protection required compared to the A-10. Currently the A-10 is rated to withstand up to 23mm projectiles, but this new design will need to improve upon that and go up to 25mm. Armor that is rated for at least 25mm will protect the aircraft from both common ground anti-air cannons and also the average caliber of aircraft mounted guns. An airframe will need to be designed that can support the weight of the increased armor while still capable of exceeding the performance of the A-10. This new CAS design will not require expensive functions such as VTOL, stealth, or thrust vectoring engines so development costs will be cut down. The FAFCAS design will also address the gun and payload option issue of the F-35. The FAFCAS will use the 30mm caliber GAU-8 Avenger cannon, which is the same gun as the A-10. In addition no internal hard points will be used on the FAFCAS. All munitions will be mounted externally on the wing and fuselage and thus allowing for larger bombs be equipped. The FAFCAS will be designed with a payload capacity of 13,000 lbs. This will be more than the light attack aircrafts and comparable with the A-10 and F-35.

The FAFCAS will be designed to have some performance improvements over the A-10. Performance wise, the FAFCAS will need to improve upon the A-10 with respect to landing/take off distance, range, and turn rate. Double canted vertical stabilizers will be mounted on the tail of the aircraft. These will contribute to the horizontal stabilizer effects and act as backup stabilizers in case one of the horizontal stabilizers is damaged. The canted vertical stabilizers will also act as air brakes when landing, and thus decreasing the required landing distance. The combat radius of the FAFCAS will also be designed to be higher than the A-10. The FAFCAS will also be designed to have a large wing and fuselage, allowing for more fuel to be stored. The increase in fuel capacity will increase the range of the aircraft. The cruise speed of the FAFCAS will be set at 480 knots, which is higher than the 300 knots on the A-10. This will allow the aircraft to reach the mission area faster and provide quicker response to close air support requests. These performance improvements while keeping the advantages of the A-10 will allow the USAF to maintain its close air support capabilities with the A-10 retired.

2.1. Mission Specification and Comparative Study

To begin the design process of the FAFCAS, the mission specification has to be stated. From Roskam Part I, a benchmark should be made by comparing different aircrafts with similar mission types. This benchmark will be used to make an initial estimate to the FAFCAS mission specification

2.1.1. Comparative Study of Similar Planes

The A-10, Su-25K, Su-34, F-35B, and the Harrier II are all military aircraft that can provide close air support. Each of their mission capabilities are tabulated on Table 2.1 and their respective design parameters tabulated on Table 2.2.

Table 2.1: Comparison of Mission Capabilities of Modern CAS Aircraft

	A-10	Su-25K	Su-34	F-35B	Harrier II
Hard points	11	11	12	8	6
Payload (lbs)	16,000	8820	17,637	15,000	9,000
Combat Radius (km)	460	750	1000	833	229
Range (km)	1,287	1,000	4,500	2,000	1667
Max Speed (km/h)	676	950	1,900	1,931	1,083
Service Ceiling (km)	13.7	7	14.65	15	13.1
Max Takeoff Weight (lbs)	51,000	42,550	99,428	60,000	31,000
Thrust/weight	0.36	0.47	0.68	0.9	0.76
Gun Caliber/Capacity	30mm/1174 Rounds	30mm/250 Rounds	30mm/180 Rounds	25mm/220 Rounds	25mm/300 Rounds

Table 2.2: Comparison of Design Parameters of Modern CAS Aircraft

	A-10	Su-25K	Su-34	F-35B	Harrier II
WE	24,959 lb	21,605 lb	49,608 lb	32,442 lb	13,968 lb
WF	11,000 lb	n/a	26,675 lb	13,325 lb	7,500 lb
T	2x 9,065 lbf	2x 9,921 lbf	2x 30,300 lbf	28,000 lbf	22,200 lbf
S	506 ft ²	323 ft ²	667.8 ft ²	460 ft ²	243.4 ft ²
B	57ft 6 in.	47ft 2 in.	48ft 3 in.	35 ft	30 ft 4 in.
AR	6.54	6.12	3.48	2.68	3.78

From the comparisons of different CAS aircrafts, there can be seen a difference in design philosophy between dedicated close air support aircraft and multirole aircraft. Dedicated CAS aircrafts such as the A-10 and Su-25K have high aspect ratios, low thrust to weight ratios, large quantities of hard points for weapons, low range, and low max speed. The Harrier II, while being used commonly as a CAS aircraft too, doesn't share all the same characteristics as the former aircrafts due to incorporating a STVOL system and thus not being able to carry as many ordinances. In addition, CAS aircraft such as the A-10 and Su-25K normally operate in forward operating bases and thus their designs doesn't require them to need high operating range, combat radius, or fuel capacity as compared to multirole aircrafts such as the F-35B and Su-34 traveling from farther bases. The high aspect ratio of the contemporary CAS aircrafts allow them to have less induced drag as they operate in their low speeds during CAS missions. It can also be seen that the majority of these aircrafts have 30mm guns due to their higher effectiveness against ground targets vs. a multi use 25mm gun.

2.1.2. Mission Specification

This new design will need to have flight and combat performance equal or greater than the A-10. The initial design parameters are listed in Table 2.3.

Table 2.3: Initial Design Parameters

Payload Capacity	16,000 lb
Crew member required	1
Range	1500 km
Combat radius	500 km
Cruise speed	800 km/h
Stall speed	200 km/h
Take off field length	1km
Landing field length	1km
Approach speed	260 km/h
Loiter time	2.5 hours
Turn Radius	300 m

2.1.3. Mission Profile

Using the initial design ranges, the predicted mission profile of the FAFCAS is displayed on Figure 2.1. The FAFCAS will have a short take off distance and quickly climb to a cruising altitude of 12km. Once it reaches the enemy position, the FAFCAS will descend quickly and initiate its weapon drop. The FAFCAS will also loiter to provide additional close air support as needed and then climb back up to cruising altitude once mission is done. At the end of the mission profile, the FAFCAS will quickly descend and land within a short distance. This is to simulate the short or ill-maintained runways provided by forward air bases.

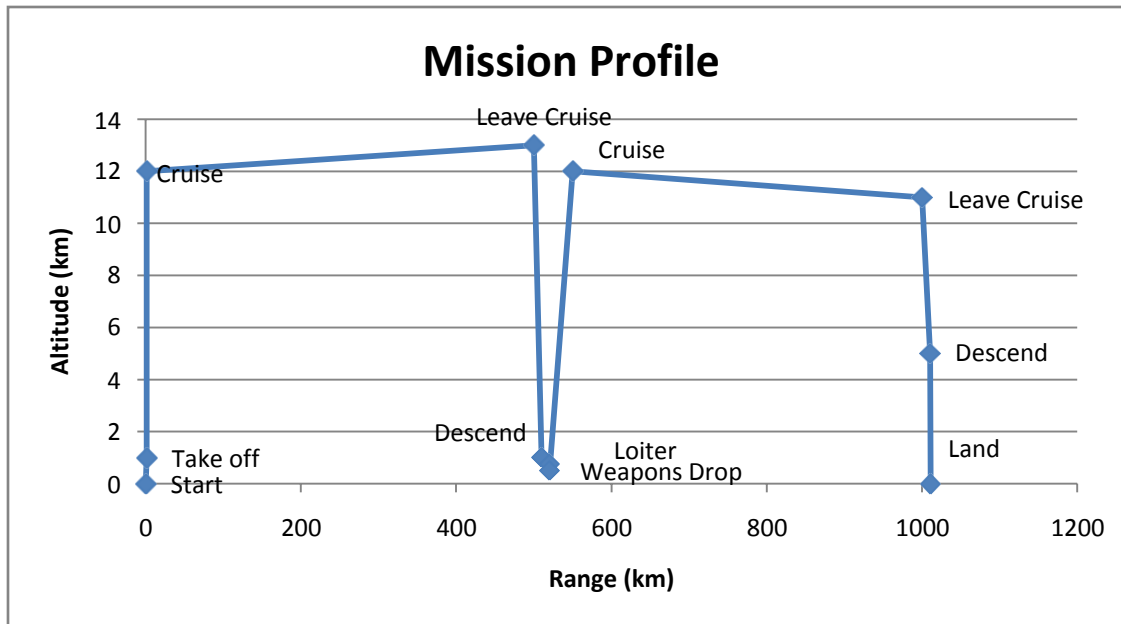


Figure 2.1: Predicted Mission Profile

2.2. Configuration Selection

The next step in the design process is the configuration selection of the aircraft. The configuration of an airplane is important during the design process. It determines where all the critical parts, such as the wing, engines, and stabilizers of an airplane will be placed. The location of each part is determined by the mission specification, as each configuration has its own pros and cons. It is important to determine this early and be firm with the decisions as future changes to the configuration after fabrication has started becomes very costly. This section will compare the configuration of other contemporary CAS aircrafts and from there determine the best configuration for this design that matches its mission specification.

2.2.1. Performance and Configuration Comparison of Similar Aircrafts

The A-10, Su-25K, Su-34, F-35B, and Harrier II are military aircrafts with similar missions but have different performance. Table 2.4 lists the aircraft's respective performance. Figure 2.2a- Figure 2.2e displays the configurations of each of the aircrafts. These 5 aircraft have different configurations but each have CAS capabilities or are air to ground focused in their design. By looking at the weight, dimensions, and wing/engine position of the different aircrafts, the FAFCAS will have a baseline on how it should look. The advantage of where the aircraft components are mounted on each of the aircraft will be analyzed to choose the best configuration for the FAFCAS.

The A-10 Thunderbolt II displayed in Figure 2.2a has a straight wing design positioned low on the fuselage, with two vertical stabilizers, and two engines mounted high on the fuselage. The wing on the A-10 has a wide aspect ratio and mounted low to the fuselage in order to create

better maneuverability at low speeds and also to decrease take off distance. Low wings also saves space on the bottom of the fuselage, which allows for more hard points to be mounted and also easier time rearming the plane. This aircraft is also expected to take fire while in CAS missions and thus a low mounted wing is safer to land with in case it needs to make an emergency landing since it can absorb some of the impact. The engines are mounted high in the fuselage in order to avoid the intake taking in foreign debris on the runway, which is common in unmaintained forward air bases and also to allow for the engines to stay on while being serviced. The engines being placed in the rear of the fuselage also allows for thrust to stay almost symmetric in case one fails and also allows for a clean wing design. Being placed high in the rear also shields it from ground fire with the rest of the body during missions. The A-10 is able to fly with just one vertical stabilizer but contains two in order for it to still maintain control in case one is damaged. They are spread apart from each other in order to avoid being disturbed by the exhaust of the engines.

The Su-25K displayed on Figure 2.2b has a conventional stabilizer configuration, with two engines mounted on the side of the fuselage, and a high aspect ratio wing mounted middle of the fuselage. The high aspect ratio on the wing gives the aircraft better maneuverability at low speeds. The wing mounted on the middle also allows for the wing to be continuous through the fuselage and also mandatory in its design as the engine is placed under the wing root, and thus unable to be placed any lower on the fuselage. The engines are mounted close to the lower sides of the fuselage in order to have a clean wing and also decrease drag as the aircraft will have a more aerodynamic shape. The inlets on the engine are far from the wing and close to the front of the fuselage, which keeps the air intake constant under different angle of attacks. The horizontal stabilizers are mounted high on the fuselage to avoid the exhaust of the low mounted engines.

The Su-34 displayed on Figure 2.2c has a mid wing design, with two engine exhausts to the rear of the fuselage, two inlets in the bottom of the fuselage, two vertical stabilizers, and also two canards in the front of the aircraft. The Su-34 is used as a fighter and a bomber and thus still needs good performance at high speeds. The mid wing design allows for the least drag in high speed flight, as the interference between boundary layers at wing/ fuselage junctions are minimized. This wing placement also gives the best maneuverability. Twin vertical stabilizers allow for redundancy in case one is damaged and increases the effectiveness of the horizontal stabilizers. A rear end exhaust keeps the flow away from any of the flight surfaces while the inlet mounted on the bottom of fuselage keeps the fuselage flat to mount more weapons and keep the fuselage shape aerodynamic. Due to needing to balance fighter performance and bomber performance, its configuration is not particularly well suited for close air support. The wing is designed for high speed maneuverability and doesn't have a high aspect ratio.

The F-35B displayed on Figure 2.2d has a single engine with the exhaust mounted to the rear and side scoop inlets, with two slanted vertical stabilizers, and a wing mounted in the middle of the fuselage. The F-35B is a multirole fighter that needs a balanced performance as a fighter and a bomber. Thus it uses a mid wing in order to give it lower drag and good maneuverability at

high speeds. But this wing also has low aspect ratio, which lowers its performance at low speeds. Its exhaust is mounted in the rear of the aircraft to keep the exhaust away from the flight surfaces and also to be able to point downward while VTOL. It has scoop type side inlets on the fuselage as it creates a stealthier radar profile. This design creates more drag as the scoop increases the drag and the diverter that prevents the boundary layer from affecting the intake also creates drag. To counteract this inherent flaw in scoop type inlets, the F-35 uses bumps in front of the inlet that keep good air flow into the engine and it also has a dual purpose in diverting the engines radar signature. The vertical stabilizer is slanted to deflect radar and keeps its radar signature low. It also is able to have horizontal and vertical stabilizing properties.

The AV-8B Harrier II displayed on Figure 2.2e is a VTOL capable jet with a single engine, high mounted wing, with both the horizontal stabilizers and wing pointed in an anhedral direction. Due to its VTOL design, it has 4 split exhaust nozzles on the side of the fuselage in order to be able to point down its exhaust. The inlet for the engines is far ahead of the wing and close to the front of the fuselage to get undisturbed air flow. The wing is mounted high on the fuselage to prevent it being affected by ground effects, especially during VTOL when there is a lot of interaction with the ground. The wing is also mounted high in order to not be disturbed by the side exhausts on the fuselage. It has drooped ailerons and automatic flaps on the wing to give it more lift even though it doesn't have a high aspect ratio. Due to the wing being mounted high on the fuselage, and thus above the aircraft's center of gravity, the aircraft will be under the dihedral effect which will make the aircraft side slip and also make spiraling mode too stable. The anhedral direction of the wings and stabilizer cancels out this dihedral effect and spiral stability and thus make the aircraft more maneuverable.

Table 2.4: Performance Comparison of Different CAS Aircrafts

	A-10	Su-25K	Su-34	F-35B	Harrier II
Empty Weight (lbs)	24,959	21,605	49,608	32,442	13,968
Payload (lbs)	16,000	8820	17,637	15,000	9,000
Combat Radius (km)	460	750	1000	833	229
Range (km)	1,287	1,000	4,500	2,000	1667
Max Speed (km/h)	676	950	1,900	1,931	1,083

Service Ceiling (km)	13.7	7	14.65	15	13.1
Max Takeoff Weight (lbs)	51,000	42,550	99,428	60,000	31,000
Thrust/weight	0.36	0.47	0.68	0.9	0.76
Length (ft)	53ft 4 in.	51ft	72ft 2 in.	50ft 6 in.	46ft 4in.
Wingspan (ft)	57ft 6 in.	47ft 2 in.	48ft 3 in.	35 ft	30 ft 4 in.
Wing Area(ft^2)	506	323	667.8	460	243.4
AR	6.54	6.12	3.48	2.68	3.78
Wing Shape	Straight Wing	Trapezoidal Wing	Cropped Delta Wing	Delta Wing	Anhedral Swept Wing

2.2.2. Overall Configuration

Since this design will be making an improvement over the A-10, much of its configurations that enhance its survivability will be adapted into this design while configurations that affect its flight performance will be altered to meet the mission specifications. This design will have a mid wing with leading edge root extensions, two canted vertical stabilizers with horizontal stabilizers with large control surfaces, pod mounted engines in the rear of the fuselage, and a tricycle landing gear formation.

2.2.3. Wing Configuration

The wing configuration for this design will be based off of the A-10 in that the wing will be a high aspect ratio wing due to its good performance in low speeds. But unlike the low wing on the A-10, this wing will be mounted in the middle of the fuselage due to this position being the sturdiest as it will be a single piece continuous through the fuselage. A leading edge root extension (LERX) will be implemented into the fuselage ahead of the wing. The LERX creates a vortex over the wing during high angles of attack, which is often during takeoff or a climb after a bombing run. Figure 2.3, provided by Airlines.net, visualize the vortex generated on an F/A-18's LERX. This controlled vortex keeps a smooth airflow over the wing past where the wing would normally stall and allows the wing to maintain lift. This will allow the aircraft to take off at a higher angle or pitching up more to get to a safe altitude away from gunfire. The one downside of the LERX is that the vortex downstream will break apart and affect the durability of the tail control surfaces.



Figure 2.3: Vortex Generated by LERX on a F/A-18.

2.2.4. Empennage Configuration

This aircraft design will have two vertical stabilizers as is common on many military fighter aircraft. Having two splits the area required to yaw as compared to one large vertical stabilizer. Having two vertical stabilizers is also important for a CAS aircraft as it will still have one control surface if the other one is damaged. Unlike the A-10, the vertical stabilizers on this design will be canted outward. This will allow for it to contribute to the horizontal stabilizers, which can decrease the take off distance or allow for more control during its pitching mode. The downside of a canted vertical stabilizer is that the vertical component will be diminished as it can only contribute part of its area to the vertical. The rear will have a fully movable tail with large control surfaces for its horizontal stabilizer. This will allow the horizontal tail to be able to act as an aileron and assist with the roll mode of the aircraft and also make its pitching mode more responsive. By being fully movable, it can also act as an airbrake during landing and decrease the landing distance.

2.2.5. Integration of the Propulsion System

This aircraft configuration will include two Pratt & Whitney F100 engines mounted to the rear of the fuselage. Two engines will be necessary in case one is damaged during CAS missions. Being placed in the high and to the rear of the fuselage has been proven by the A-10 to be a safer spot as the rest of the wing and armored fuselage can absorb the incoming fire. Being high on the fuselage will also allow the engines to stay on as the aircraft is being serviced on the

ground, and allow it to go back for another mission quickly. A downside to this engine position will be the risk of deep stall and it being an inconvenient location to do maintenance on.

2.2.6. Landing Gear Disposition

This configuration will have a tricycle landing gear disposition with two to the rear of the center of gravity and one near the nose of the aircraft. The downside of not using a low mounted wing like the A-10 will be that the rear landing gears can't be attached to the wings without affecting their structural integrity. The fuselage will need to be widened in order to house the landing gears wide enough that the aircraft won't tip over while landing. A wider fuselage will allow more hard points to be attached under the aircraft. The nose landing gear will be attached centerline of the aircraft as compared to the A-10, which had the landing gear offset to the side due to the gun position. The A-10's offset landing gear causes it to turn wider while taxiing in one direction over the other. A centerline nose landing gear will keep the taxiing consistent and apply a balanced weight force when landing.

2.3. Weight Sizing and Weight Specifications

Once the configuration of the aircraft is decided upon, a weight sizing analysis must be conducted. The weight sizing analysis will determine the minimum airplane and fuel weight of the design that will meet the mission requirements. These mission weights are very important to the design of the plane as it sizes the entire vehicle. By studying the how the different mission parameters affect the takeoff weight, the best design point can be found that meets the plane the mission specifications while minimizing the weight of the aircraft.

2.3.1. Mission Weight Estimates

When designing an aircraft, the aircraft weight at different conditions must be estimated. Roskam Part I provides a way to estimate the aircraft's takeoff gross weight (W_{to}), empty weight (W_{oe}), and the mission fuel weight (W_f). The takeoff weight is broken down as follows:

$$W_{to} = W_{oe} + W_f + W_{pl} \quad (2.3.1)$$

Where W_{oe} is the airplane operating weight empty, W_{pl} is the payload weight, and W_f is the mission fuel weight. Airplane operating weight empty is composed of the manufacturer's empty weight plus the fixed equipment weight. Roskam's process to obtaining values for W_{to} , W_{oe} , and W_f consists of seven steps. The seven steps are summarized below:

1. Determine W_{pl} .
2. Guess a takeoff weight.
3. Determine W_f .
4. Calculate a tentative W_{oe} from the takeoff weight guess.
5. Calculate a tentative W_{oe} assuming crew weight of 200lbs.
6. Find the allowable W_{oe} .

7. Compare the tentative and allowable empty weight and make adjustments until there is a 0.5% difference.

In Roskam Part I, it is stated that there is a linear relationship between W_{to} and W_{oe} . The equation for this linear relationship is as follows:

$$\log_{10}W_{to} = A + B\log_{10}W_e \quad (2.3.2)$$

Where A is a regression intercept coefficient obtained from data on existing airplanes with similar types and B is a regression slope coefficient obtained from the same set of airplane data. Different aircraft weights for ten aircrafts similar to the FAFCAS were obtained and tabulated in Table 2.5. The aircrafts takeoff weight is then plotted vs. their empty weight and a line of best fit drawn through the data points. This plot can be seen in Figure 2.3a. Roskam Part I also states how to calculate the fuel weight used by using the fuel-fraction method and the mission profile in Figure 2.1. The complete steps of the fuel-fraction method can be seen in Roskam Part I page 23.

Table 2.5: Comparison of Takeoff and Empty Weights of Modern Aircrafts

	Payload (lbs)	Max Takeoff Weight (lbs)	Empty Weight(lbs)	Airplane Type
A-10	16,000	51,000	24,959	2 Engine CAS aircraft
Su-25K	8820	42,550	21,605	2 Engine CAS aircraft
Su-34	17,637	99,428	49,608	2 Engine fighter-bomber
F-35B	15,000	60,000	32,442	VTOL multirole fighter
AV-8B	9,000	31,000	13,968	1 Engine ground attack aircraft
Tornado GR4	19,800	61,700	30,620	2 Engine variable sweep multirole aircraft
Mirage 2000	13,900	37,500	16,350	1 Engine multirole fighter
F-15E	23,000	81,000	31,700	2 Engine Multirole fighter
F/A-18	13,700	51,900	23,000	2 Engine Multirole Fighter
Saab Gripen	11,700	31,000	14,990	1 Engine Multirole Fighter

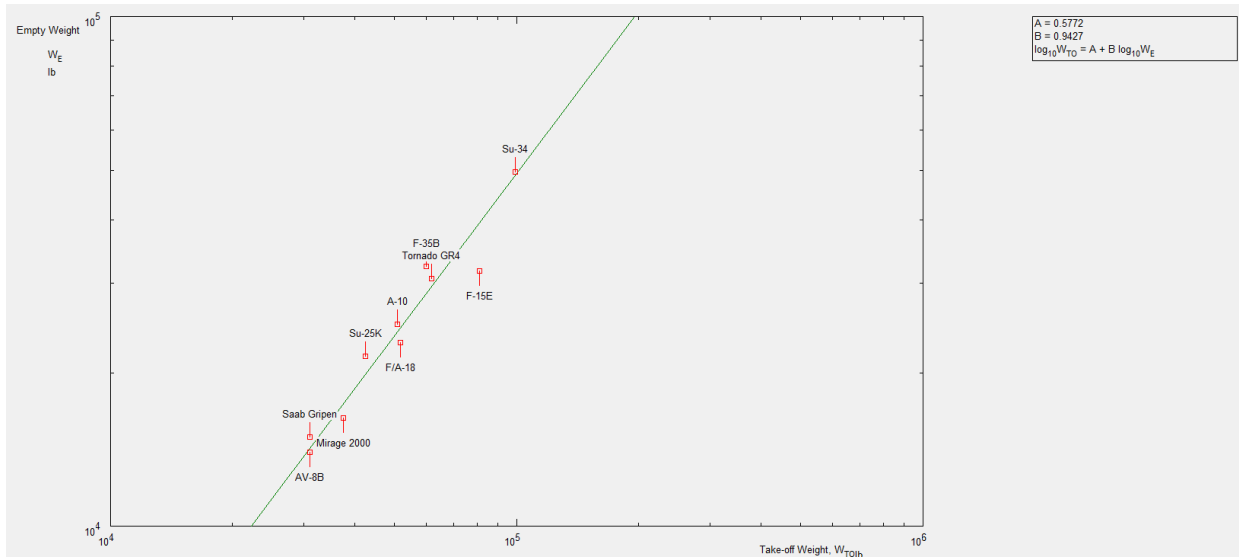


Figure 2.3a: Weight Trends for Fighters

From Figure 2.3a, the regression points are $A=.5772$ and $B=.9427$. In Roskam Part I, Roskam obtained regression points of $A=.5091$ and $B=.9505$ for military aircraft with external loads.

2.3.2. Calculation of Mission Weights

The manual calculation of the FAFCAS mission weights can be seen in Appendix 2B. In the manual calculation the takeoff weight guess was 60,000 lbs and the resulting tentative empty weight was at 20,800 lbs. With Roskam’s regression coefficients, the allowable empty weight was at 31,000 lbs. This difference was too large and needed iteration.

Due to the large difference, Advanced Aircraft Analysis (AAA) by DARcorporation was used in the next iteration to calculate the mission weights. AAA is an aircraft design program used by the industry for preliminary aircraft design. The design program is structured to follow the Class I and Class II design procedure. AAA separates the design process into ten modules to calculate different aircraft characteristics. Figure 2.3b displays the mission profile fuel fractions to be used in AAA. Figure 2.3c displays the mission weights calculated by AAA. Using the regression points $A=.5772$ and $B=.9427$ calculated from Eqn. 2.3.2, AAA plots takeoff weight vs. empty weight using the regression points and by varying the fuel weight. This plot can be seen in Figure 2.3d. The point where the two lines intercept in Figure 2.3d is the design point and determines the takeoff weight. Using an initial takeoff weight guess of 85,000 lbs and payload weight of 13,000 lbs, the resulting mission weights are shown in Table 2.6.

Table 2.6: Mission Weights

Weight takeoff with stores	96,650 lbs
Weight takeoff without stores	83,650 lbs
Weight empty	47,400 lbs

Weight fuel

23,000 lbs

The screenshot displays the 'Weight' module of the Advanced Aircraft Analysis 3.7 software. The interface includes a menu bar with options like File, Edit, Window, Airfoil, and Help. Below the menu bar are several toolbars for different analysis areas: Weight, Aerodynamics, Performance, Geometry, Propulsion, Stability & Control, Dynamics, Loads, Structures, and Cost. The main workspace is titled 'Weight' and contains several sub-sections: 'Weight Sizing' with 'Class I' and 'Class II' tabs; 'Mission Profile' with options for W_{T0} , W_E , W_F ; W_{T0} , W_F given W_E ; L/D from Weights; Regression; Sensitivity; and Useful Load; and 'Segment Input and Fuel-Fraction Calculation' with 'New Segment', 'Delete Segment', 'Insert Segment', and 'Move Segment' buttons. A table on the left lists mission profiles and their corresponding fuel fractions (M_{ff}):

Mission Profile	M_{ff}
Cruise	0.9340
Loiter	0.9314
Descent	0.9900
Cruise	0.9692
Payload Expend	1.0000
Cruise	0.9767
Climb	0.9861
Cruise	0.9435
Descent	0.9900
Land/Taxi	0.9950

The bottom of the interface shows a toolbar with icons for Configuration, Controls, Flap/Slat, Gear, Structure, Engine, Nozzle, Propeller/Fan, Store, Flight Cond, Recalculate, Notes, Copy WNF, Print, Atmosphere, Help, and Exit. The status bar at the bottom indicates the company name, project name 'Advanced Aircraft Analysis 3.7 Project', date '10/02/17', and time '4:31 PM'.

Figure 2.3b: AAA Mission Profile Fuel Fractions.

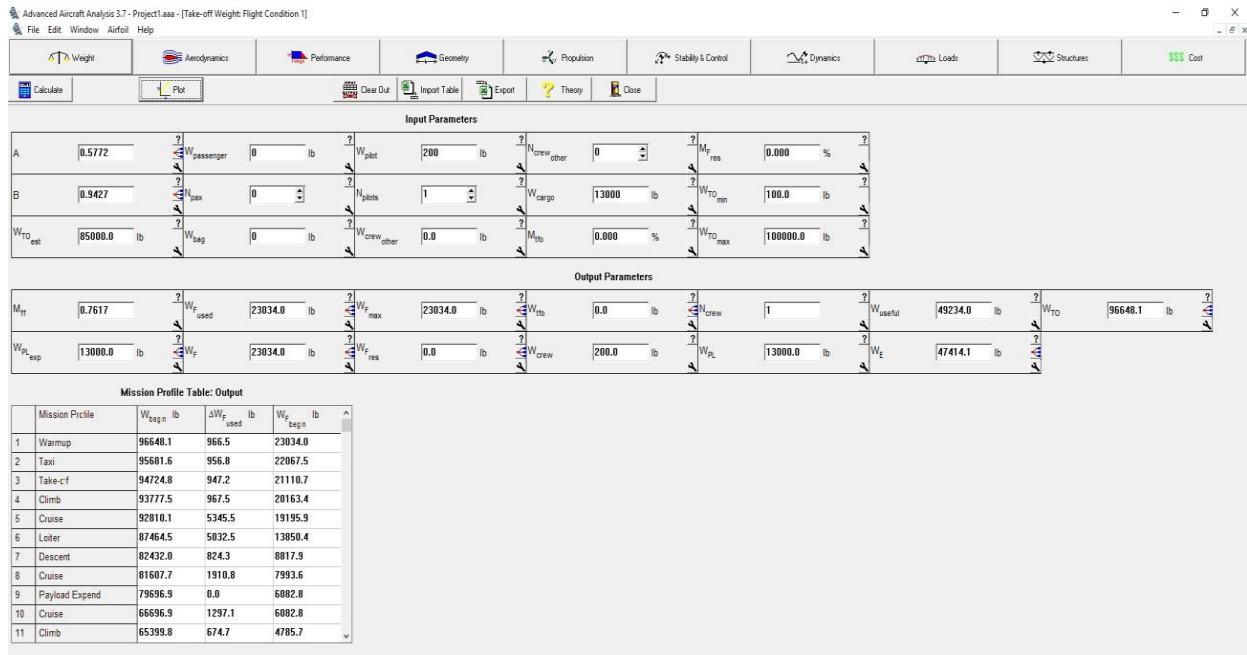


Figure 2.3c: AAA Calculation of Mission Weights.

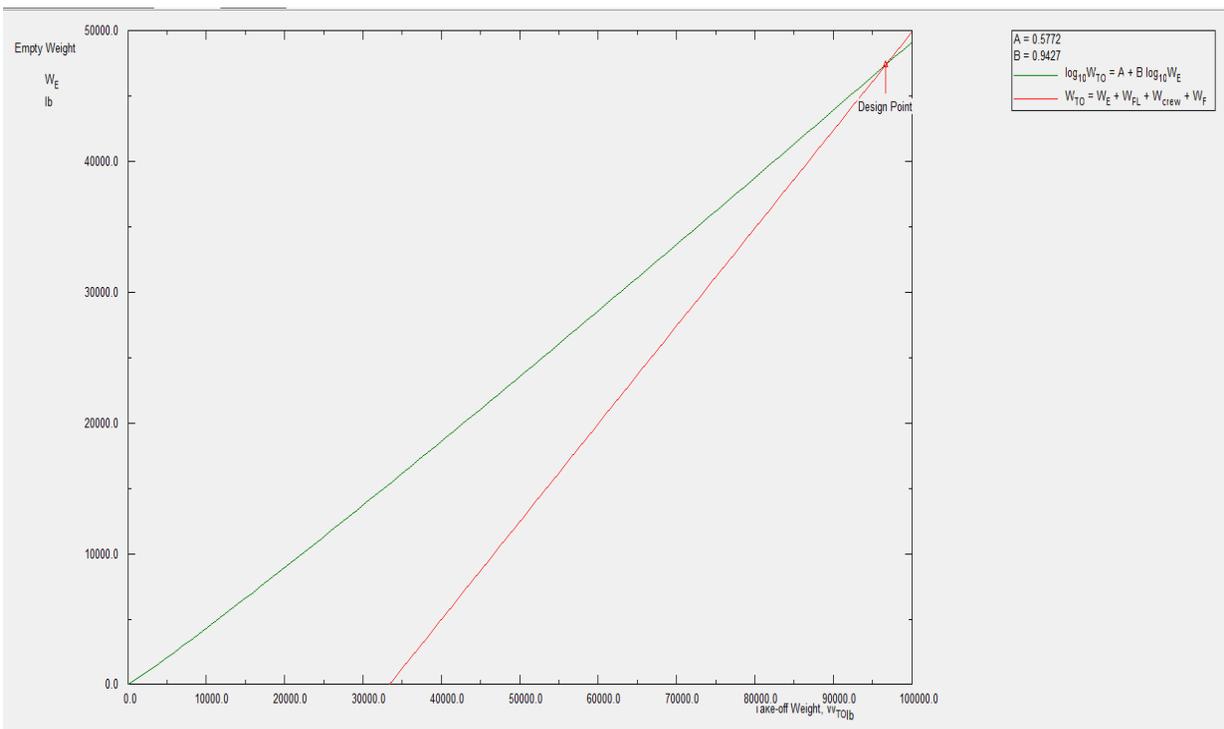


Figure 2.3d: AAA Design Point.

2.3.3. Discussion of Mission Weight Analysis

From this mission weight analysis, the original mission requirements had to be lowered in order for this aircraft design to be within the realms of comparable mission weights. The original

loiter time of 2.5 hours and payload of 16,000 lbs was too optimistic for current airplane technology and had to be lowered. The range of the aircraft was reduced from 1,500 km to around 1,300 km to lower the fuel weight. The resulting design has a takeoff weight of 96,650 lbs, with a payload weight of 13,000 lbs, fuel weight of 23,000 lbs, and an empty weight of 47,400 lbs. These weights are comparable to contemporary twin-engine multirole fighter aircrafts and heavier than the A-10 which this is intended to replace. The regression points using 10 modern fighter aircrafts were $A = .5772$ and $B = .9427$. These constants are similar to the constants calculated by Roskam for fighter aircraft with external loads. They are similar due to both set of airplanes have similar mission specifications.

2.3.4. Takeoff Weight Sensitivities.

From the mission weight analysis using AAA, the takeoff weight can be seen to vary with multiple parameters such as payload, empty weight, range, endurance, and specific fuel consumption. Thus a sensitivity study has to be conducted to see which parameter drives the design. In Roskam Part I, the following sensitivities are derived:

- Sensitivity of takeoff weight to payload weight.
- Sensitivity of takeoff weight to empty weight.
- Sensitivity of takeoff weight to range, endurance, speed, lift-to-drag ratio, and specific fuel consumption.

The partial derivative of takeoff weight to the different parameters is called growth factors. Using an initial takeoff weight guess of 60,000 lbs and the equations listed in Chapter 2.7 of Roskam Part I, the sensitivities are manually calculated. The resulting calculations can be seen in Appendix 2C. Due to the final takeoff weight much higher than 60,000 lbs, the manual calculation in Appendix 2C is not applicable. AAA was used to recalculate the weight sensitivities for the takeoff weight of 96,650 lbs. The sensitivities were studied during the aircraft's climb, cruise to target, loiter, descent, payload expenditure, climb, and cruise back to base. These points in the mission profile are observed as the takeoff weight changes the most during these events. Figure 2.3e shows the AAA calculation of the takeoff weight sensitivities.

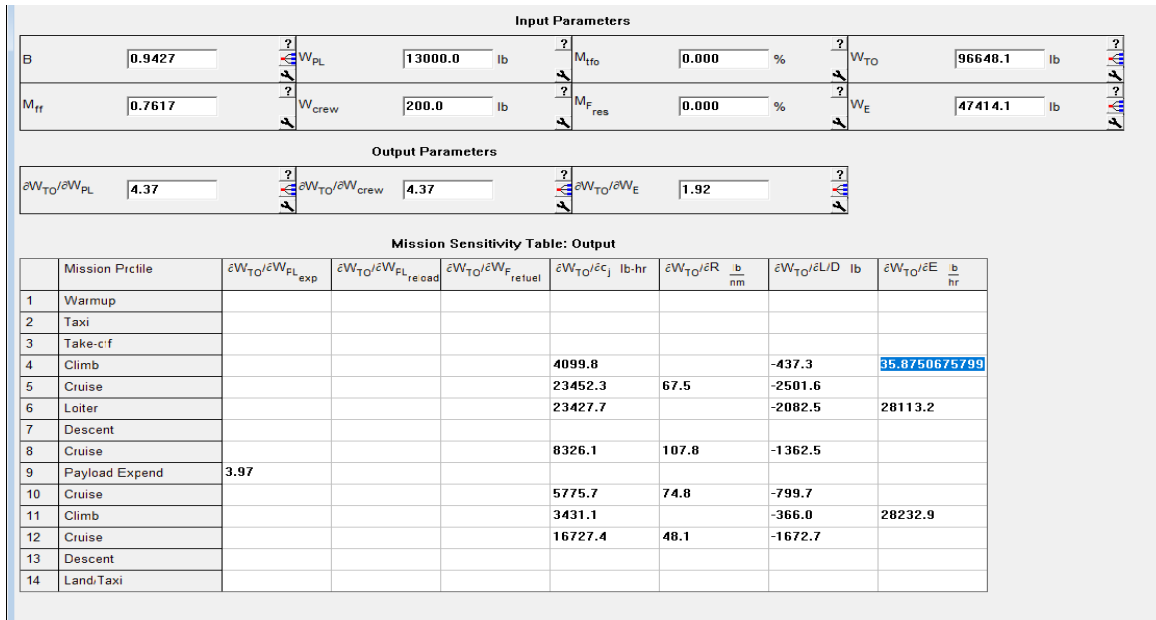


Figure 2.3e: AAA Calculations of Takeoff Weight Sensitivities

The resulting growth factors using the AAA program are as follows:

- Payload Weight Growth Factor:

$$\frac{\partial W_{to}}{\partial W_{pl}} = 4.37.$$

Every 1 lb of payload weight that is increased, the takeoff weight increases by 4.37lbs.

- Empty Weight Growth Factor:

$$\frac{\partial W_{to}}{\partial W_e} = 1.92.$$

Every 1 lb of empty weight that is increased, the takeoff weight increases by 1.92lbs.

- Non-Payload Weight Parameters:

Table 2.7: Growth Factors for Non-Payload Weight Parameters at Different Flight Phases

Mission Profile	$\frac{\partial W_{to}}{\partial C_j}$	$\frac{\partial W_{to}}{\partial R}$	$\frac{\partial W_{to}}{\partial L/D}$	$\frac{\partial W_{to}}{\partial E}$
Climb	4099.8	n/a	-437.3	33735.9
Cruise Out	23452.3	67.5	-2501.6	n/a
Loiter	23427.7	n/a	-2082.5	28113.2
Dash Out	8326.1	107.8	-1362.5	n/a
Dash In	5775.7	74.8	-799.7	n/a

Climb	3431.1	n/a	-366.0	28232.9
Cruise In	16727.4	48.1	-1672.7	n/a

As can be above, for the range case the Dash-Out has the most sensitivity in regards to takeoff weight. In the specific fuel consumption case, the cruise out phase has the highest sensitivity. In the L/D case, the cruise-out phase also has the highest sensitivity. In the endurance case, the initial climb after takeoff has the highest sensitivity. Optimizing the parameters in the dash-out and cruise out phases will save the most amount of takeoff weight for the airplane design.

2.3.5. Trade Studies

A trade study is conducted along with the sensitivity study in order to see how other parameters affect each other. In Figure 2.3f plots the cruise back to base L/D ratio over the takeoff weight. In Figure 2.3g, the cruise back to base specific fuel consumption is plotted vs. the takeoff weight. In Figure 2.3h, the range is plotted vs. the payload weight. From Figure 2.3f, it can be seen how the takeoff weight can be cut down by increasing the L/D during the cruise out phase of the flight. Observing Figure 2.3g, by increasing the specific fuel consumption of the engine during the cruise out phase of the flight, the takeoff weight of the airplane will be reduced by a significant amount. Figure 2.3h shows the range of the aircraft as the payload weight is being traded off while keeping takeoff weight constant.

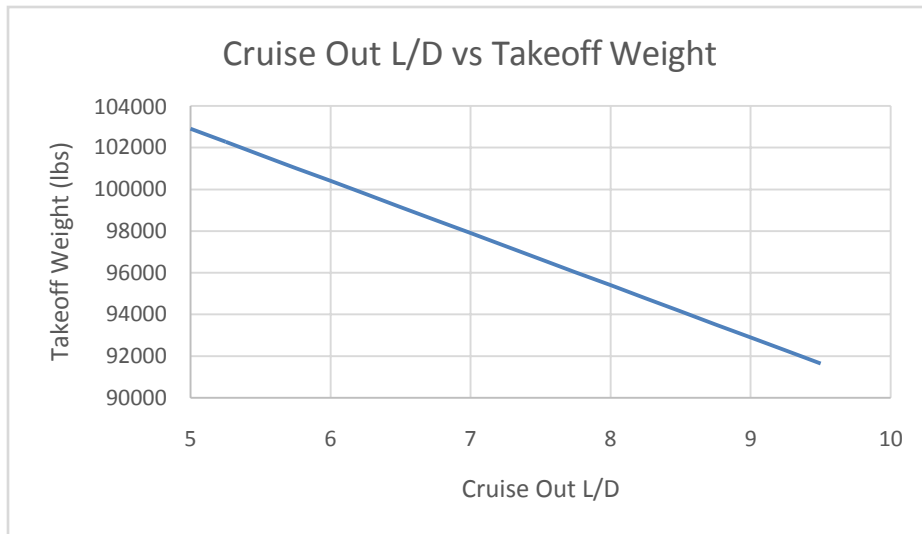


Figure 2.3f: Cruise-Out L/D vs. Weight Takeoff

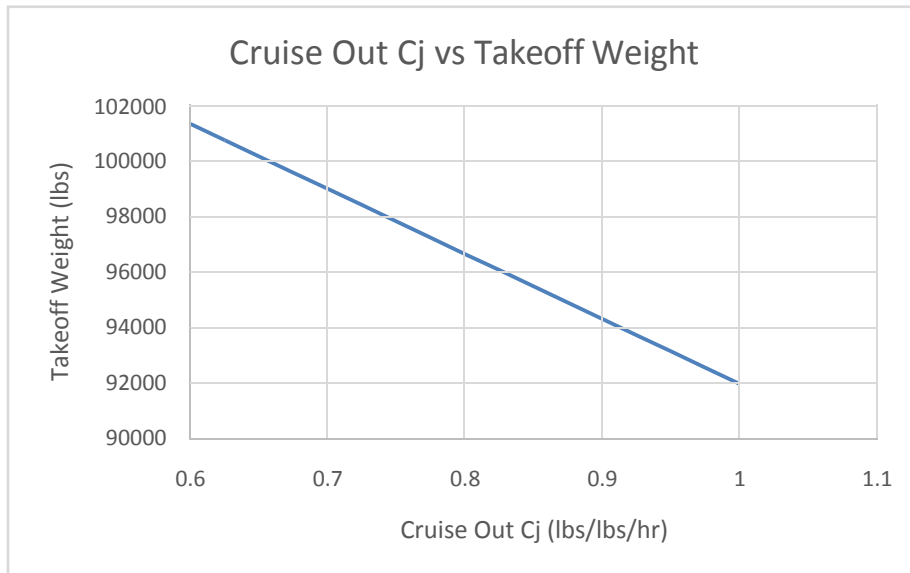


Figure 2.3g: Cruise Out Specific Fuel Consumption vs. Weight Takeoff

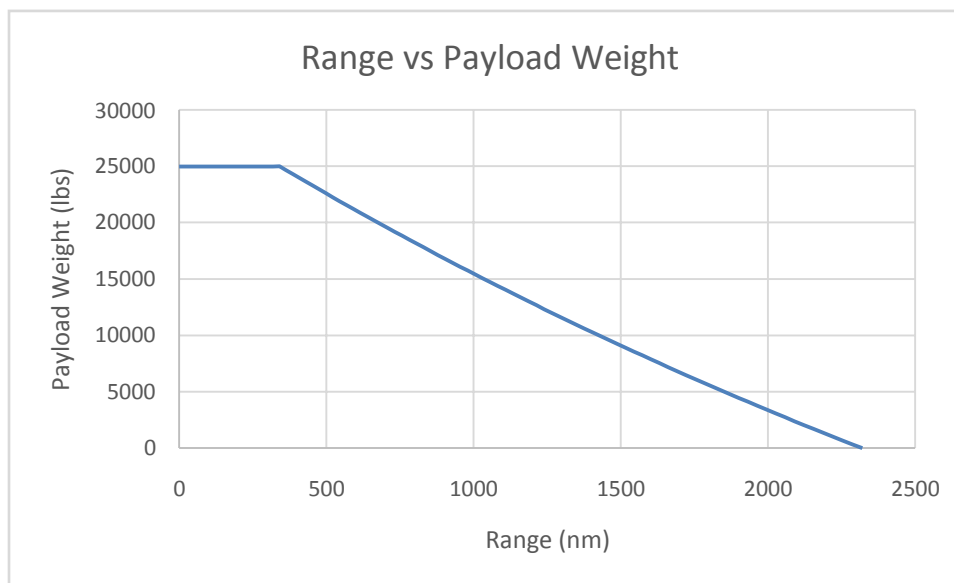


Figure 2.3h: Range vs. Payload Weight

2.3.6: Discussion of Weight Sensitivities and Trade Studies

While determining the optimal takeoff weight, it has shown that the mission weights are a function of the aircraft's flight parameters. In §2.3.4, the takeoff weight's sensitivities to the flight parameters are listed. As the parameters are increased or decreased, the sensitivities show how much the takeoff weight will be adjusted. This will be used to determine which part of the aircraft's flight characteristics and at which phase of the flight needs to be changed to meet the mission requirement. As can be seen in Table 2.7, the loiter and cruise out phase has high sensitivity with the specific fuel consumption. This lets us know if we want to minimize the

takeoff weight, the C_j needs to be increased during this phase or find a more efficient engine. The dash-out and dash-in ranges could also be lowered to save weight on the takeoff weight. This will need to be done cautiously though as if it is lowered too much it will limit its combat radius and affect its operational capability. Trade studies compare different parameters together and plots them over a range of values. Figure 2.3f to Figure 2.3h can be used to quickly find a value for a flight parameter if another flight parameter value has already been decided. In Figure 2.3h, the payload weight was set at a limit of 25,000 lbs as that is near the upper limit for fighter aircraft.

With the mission weights listed in section 2.3.2, this aircraft will likely be the size of other large body, twin-engine multirole fighters such as Su-34 or F-15E. Now that the sensitivities are calculated, the weight consequences of future adjustments to the aircraft's flight parameters during the performance sizing can be determined. These mission weights will act as constraints on the rest of the aircraft design to keep it within the mission specifications.

2.4. Performance Constraint

In an airplane design, the initial sizing of the aircraft is determined by a weight and performance constraint analysis. The future Air Force close air support aircraft is a military aircraft design and will be using military aircraft certification base during the performance constraint analysis. The design aircraft is designed to be a replacement for the A-10 and will need to have low stall speed, short takeoff and landing distance, high maneuverability and climb rate. These performance constraints will determine the necessary propulsion system to power this design. The following design parameters have a major impact on the performance:

- Wing Area
- Take off Thrust
- C_{Lmax}
- C_{LmaxTO}
- C_{LmaxL}

2.4.1. Manual Calculation of Performance Constraints

In Roskam Part I, the author provides a step by step process to estimate the design parameters that impact aircraft performance. The manual calculation of the performance constraints is listed in Appendix 2D. The performance constraints are based off of the MIL-C-005011B and MIL-STD-3013A military aircraft certification. Once the design parameters are estimated, the wing loading, thrust loading, and maximum lift coefficient can be determined. With the highest possible wing loading and lowest possible thrust loading obtained, the wing area and takeoff thrust can be calculated.

2.4.1.1 Stall Speed: Manual Calculation

At sea level with density = $.002378 \frac{\text{slugs}}{\text{ft}^3}$, $C_{lmax}=1.8$ and a desired stall speed of 138mph, the resulting $\frac{W}{S_{to}} = 87.67$. If C_{lmax} was increased to 2.6, then $\frac{W}{S_{to}} = 126.64$. The design has to use the lower of the $\frac{W}{S_{to}}$ value 87.67 for margin of safety.

2.4.1.2 Takeoff Distance: Manual Calculation

Military aircraft certification requires the aircraft to be able to fly above a 50 feet tall obstacle by the end of the runway. With a takeoff weight from the weight sizing, $W_{to}=96,650$ lbs, a bypass ratio = 6.22, $\mu_g=.05$ for hard turf, at sea level and a desired takeoff distance of 3280 ft the resulting $\frac{W}{S_{to}} = 34.5432$.

2.4.1.3 Landing Distance: Manual Calculation

For military fighters the ratio of landing weight and takeoff weight is around 0.8. The certification also requires the approach velocity to be 1.2 times the stall speed. The aircraft will also have to be able to pass a 50 feet tall obstacle before touching down. Using FAR 25 certification charts, the approach speed for a runway of 3300 ft is around 105 knots. Under military certification, the required approach speed will have to be 87.4 knots. The resulting $\frac{W}{S_{to}} = 32.34 * C_{lmax}$.

2.4.1.4 Drag Polar Estimation: Manual Calculation

For this initial estimate of the airplane design, the parameters for the drag are listed as:

- $AR=6$
- $C_f=0.04$
- $S=500$
- $W_{to}=96,650$ lbs.

In Roskam Part I Chapter 3, the author states that the zero lift drag coefficient can be expressed as equivalent parasite area divided by wing area. The parasite area can then be related to the wetted area by Roskam's correlation coefficients a & b, which are based off of C_f . The S_{wet} was also determined by Roskam to correlate to W_{to} and can be related by regression coefficients c & d. The resulting Roskam correlation coefficients for drag are; $a=-2.4$, $b=1$, $c=-0.1289$, $d=0.7506$. With these coefficients, the drag coefficient can be determined.

2.4.1.5 Climb Constraints: Manual Calculation

MIL-C-005011B requires the aircraft to be able to takeoff with the most critical engine inoperative. In this aircraft design's case, it would be one out of the two engines inoperative. The takeoff velocity V_{to} also needs to be 1.1 times the V_S at takeoff with a climb gradient of at least

0.005. The L/Dmax is calculated to be 10.69 at sea level. For a desired rate of climb (RC) of 500 fpm, the resulting velocity and $\frac{T}{W_{TO}}$ are listed on Table 2.8.

Table 2.8: $\frac{T}{W_{TO}}$ for Different $\frac{W}{S_{to}}$ and One Engine Inoperative

$\frac{W}{S_{to}}$	V(fps)	RC/V	$\frac{T}{W_{TO}}$ 1 engine	$\frac{T}{W_{TO}}$ 2 engines
40	218	.038	.131	.262
60	267	.031	.125	.25
80	309	.027	.121	.242
100	345	.024	.118	.236

2.4.1.6 Maneuvering Constraints: Manual Calculation

For this aircraft design, a combat speed of 510 mph at an altitude of 1000ft is desired. The plane will also need to be able to make a 3.5g turn maneuver. The resulting relationship between $\frac{T}{W}$ and $\frac{W}{S}$ for these parameters is:

$$\frac{T}{W} = \frac{21.3}{\frac{W}{S}} + .001258 * \frac{W}{S} \quad (2.4.1)$$

2.4.1.7 Speed Constraints: Manual Calculation

A cruise speed of 480 knots is desired at an altitude of 40,000 ft. Using atmospheric data from the MIL-STD-3013A certification, the resulting Mach #= 0.73 and pressure= 2040.86 lbs/ft². An additional compressibility drag is included to the C_{d0} due to the high Mach #. The resulting relationship between $\frac{T}{W}$ and $\frac{W}{S}$ for these parameters is:

$$\frac{T}{W} = \frac{27.4}{\frac{W}{S}} + .000087 * \frac{W}{S} \quad (2.4.2)$$

2.4.2. Calculation of Performance Constraints with AAA Program

Another method to do a performance constraint analysis is to make a matching graph in AAA by plotting takeoff wing loading vs. thrust to weight ratio for each of the design parameters. A point is then chosen where the lines intersect to determine the design aircraft's wing area and takeoff thrust.

2.4.2.1. Stall Speed: AAA

In Figure 2.4a, the parameters for the design aircraft's stall speed are inputted to output the wing loading at stall speed and clean configuration. Figure 2.4b displays the resulting wing loading plot vs. T/W.

Input Parameters							
h_s	1000 ft	ΔT_s	0.0 deg F	V_{s_clean}	120.00 kts	V_{s_WTO}	100.00 kts
						W_s/W_{TO}	1.000
						$C_{L_max_s_dn}$	2.000
						$C_{L_max_s}$	2.600

Output Parameters	
$(W/S)_{TO_s_dn}$	94.68 $\frac{lb}{ft^2}$
$(W/S)_{TO_s}$	85.48 $\frac{lb}{ft^2}$

Figure 2.4a: AAA Parameters for Stall Speed

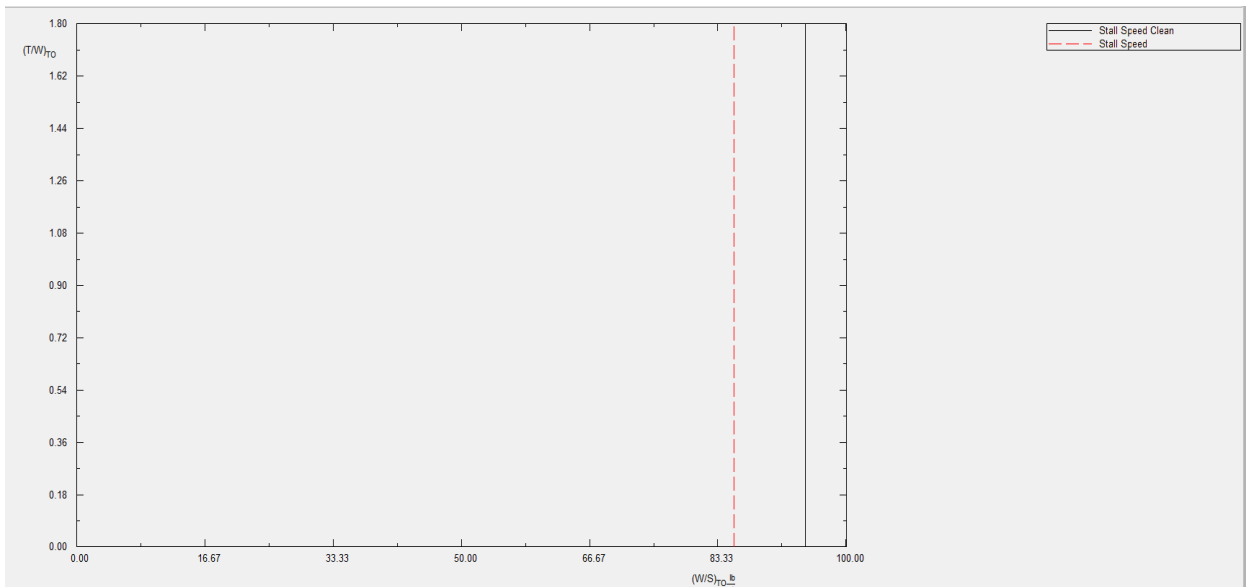


Figure 2.4b: AAA T/W vs. W/S for Fixed Stall Speed

2.4.2.2. Takeoff Distance: AAA

In Figure 2.4c, the parameters for the design aircraft's takeoff distance are inputted to output the wing loading. Figure 2.4d displays the resulting wing loading plot vs. T/W for a fixed takeoff distance and varying max lift coefficients.

Input Parameters							
h_{TO}	0 ft	ΔT_{TO}	0.0 deg F	Plot ΔC_{L_max}	0.200	$C_{D_{0_TO_down}}$	0.0580
						BPR	6.22
F_{TO}	1.000	$C_{L_max_TO}$	2.000	S_{TOG}	3280 ft	H_G	0.0500

Figure 2.4c: AAA Parameters for Takeoff Distance

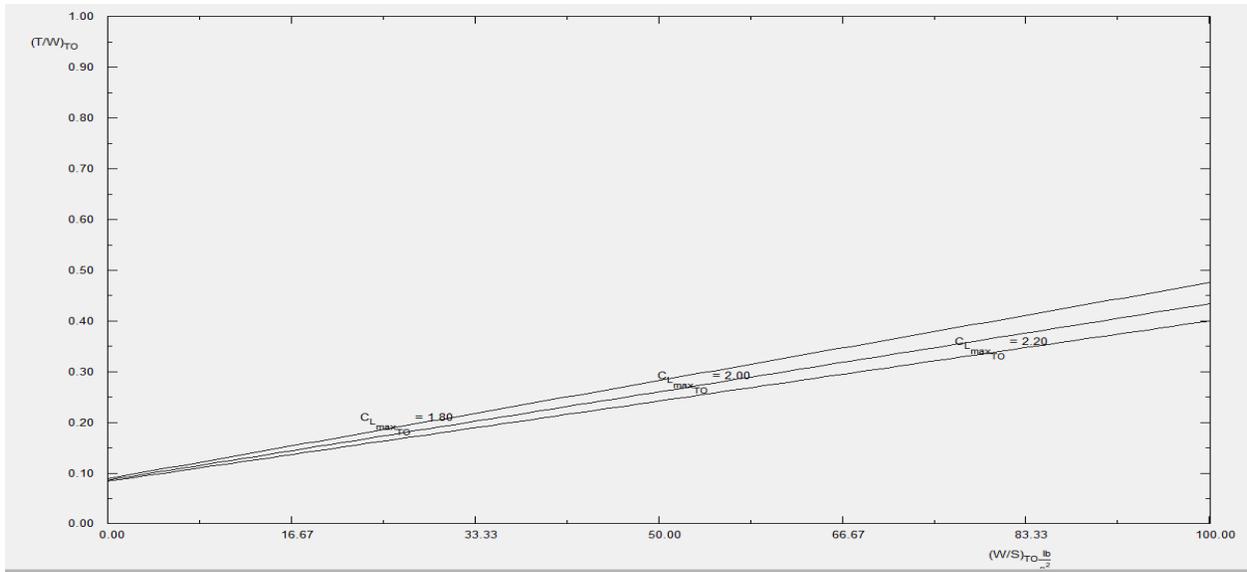


Figure 2.4d: AAA T/W vs. W/S for Different $C_{L,max}$ with Fixed Takeoff Distance

2.4.2.3. Landing Distance: AAA

In Figure 2.4e, the parameters for the design aircraft's landing distance are inputted to output the wing loading. Figure 2.4f displays the resulting wing loading plot vs. T/W for a fixed landing distance and varying max lift coefficients.

Input Parameters														
h_L	<input type="text" value="0"/>	ft	ΔT_L	<input type="text" value="0.0"/>	deg F	W_L/W_{TO}	<input type="text" value="0.762"/>	C_{L,max_L}	<input type="text" value="2.600"/>	Plot $\Delta C_{L,max}$	<input type="text" value="0.200"/>	S_{FL}	<input type="text" value="3280"/>	ft
Output Parameter														
$(W/S)_L$	<input type="text" value="87.71"/>	lb/ft ²												

Figure 2.4e: AAA Parameters for Landing Distance

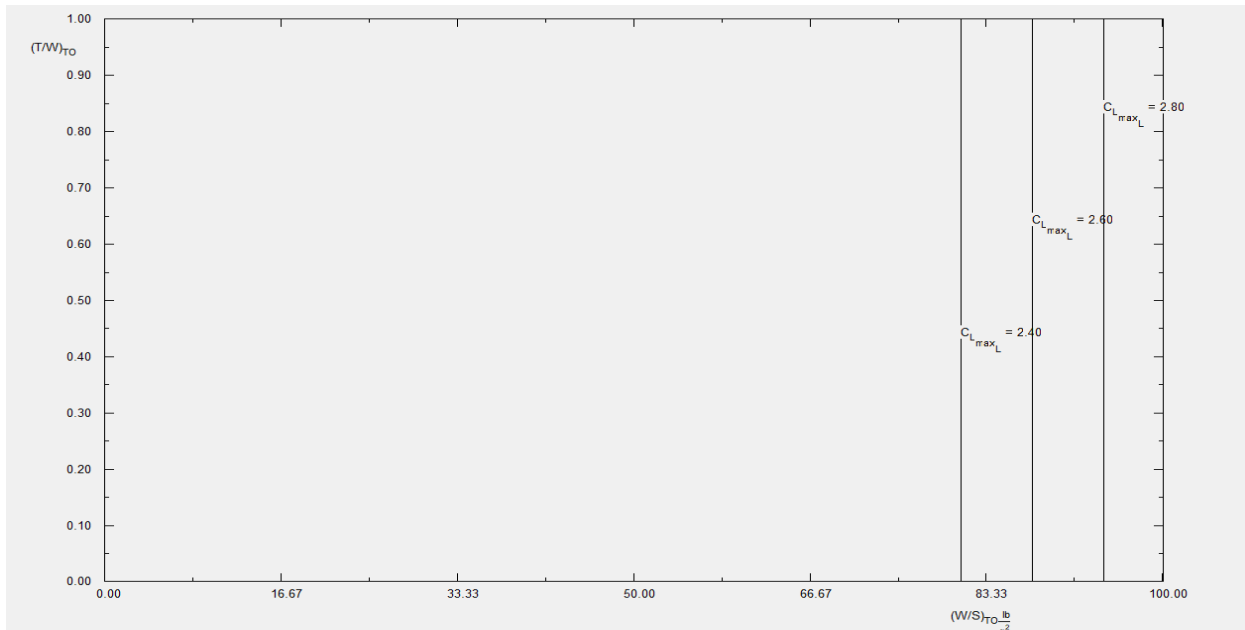


Figure 2.4f: AAA T/W vs. W/S for Different $C_{L_{max}}$ with Fixed Landing Distance

2.4.2.4. Drag Polar Estimation

The drag coefficients for five different configurations of the aircraft with a NACA 6716 Airfoil are documented in Table 2.9. The plots of C_L vs C_D for these five configurations are listed on Figure 2.4g.

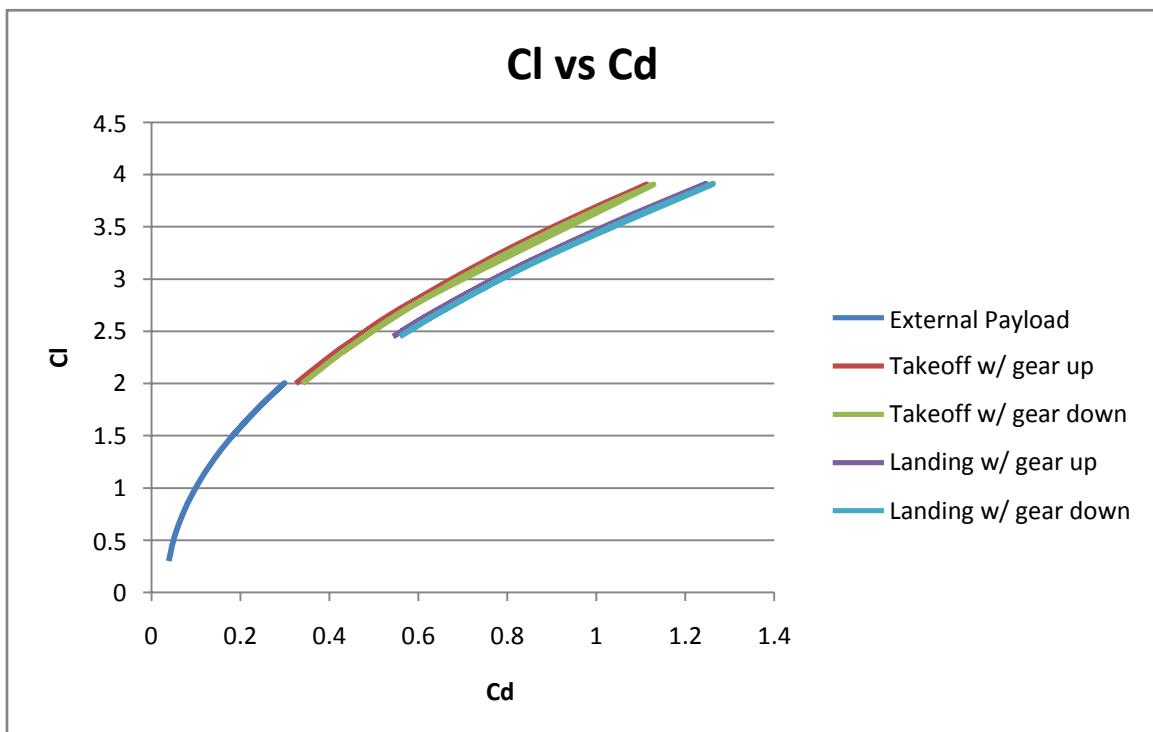


Figure 2.4g: C_L vs C_D for Five Different Flight Configurations

Table 2.9: Drag Coefficient of Aircraft under five configurations

Configuration	Drag Coefficient
With external payload	$Cd=0.033+0.0663*Cl^2$
Takeoff with gear up	$Cd=0.043+0.0703*Cl^2$
Takeoff with gear down	$Cd=0.058+0.0703*Cl^2$
Landing with gear up	$Cd=0.088+0.0758*Cl^2$
Landing with gear down	$Cd=0.103+0.0758*Cl^2$

2.4.2.5. Climb Constraints

In Figure 2.4h, the parameters for climb constraints are inputted into AAA to output the wing loading. Figure 2.4i displays the resulting wing loading plot vs. T/W for climb to a set altitude of 40,000 ft.

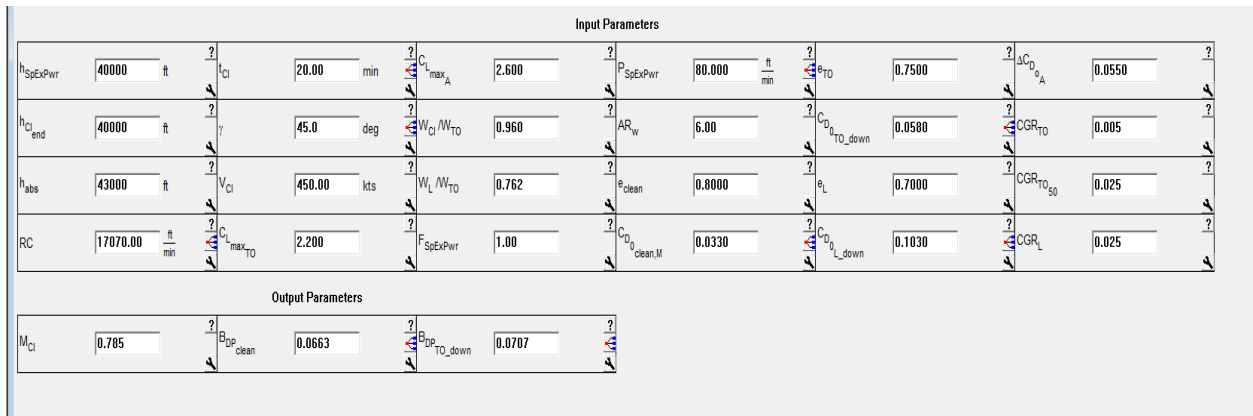


Figure 2.4h: AAA Parameters for Climb Constraints

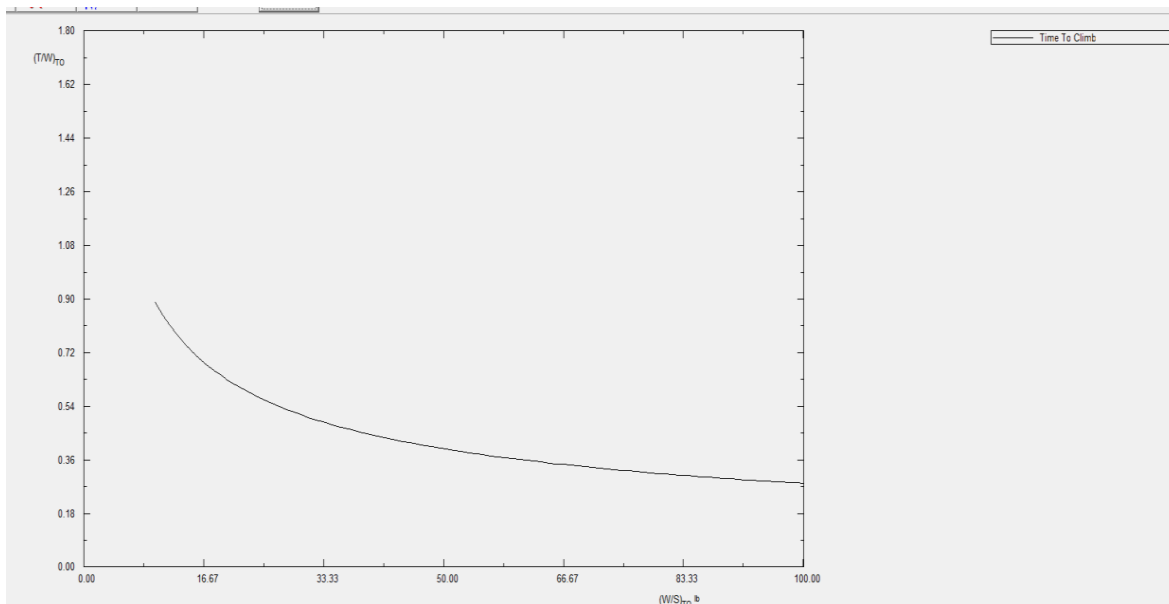


Figure 2.4i: AAA T/W vs. W/S for Climb to Altitude of 40,000 ft.

2.4.2.6. Maneuvering Constraints: AAA

In Figure 2.4j, the parameters for maneuvering are inputted into AAA to output the wing loading for a load factor of 3.5. Figure 2.4k displays the resulting wing loading plot vs. T/W for an altitude of 1,000 ft.

Input Parameters							
h_M	1000	ft	n	3.50	g	F_M	1.000
V_M	443.00	kts	W_M/W_{TO}	0.825		AR_W	6.00
						$C_{D_{0, clean, M}}$	0.0330
						e_{clean}	0.8000
Output Parameters							
M_M	0.672		$B_{DOP, clean}$	0.0663		TurnRate	0.1443 $\frac{rad}{s}$

Figure 2.4j: AAA Parameters for Maneuvering

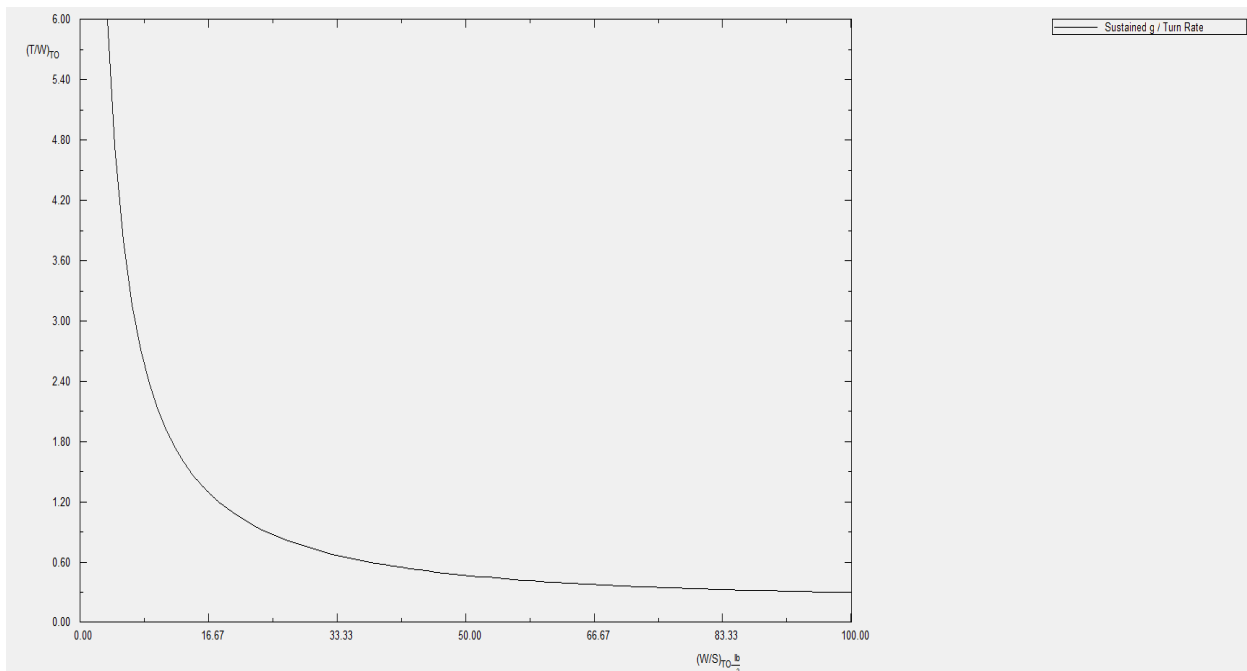


Figure 2.4k: AAA T/W vs W/S for Load Factor of 3.5 at Altitude of 1000ft.

2.4.2.7. Speed Constraints

In Figure 2.4l, the parameters for aircraft speed are inputted into AAA to output the wing loading. Figure 2.4m displays the resulting wing loading plot vs. T/W for an altitude of 40,000 ft at max cruise speed of 480 knots.

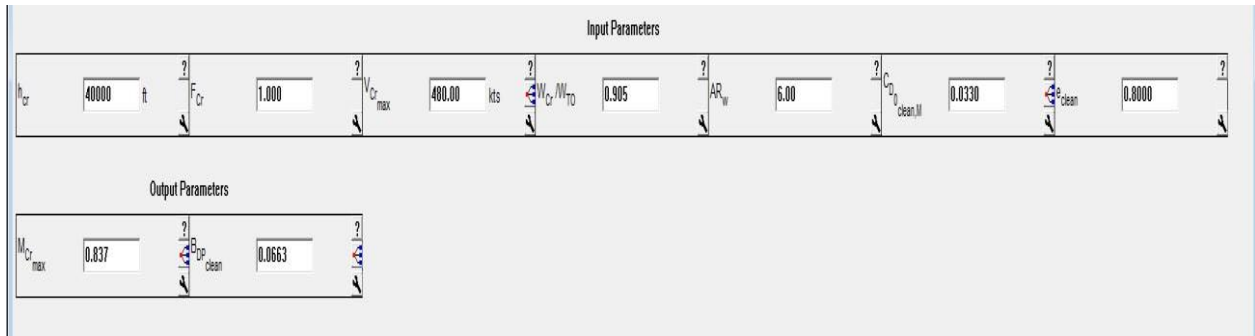


Figure 2.4l: AAA Parameters for Speed Constraints

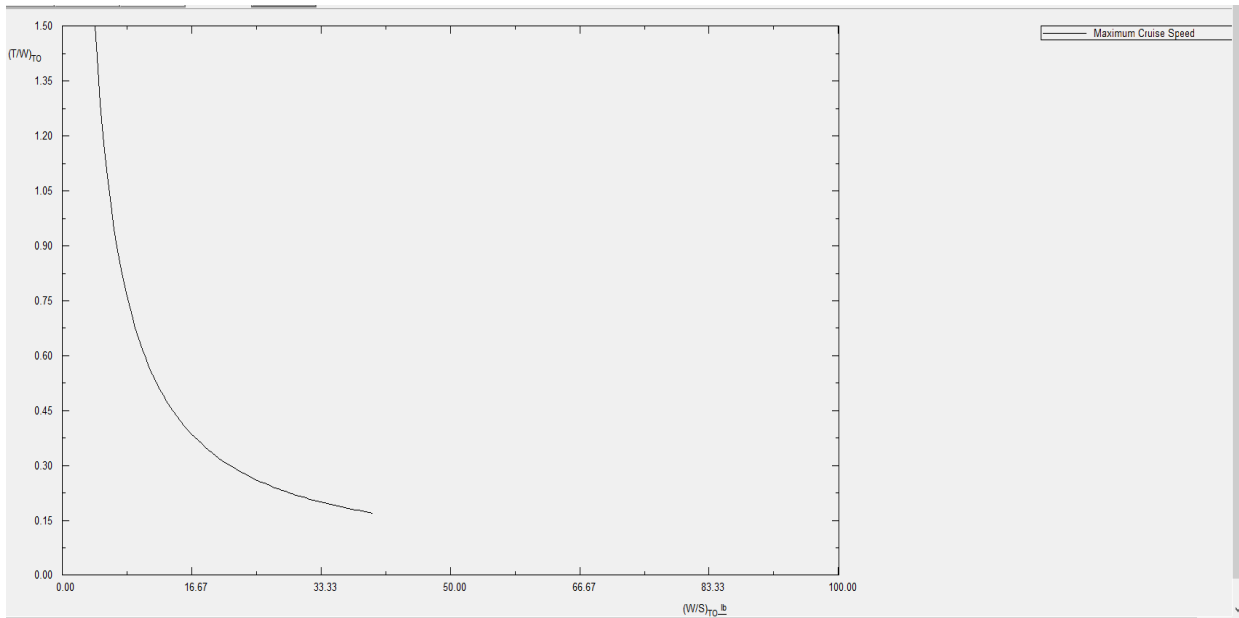


Figure 2.4m: AAA T/W vs W/S for Max Cruise Speed of 480 knots at 40,000 ft

2.4.3. Summary of Performance Constraints

The seven plots from §2.4.2.1-§2.4.2.7 are put together into one graph in order to choose a design point for the wing loading and thrust to weight ratio. The graph can be seen in Figure 2.4n.

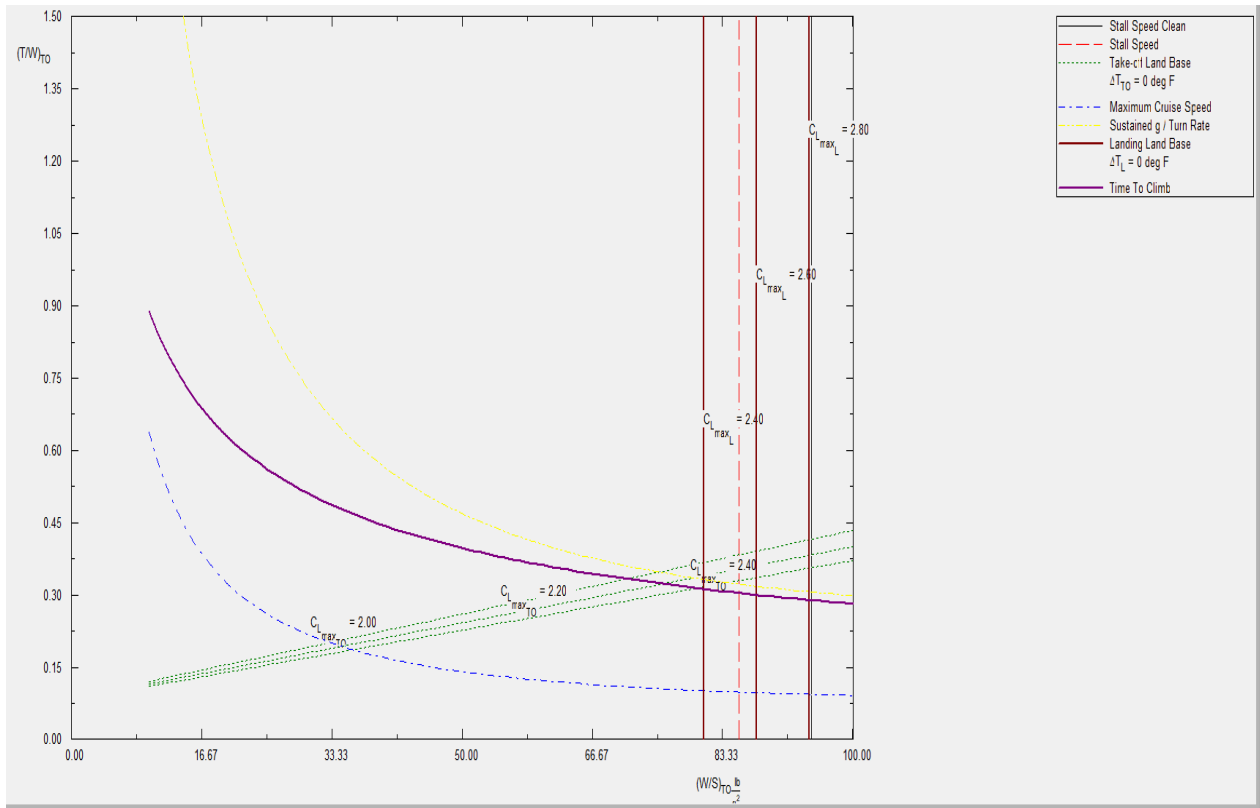


Figure 2.4n: AAA Matching Graph of Performance Constraints

For takeoff, a $C_{LmaxTO} = 2.2$ will be chosen. For landing, a $C_{LmaxL} = 2.4$ will be chosen. The stall speed plot of a clean configuration is seen far away from the rest of the plots and can thus be more liberally chosen. A $C_{LmaxClean} = 2.0$ will be chosen. To choose the matching point from Figure 2.4n, multiple criteria have to be met. The matching point has to meet the following:

- Run along the green lift coefficient line.
- Be above the blue cruise speed line.
- Below yellow maneuverability and purple time to climb line.
- To the left of the red stall speed line.

Using this criteria, a matching point at $\frac{T}{W_{TO}} = 0.3$ and $\frac{W}{S_{TO}} = 80$ psf is chosen. With an aspect ratio chosen to be 6 and a $W_{to} = 96,650$ lbs the resulting design parameters are as follows:

- Wing Area $S = 1208$ ft²
- Thrust at Takeoff = 29,000 lbs

2.4.4. Discussion of Performance Constraints

The military aircraft certification MIL-C-005011B and MIL-STD-3013A were used to choose initial parameters to perform a performance constraint analysis. From these parameters

inputted into the AAA program, various plots of T/W vs. W/S were created for each performance constraint.

Stall speed was calculated at sea level and was set at a low speed as this aircraft design will need to provide air support for ground troops at a low altitude and speed. The wing loading at a stall speed of 138mph is 85 psf for a clean configuration and 95 psf in normal flying conditions with payload. This tells us the matching point will need to be less than 85 psf to support this stall speed.

The landing and takeoff distance was set at 3280 feet to allow this aircraft to operate in remote smaller air bases. Under MIL-C-005011B and MIL-STD-3013A, the aircraft will need to be able to fly above a 50 ft obstacle before landing or taking off. T/W vs. W/S were plotted for both landing and takeoff with three different C_{Lmax} . From looking at Figure 2.4b and Figure 2.4f, the landing plots are in similar positions as the stall speed as such will have similar impact to the design. Figure 2.4g and Table 2.9 lists the drag coefficients for five different configurations: with external payload, takeoff flaps with landing gear up and down, and landing flaps with landing gear up and down. A NACA 6716 Airfoil was chosen to plot the C_L vs C_D under these configurations as the A-10 uses this airfoil on its wing and it has the closest mission requirements as this design aircraft. Looking at Table 2.9, the landing flaps with landing gear has the highest zero-lift drag coefficient. This corresponds with the theory that the aircraft requires high drag as it is landing. In Figure 2.4g the C_L goes up to nearly four when taking off with the landing gear is up.

At cruising altitude of 40,000 ft, the max Mach number is 0.83, which is approaching transonic. There will be some normal shocks forming above the wing at this speed. In addition vibration on the wing will need to be taken into account. As the wing will be designed for a combat aircraft, the wing spar will be stiff and durable to survive enemy fire and tight maneuvers. As such, the wing vibrations from transonic flight will be assumed negligible. An altitude of 1000 ft and a load factor of 3.5g are selected as the parameter for the maneuvering constraint as this aircraft will need to fly low during close air support and also need to make tight turns repeatedly to make repeated strafing runs.

The plots of the T/W vs. W/S of each performance constraints are combined together on Figure 2.4n. From this figure, the speed constraint is observed to be far off from the rest of the performance constraints and as such is not a critical constraint to the design. Thus, a higher max cruising speed can be chosen without affecting the design. The climbing and maneuvering constraint are close to each other and as such are critical constraints. Where they match up with the takeoff constraint is also close to the landing and stall constraints plots. This tells us there is a very narrow region where a matching point can be chosen to support these performance requirements. In particular, the climbing constraint parameters in Figure 2.4h affected this design the most while performing the performance constraint analysis. The original design desired a climb time of 5.8 minutes with at least a rate of climb of 500 feet per minute per military

certification. This climb time was too short and did not allow the matching plot to converge to an answer. The climb performance had to be sacrificed by increasing the climb time to 20 minutes with a steep climb angle of 45 degrees to allow for the rest of the performance constraints to converge to an answer. The load factor of 3.5 also caused the matching point to be nearing the stall speed limit. With the narrow matching point area made by the landing, takeoff, climbing, and maneuverability constraints the matching point was chosen at $\frac{T}{W_{TO}} = 0.3$ and $\frac{W}{S_{TO}} = 80$ psf.

The resulting wing loading is similar to the range of contemporary fighters as the A-10 and Su-34 has wing loading of at least 100 psf. But this design with a $W_{TO} = 96,650$ lbs leads to a wing area of 1208 ft², which is larger than most fighter aircrafts. The thrust to weight of 0.3 is lower than other contemporary fighters, which have an average thrust to weight of 0.36.

Based off the matching plot on Figure 2.4n and the performance constraint analysis, the maneuverability and the climb rate of the aircraft will be the characteristics that have the most impact to this design. These two characteristics approach the limits set by the stall speed and as such, changes to these two flight performance parameters will need to be done carefully to avoid passing the stall speed constraints. The climb constraint had high sensitivity in regards to the climb angle and climb time. A longer than expected climbing time was required to meet the performance constraints. This will mean the aircraft will need a large radius of safe airspace to climb to its cruising altitude. The load factor of 3.5gs will also be limit of this aircraft's turn rate as anymore and it will also past the landing and stall constraints. The design of this aircraft will need to keep in mind of the slow climb performance and max turn rate.

2.5. Fuselage Design

The next step in the design process is the fuselage design. With the weight of the aircraft determined and the area of the wing calculated the airplane can start taking shape. Airplane dimensions for various military fighters will be observed and used as a reference for the initial fuselage design. The Future Air Force Close Air Support Aircraft will need ample space to hold its 13,000 lbs in payload and also be able to support the wing area determined in the performance constraint analysis.

2.5.1. Cockpit Design

In Roskam Part III, the author provides general pilot, control stick, and ejection seat dimensions to be used during the cockpit design. During the cockpit design, multiple things have to be taken in consideration. The ejection seat has to have enough clearance in the cabin to eject safely and the seat has to be at an angle for the pilot to maintain good line of vision. Vision is critical for fighter pilots to maintain situational awareness. Figure 2.5a displays the layout of the ejection seat and flight controls.

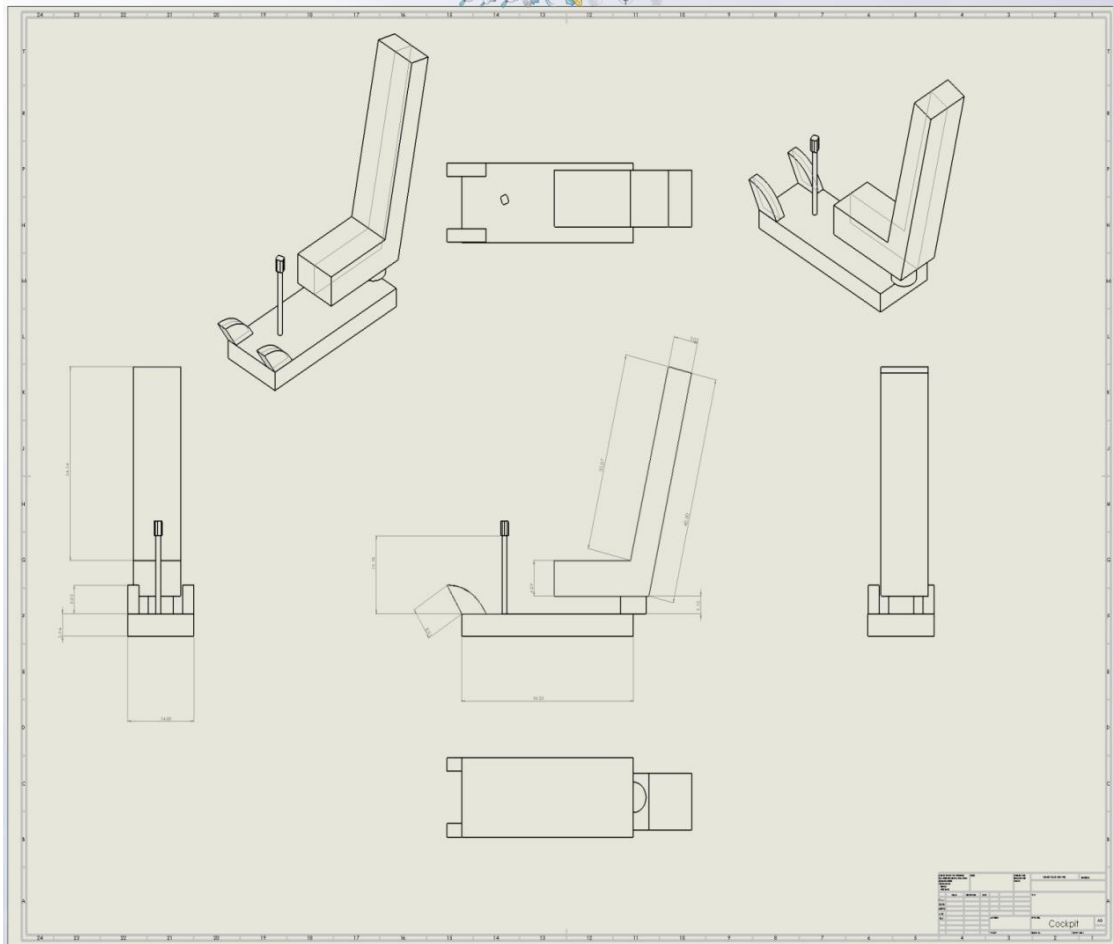


Figure 2.5a: Layout Design of Cockpit

2.5.2. Fuselage Design

In Roskam Part III, the author provides a step by step process to design the fuselage for military aircraft. In the case of the FAFCAS, the aircraft will have the ammunition container behind the pilot, gun mounted forward and below the pilot, main landing gear retract forward of the nose, and the engines mounted behind the ammunition container. When designing the fuselage, the primary design parameters are the following:

- Height of the fuselage, df
- Length of the fuselage, lf
- Distance from end of fuselage to beginning of tail section, lfc
- Angle from top of tail section to bottom of fuselage, θ_{fc}

Figure 2.5b shows the definition of the fuselage parameters provided by Roskam Part II.

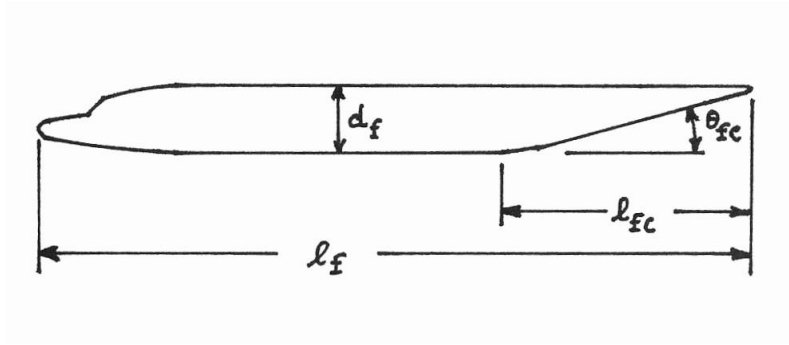


Figure 2.5b: Definition of Fuselage Design Parameters.

In Roskam Part II, the author provides values for suggested geometric parameters for fighters to use. Table 2.10 shows the suggested parameters and the parameters chosen for the FAFCAS.

Table 2.10: Suggested and Design Fuselage Geometric Parameters

Geometric Parameter	Suggested	FAFCAS Design
l_f/d_f	7-11	11
l_{fc}/d_f	3-5	3
θ_{fc}	0-8	0

With the fuselage parameters chosen in Table 2.10, the initial fuselage design has the following dimensions:

- $l_f = 66$ ft.
- $d_f = 6$ ft.
- $l_{fc} = 18$ ft.
- $\theta_{fc} = 6$ degrees

Using these dimensions, the resulting layout of the fuselage and model of the fuselage can be seen in Figure 2.5c and Figure 2.5d respectively.

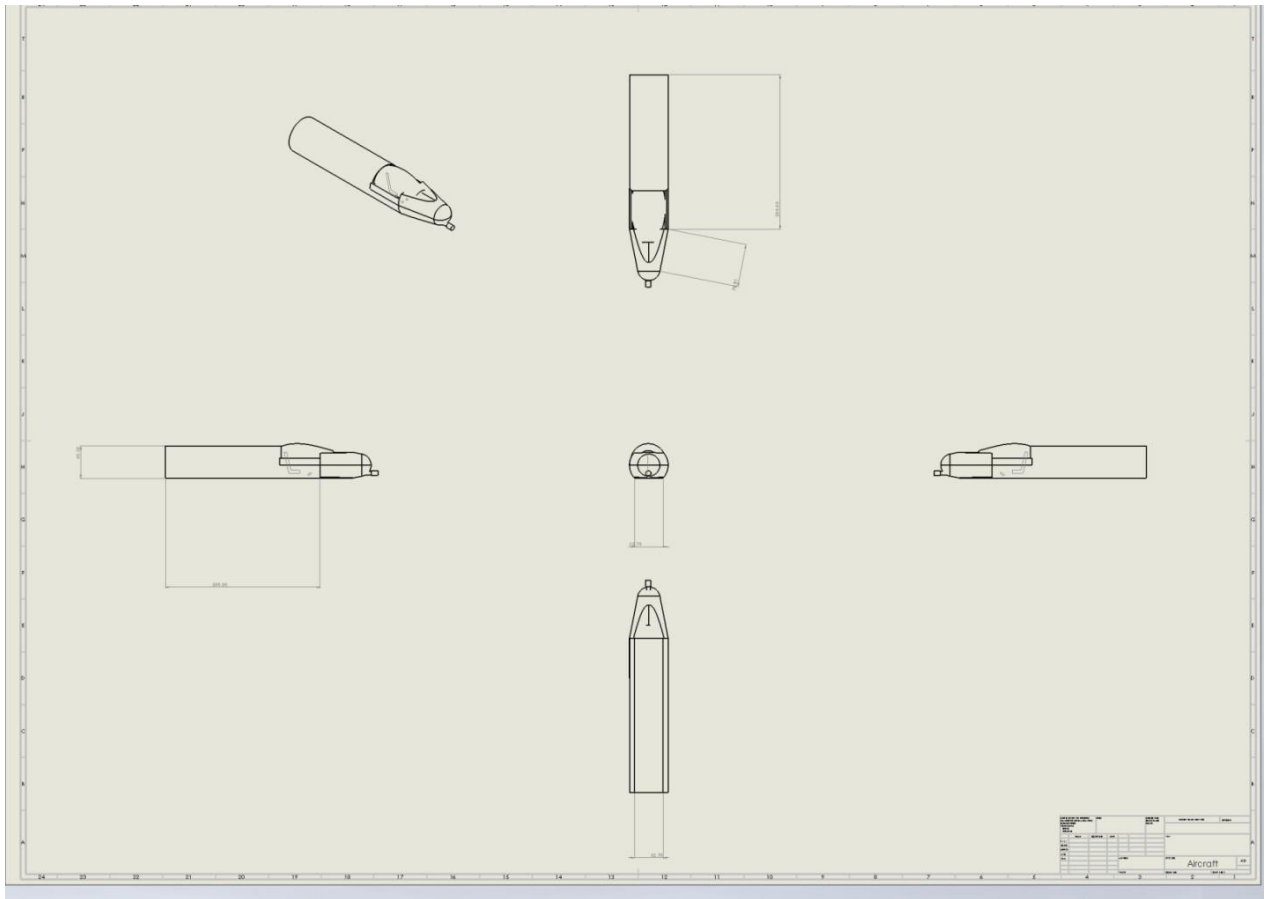


Figure 2.5c: Layout of the Fuselage

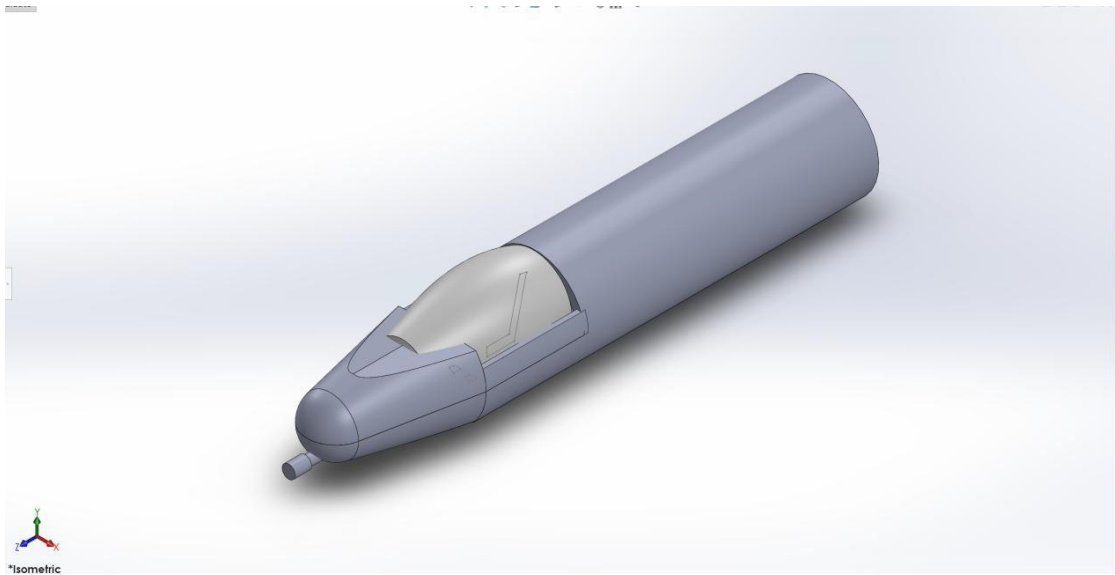


Figure 2.5d: Fuselage Model

2.6. Wing, High-Lift System, and Lateral Control Design

With the weight sizing and performance constraint analyzed and the initial fuselage design made, the next step will be to design the wing and other flight surfaces of the aircraft. The wing area and aspect ratio determined from previous analysis will be used to design the wing planform shape. Afterwards the airfoil and the high-lift devices will be chosen based on the mission requirements of the FAFCAS. Equations in Roskam Part II Chapter 6 and Chapter 7 will be used to design the wing and high lift design. The wing will need to provide sufficient lift at low speeds and low altitude due to the FAFCAS's primary role in close air support.

2.6.1. Wing Planform Design

Using the performance constraint analysis in §2.4.3, the design aircraft's wing dimensions are determined to be:

- $S = 1208 \text{ ft}^2$
- $AR = 6$

The resulting wingspan is 85 ft. The wing area and the wing span is approaching transport aircraft dimensions and thus needs to be lowered.

Using the matching graph from the performance constraint analysis the following changes were made in the matching point:

- Keep the $\frac{T}{W_{TO}}$ the same at 0.3.
- Increase the C_{Lmax} at takeoff to 2.4
- Increase the C_{Lmax} at landing to 2.8.

The resulting $\frac{W}{S}$ from this new matching point is at 93 psf. With these new parameters, the resulting wing dimensions are:

- $S = 1040 \text{ ft}^2$
- $AR = 6$
- $B = 79 \text{ ft}$

Using contemporary wing data of other fighter aircrafts from Roskam Part II Chapter 6, the dihedral angle and taper ratio are chosen as:

- $\Gamma_w = 0 \text{ degrees}$
- $\Lambda = 0.45$

A dihedral angle of zero degrees was taken because a mid wing configuration was chosen for this airplane design. Most contemporary fighter aircrafts that have mid wing configuration such as the F-16 are already unstable and doesn't need additional instability from dihedral effects. Taper

ratio was chosen to be 0.45 as it is a midpoint between low taper ratio high speed fighter and high taper ratio low speed aircraft.

2.6.1.1. Sweep Angle- Thickness Ratio Combination

A critical Mach # of 0.84 was chosen as the design point of the wing. The resulting C_{Lcr} is 0.43 at an altitude of 40,000 ft. With the thickness ratio equation from Torenbeek 1988, the thickness ratio and resulting wing weight are listed on Figure 2.6a. See Appendix 2E for equations used to determine wing weight and thickness ratio.

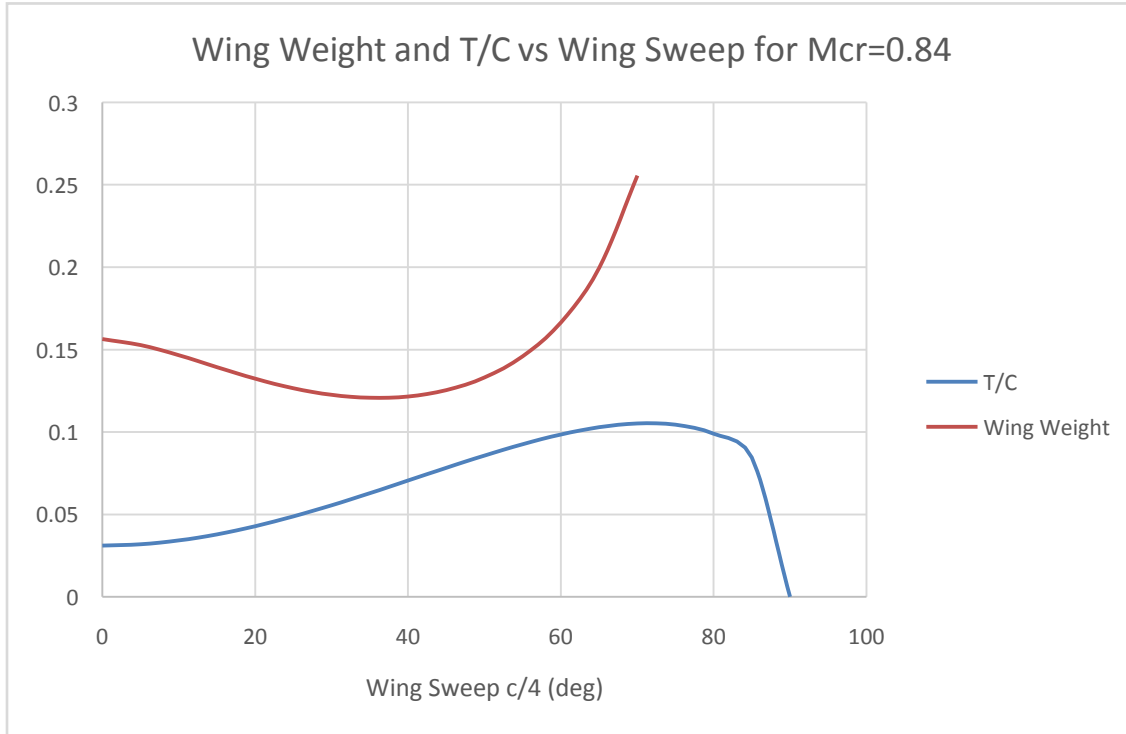


Figure 2.6a: Wing Weight and Thickness Ratio for Different Wing Sweep

Given the requirement of thickness ratio greater than 0.1, a thickness ratio of 0.1 at a sweep angle of 60 degrees will be chosen to satisfy the $M_{cr}=0.84$. The resulting wing weight for this wing sweep and thickness ratio is 11670 lbs.

2.6.2. Airfoil Selection

A NACA 6716 airfoil will be chosen for this aircraft design. From contemporary fighter aircraft data listed by Roskam Part II, an incidence angle of zero will be chosen to reduce cruise drag. A twist angle of -1 degrees will be chosen as a washout design has lower wing weight and to delay tip stall.

2.6.3. Wing Design Evaluation

Using the taper ratio of 0.45 and a thickness ratio of 0.1, a root chord of 15 ft and a tip chord of 6.75 ft were selected. These parameters are inputted into AAA and the result can be seen in Figure 2.6b and Figure 2.6c.

Figure 2.6b: AAA Parameters for Wing Airfoil Lift Coefficients Case 1

Figure 2.6c: AAA Wing Maximum Lift Verification Case 1

As can be seen in Figure 2.6c, this current design of the wing does not meet the required C_{Lmax} within +/- 5% and the wing planform area needs to be redesigned. The wing sweep angle from §2.6.1.1 is too high for contemporary fighter aircrafts. In Figure 2.6d, a redesigned planform area is chosen that meets the required C_{Lmax} .

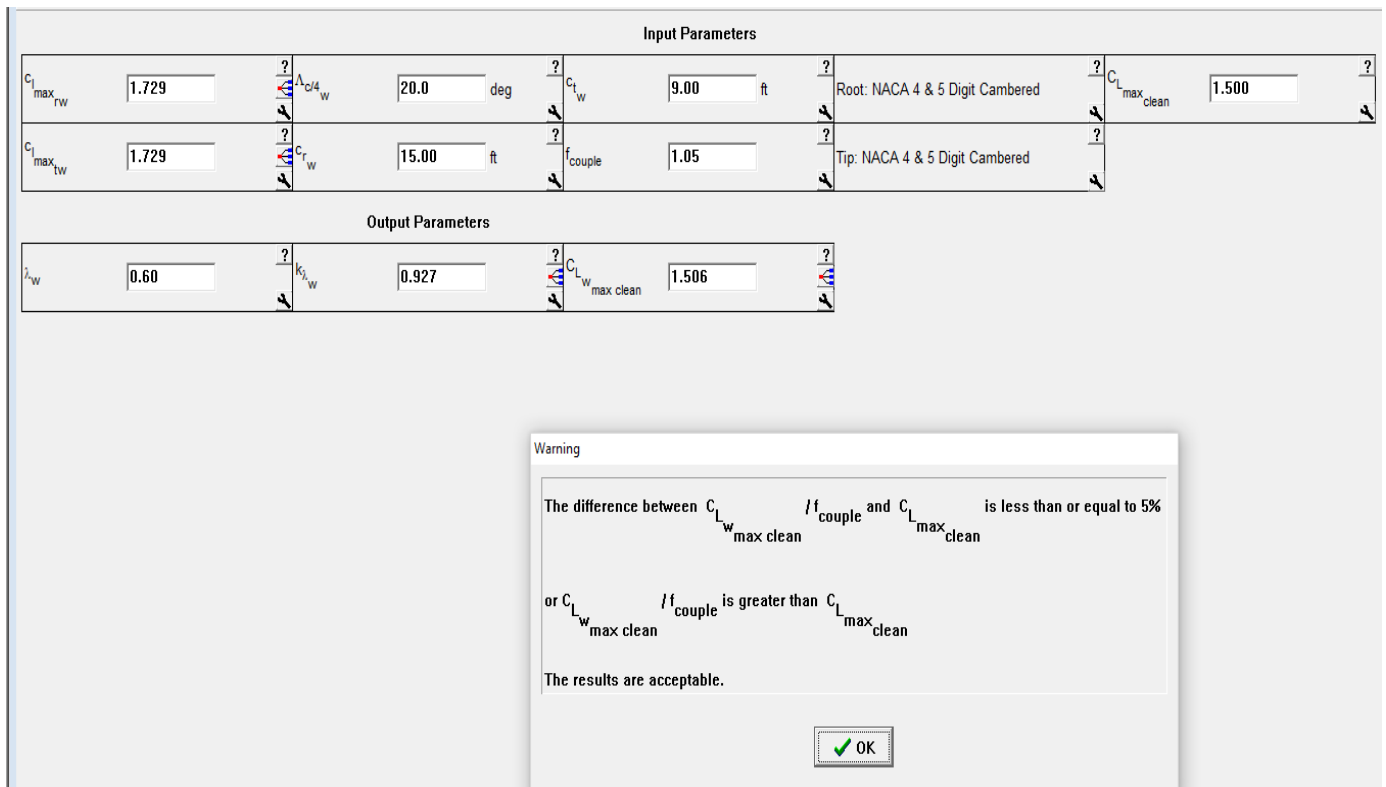


Figure 2.6d: AAA Wing Maximum Lift Verification Case 2

In this new planform area configuration, the taper ratio was increased from 0.45 to 0.6 which results in a wing root chord of 15 ft and a tip root chord of 9 ft. The sweep angle was decreased from 60 degrees to a more realistic 20 degrees. With a required C_{Lmax} of 1.5, this new design meets this number within +/- 5%. The new wing weight of this design is 8550 lbs.

2.6.4. Design of the High-Lift Devices

From the performance constraint analysis the lift coefficients used to design the high-lift devices are:

- $C_{LmaxTo} = 2.4$
- $C_{LmaxL} = 2.8$
- $C_{Lmax} = 1.5$

See Appendix 2F for the calculation of the high-lift devices. The flap geometries of this design to meet the requirements are:

- $\frac{S_w}{S} = 1.0$
- $\frac{C_f}{C} = 0.3$
- $\delta_{fL} = 40$ degrees
- $\delta_{fTo} = 25$ degrees

Full length Fowler Flaps with spoilers will be used to meet this design.

2.6.5. Design of the Lateral Control Services

An aircraft length of 50 ft, wing area of 1040 ft², and wing span of 79 ft are used parameters to design the lateral control services. Using Roskam Part II's contemporary fighter aircraft data, the summary of lateral control service geometry are listed in Table 2.11.

Table 2.11: Geometry of Lateral Control Services

	Horizontal Stabilizer	Vertical Stabilizer
Area (ft ²)	220	183
Dihedral Angle (deg)	0	75
Incidence Angle (deg)	0	0
AR	4	1
Sweep Angle (deg)	20	25
Taper Ratio	0.5	0.4

2.6.6. Preliminary Sketch of Wing

Using the wing dimensions from §2.6.3, a preliminary sketch is drawn for the main wing which is seen in Figure 2.6e. The main wing properties are as follow:

- Mean Aerodynamic Chord (MAC)= 13.2 ft.
- Mean geometric chord (MEC)= 13.2 ft.
- Leading edge wing sweep= 20 deg.
- Trailing edge wing sweep= 12 deg

For the aerodynamic center in reference to the leading edge and wing root (x=0, y=0):

- $x_{ac} = 17.7\text{ft}$
- $y_{ac} = -8.86\text{ft}$

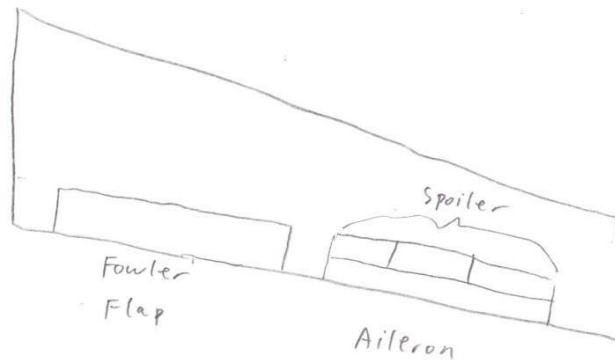
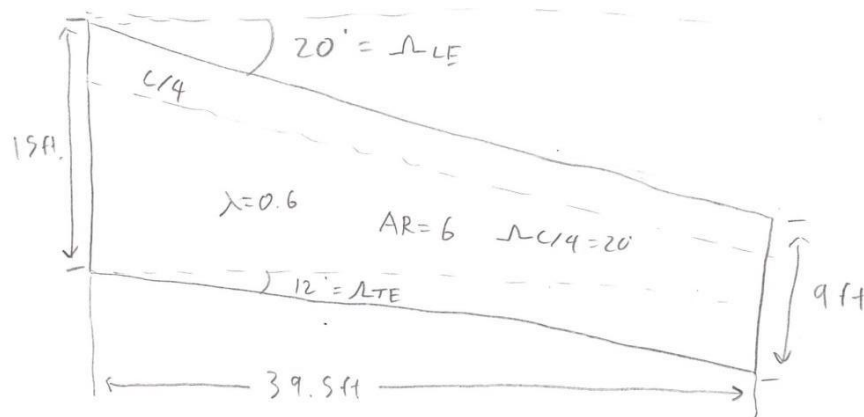


Figure 2.6e: Sketch of Main Wing

2.6.7. Discussion of Wing Design

The initial parameters in §2.6.1 was shown to be insufficient for the required C_L . The original wing area was too large for a fighter jet and the C_{Lmax} of 2.0 was higher than necessary. By using the matching graph from the performance constraint, another matching point was chosen to lower the wing area to 1040 ft² and lower the C_{Lmax} to 1.5. In §2.6.1.1, the wing sweep of 60 degrees was chosen from Figure 2.6a. Using AAA, this wing sweep was too high and not sufficient to sustain the required C_{Lmax} of 1.5. Thus the taper ratio was increased to 0.6 from 0.45 and the wing sweep changed to 20 degrees.

When designing the high-lift devices, it was observed that the landing C_{LmaxL} was the critical factor and thus a Sw/S ratio of 1.0 and flap angle of 40 degrees was chosen. Using Roskam's data for lateral control services for fighter aircrafts, the parameters for the tails of the FAFCAS were chosen. The areas of the wing and the control surfaces are larger than most of the other

contemporary fighter aircrafts. Due to the C_{Lmax} requirements in takeoff and landing, Fowler flaps and spoilers were chosen as Fowler Flaps doesn't interrupt the top surface of the wing.

2.7. Empennage Design

The next part of the FAFCAS that will be designed is the longitudinal and directional empennage. The horizontal and vertical stabilizers at the tail stabilize the aircraft and also act as the control surfaces. With the main wing designed, the initial parameters to design the empennage can be derived. Various other fighter aircrafts will be analyzed to create a starting point for the design.

2.7.1. Overall Empennage Design

In Roskam Part II Chapter 8, the author provides a step by step process in designing the empennages which is used to design the empennage. From the wing design geometry in §2.6 and using a database of contemporary fighter aircraft empennage sizes found in Roskam Part II Chapter 8, the first estimate of the FAFCAS empennage geometry are as follows:

- Conventional Configuration
- $S_{\square} = 82 \text{ ft}^2$ (1 Horizontal Stabilizer)
- $S_v = 73 \text{ ft}^2$ (1 Vertical Stabilizer)
- $x_{\square} = 407 \text{ in.}$
- $x_v = 407 \text{ in.}$

Roskam's vertical and horizontal tail database for various fighters can be found in Appendix 2G.

2.7.2. Design of the Horizontal Stabilizer

In Table 2.12, the parameters for the FAFCAS horizontal stabilizer design will be listed. These parameters are determined by observing geometries of other fighter aircrafts provided by Roskam Part II Chapter 8.

Table 2.12: FAFCAS Horizontal Stabilizer Parameters

Aspect Ratio	4
Taper Ratio	0.5
Sweep Angle	20 deg
Thickness Ratio	.1
Airfoil	NACA 6716/6713
Incidence Angle	0
Dihedral Angle	0 deg

A dihedral angle of 0 degrees was chosen as it will be a conventional configuration and with no requirement to contribute to the vertical stability. Two vertical stabilizers will be sufficient for

the vertical stability. A NACA 6716/6713 airfoil used by the A-10 is chosen for the horizontal stabilizer as the A-10 share a similar horizontal tail area and they will also be flying under the same conditions. The sweep angle, aspect ratio, and taper ratio are within the ranges of planform design parameters of fighter aircrafts as listed in the database by Roskam Part II.

For a conventional configuration, volume coefficients are used to make an initial estimate of the tail size. The definition of the volume coefficients by Roskam can be seen in Figure 2.7a. The volume coefficients are used to calculate the tail areas by the following equations from Roskam Part II:

$$\begin{aligned} S_h &= \bar{v}_h \bar{S} \bar{c} / x_h \\ S_v &= \bar{v}_v S b / x_v \end{aligned} \tag{2.7.1}$$

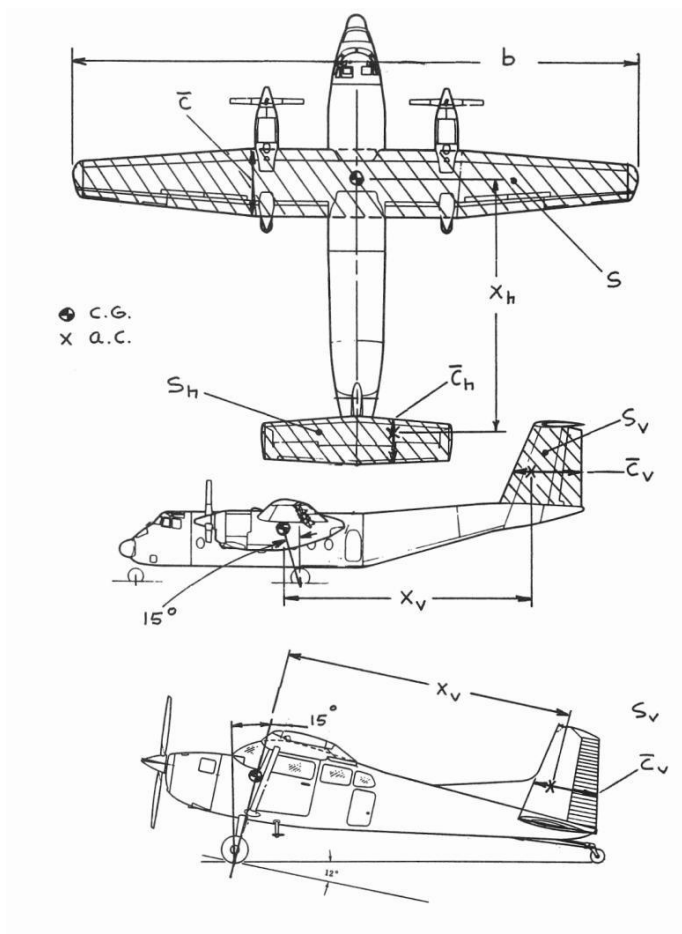


Figure 2.7a: Volume Coefficient Definitions

In Table 2.13 the FAFCAS's horizontal stabilizer volume coefficients and control surface size data will be compared to other contemporary fighter aircraft.

Table 2.13: Horizontal Tail Volume Comparison

	V _h	Se/Sh
FAFCAS	0.41	1
A-10	0.41	0.32
A6A	0.46	1
F-16	0.3	1
F-15	0.2	1

As can be seen in the airplane comparison in Table 2.13, higher speed multirole aircraft such as the F-16 and F-15 have smaller volume coefficients as compared to slower attack aircrafts such as the A-10 and A6A. As the FAFCAS will be flying in low speeds, a V_{\square} of 0.41 will be chosen. In the A6A, F-15, and F-16 the whole tail acts as the elevator while the A-10 has only part of the tail area act as the elevator. The FAFCAS will have split horizontal stabilizers like the F-15 and F-16 and thus will have a Se/Sh of 1.0.

2.7.3. Design of the Vertical Stabilizer

In Table 2.14, the parameters for the FAFCAS vertical stabilizer design will be listed. These parameters are determined by observing geometries of other fighter aircrafts provided by Appendix 2G.

Table 2.14: FAFCAS Vertical Stabilizer Parameters

Aspect Ratio	1
Taper Ratio	0.4
Sweep Angle	25 deg
Thickness Ratio	.135
Airfoil	NACA 6716/6713
Incidence Angle	0 deg
Dihedral Angle	80 deg

The aspect ratio, taper ratio, incidence angle, and sweep angle chosen are within the ranges of fighter aircraft planform design parameters for vertical tails. A dihedral angle of 80 degrees is chosen to cant the vertical stabilizers. Canting the vertical stabilizers reduces the radar cross section and also allows it to contribute to the vertical and horizontal control of the aircraft as the aerodynamic forces acting on it will be split. Two vertical stabilizers are also used so the stabilizers avoid the expansion wave of the behind the wing as the plane flies near supersonic. The vertical stabilizers are also swept back for aesthetic reasons.

In Table 2.15 the FAFCAS's vertical stabilizer volume coefficients and control surface size data will be compared to other contemporary fighter aircraft.

Table 2.15: Vertical Tail Volume Comparison

	V_v	S_r/S_v
FAFCAS	.06	0.2
A-10	.06	0.28
A6A	.069	0.21
F-16	.094	0.25
F-15	.098	0.25

As can be seen in Table 2.15, higher speed multirole fighter aircrafts have higher V_v than lower speed attack aircrafts. Due to the FAFCAS will be operating in low speeds while flying close air support, a V_v of 0.06 will be chosen. The rudder area (S_r) to vertical tail area ratio of 0.25 will be chosen for the FAFCAS. This is chosen by taking the average of the S_r/S_v values of the high speed and low speed attack aircrafts.

2.7.4. Empennage Design Evaluation

With the initial empennage parameters determined, the vertical and horizontal designs are evaluated on the AAA program. Figure 2.7b and Figure 2.7c lists the parameters of the horizontal parameters and its lift coefficient. Figure 2.7d and 2.7e lists the parameters and lift coefficient of the vertical tail.

Figure 2.7b: AAA Horizontal Tail Input Parameters with Root and Tip C_{lmax}

Figure 2.7c: AAA Horizontal Tail Clmax Clean

In Figure 2.7b it is shown that a horizontal root chord length of 7.4 ft and a horizontal tip chord length of 3.7 ft were chosen for a taper ratio of 0.5. The resulting C_{Lmax} at the root is 1.73 and at the tip 1.79. In Figure 2.7c, the horizontal tail parameters are inputted into AAA and with a sweep angle of 20 degrees, the resulting C_{Lmax} for the horizontal tail is 1.55.

Input Parameters									
Altitude	40000 ft	V_{S_clean}	480.00 kts	c_{t_v}	2.80 ft	$(t/c)_t$	13.5 %	Tip Airfoil	NACA 4 & 5 Digit Cambered
ΔT	0.0 deg F	c_{r_v}	7.00 ft	$(t/c)_{r_v}$	13.5 %	Root Airfoil	NACA 4 & 5 Digit Cambered		
Output Parameters									
Re_{r_v}	11.2148 x 10 ⁶	$C_{l_max_rv}$	1.808	Re_{t_v}	4.4859 x 10 ⁶	$C_{l_max_tv}$	1.676		

Figure 2.7d: AAA Vertical Tail Input Parameters with Root and Tip Clmax

Input Parameters													
$C_{l_max_rv}$	1.808	$C_{l_max_tv}$	1.676	c_{r_v}	7.00 ft	c_{t_v}	2.80 ft	Root Airfoil	NACA 4 & 5 Digit Cambered	Tip Airfoil	NACA 4 & 5 Digit Cambered	Λ_v^4	25.0 deg
Output Parameters													
l_v	0.40	k_v	0.950	$C_{l_max_clean}$	1.500								

Figure 2.7e: AAA Vertical Tail Clmax Clean

Two vertical tails are used in this design. In Figure 2.7d, it is shown that a vertical root chord length of 7 ft and a vertical tip chord length of 2.8 ft were chosen for a taper ratio of 0.4. The resulting C_{Lmax} at the root is 1.81 and at the tip 1.68. In Figure 2.7e, the vertical tail parameters are inputted into AAA and with a sweep angle of 25 degrees, the resulting C_{Lmax} for the vertical tail is 1.5.

2.7.5. Design of the Longitudinal and Directional Controls

In Table 2.14 and Table 2.15, the control surface to empennage area surface areas was chosen for the FAFCAS. In Table 2.14, S_e/S_h was chosen to be 1. This would mean the whole horizontal tail acts as the elevator. Thus the whole tail will need to rotate when the aircraft is

pitching up or down. In Table 2.15, S_r/S_v was chosen to be 0.2. This would mean the rudder area would be 20% of the vertical tail area.

Using these ratios and the tail areas, the areas of the control surfaces are calculated to be:

- Elevator Area (S_e)= 82 ft²
- Rudder Area (S_r)= 14.6 ft²

2.7.6. Empennage Drawings

The empennage dimensions and a sketch of the empennages can be seen in Figure 2.7f. With the empennage and wing dimensions calculated, the model of the FAFCAS can be updated. The updated model can be seen in Figure 2.7g.

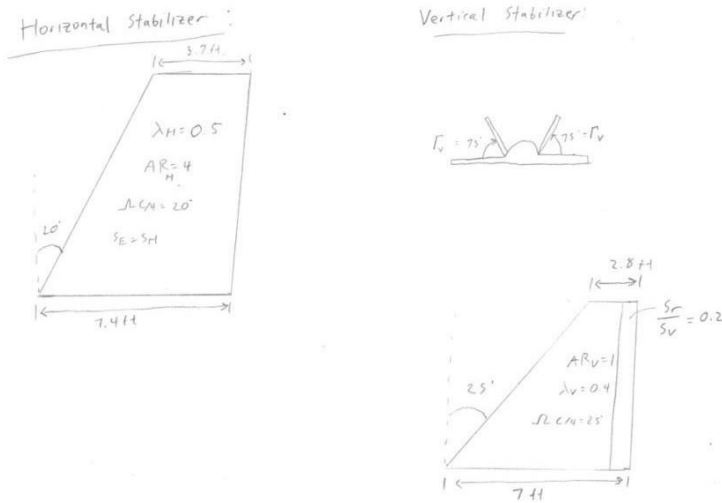


Figure 2.7f: Empennage Dimensions and Drawing



Figure 2.7g: CAD Drawing of Fuselage, Wing, and Empennage.

2.7.6. Discussion of Empennage Design

In §2.7.1 the empennage configuration was chosen to be two vertical stabilizers and two horizontal stabilizers. In the military aircraft certification MIL-C-005011B and MIL-STD-3013A it is recommended that fighter aircraft have two vertical stabilizers to reduce the required empennage area and also as precaution in case one gets damaged. This will be likely as this aircraft will be flying at low altitude to provide close air support. The horizontal stabilizers will also be split into two as the tail section will interrupt the geometry of the empennages. The location of X_h and X_v were determined by locating the aerodynamic center of the main wing that was solved for in the §2.6. These two positions help determine where to place the stabilizers in the FAFCAS. The horizontal and vertical empennages dimensions were determined by using Appendix 2G. Each of the fighter aircraft had a volume coefficient and a control surface/wing area ratio. Fighter aircrafts tabulated by Roskam have different mission focus such as air superiority, close air support, attack, or multirole. Thus volume coefficients and control surface area ratios were chosen that were close to attack aircraft like the A-10. The only exception is the area of the elevator which was chosen more in line with typical multirole and air superiority fighters. The FAFCAS has the whole horizontal stabilizer act as the elevator for a more sensitive pitch control as during close air support missions the aircraft will be constantly lowering and raising its altitude. During the empennage evaluation in AAA, it was observed that the calculated Cl_{max} for the root and tip can be raised by using different airfoils.

2.8. Landing Gear Design and Weight Balance

The FAFCAS currently has the fuselage, wing, and the empennages designed. The next component that will be developed is the landing gear. The landing gear is an important component and has to be carefully designed during the design process. It needs to be able to

support the weight of the aircraft while landing and taking off without buckling. The length, position, and number of landing gears are important design points that will have to be determined. Once all the components are designed, each components weight has to be determined and their center of gravity located to balance the aircraft.

2.8.1. Estimation for the Center of Gravity Location for the FAFCAS

This initial analysis of the FAFCAS center of gravity will be before the landing gear is designed. Once the landing gear is designed, another center of gravity analysis will be conducted. Roskam Part V provides a step by step process in component weight estimation, which will be used in the weight balance. Four different fighter aircraft will be compared and their component weights tabulated. The component weights will be averaged and the averaged component weight to gross weight ratio will be used to determine the FAFCAS component weights. The results are listed in Table 2.16.

Table 2.16: Component Weight to Gross Weight Ratios of Four Different Fighter Aircraft and the FAFCAS

Aircraft	A2F (A6)	F105B	F/A-18A	AV-8B	FAFCAS
Pwr Plt/Gw	.162	.246	.194	.219	.205
Fix Eqp/Gw	.159	.155	.158	.12	.148
We/Gw	.651	.797	.71	.557	.679
Wing Grp/Gw	.136	.109	.117	.063	.106
Emp Grp/Gw	.024	.031	.029	.016	.025
Fus Grp/Gw	.102	.187	.145	.090	.131
Eng Sect/Gw	.002	.003	.004	.006	.00375
Landing Gear/Gw	.067	.059	.062	.044	.058
Engine(s)/Gw	.115	.197	.133	.166	.153
Nult/Gw	n/a	13	11.25	10.5	11.58
Gw/Wto	1	.92	.623	.771	.829

These four aircrafts were chosen due to their engines are located in the fuselage, share similar mission requirements in that they can act as close air support, and similar wing shape as the FAFCAS. We/Gw average value in Table 2.16 is 0.679 while using the mission weights in §2.1 the We/Gw was 0.592. The difference is due to older fighter aircrafts are used in this analysis to get the average such as the F105B.

Using the ratios in Table 2.16, the initial component weights can be determined. The results will be tabulated in Table 2.17.

Table 2.17: Component Weight of Initial and Class I FAFCAS

	Initial Estimate	FAFCAS Class I Weight (w/adjustments)

Power Plant (lbs)	16415	
Fix Equipment (lbs)	11850	
Wing (lbs)	8488	10000
Empennage (lbs)	2002	3600
Fuselage (lbs)	10490	11600
Engine Section 1 (lbs)	300	300
Landing Gear (lbs)	4644	5000
Engine Section 2 (lbs)		4164
Engine (lbs)	12251	Actual: 2886
Ammo (lbs)	2000	
Fix Equipment- Ammo (lbs)	9850	
GAU-8 Actual Weight (lbs)		2014
Fix Equipment-Gun (lbs)		7836
Empty Weight (lbs)	54189	47400

The initial empty weight from the weight ratios was 54,189 lbs. This was more than the desired 47,400 lbs empty weight. By changing the estimated engine weight to the actual engine weight of 2886 lbs, this reduced the empty weight significantly below the desired empty weight. With this extra allotment of weight, the weight of the wing, empennage, fuselage and the landing gear was increased from the initial to simulate extra armor being applied. Table 2.18 lists the component weights that will be used for weight and balance analysis of the FAFCAS.

Table 2.18: FAFCAS Component Weight and Mission Weights

Wing (lbs)	10000
Empennage (lbs)	3600
Fuselage (lbs)	11600
Engine Section 1 (lbs)	300
Landing Gear (lbs)	5000
Engine Section 2 (lbs)	4164
Engine (lbs)	2886
GAU-8 Gun Actual Weight (lbs)	2014
Fix Equipment-Gun (lbs)	7836
Empty Weight (lbs)	47400
Pilot (lbs)	250
Payload (lbs)	26000
Fuel (lbs)	23000
Takeoff Gross Weight (lbs)	96650

The center of gravity of each component is listed on Table 2.19. The reference plane was recommended by Roskam as left and below the aircraft as possible to avoid negative signs on the numbers. Thus the reference point was placed 100inches under the middle of the fuselage with

the length axis starting at the gun barrel tip. The reference plane and center of gravity for each component can be seen in Appendix 2H.

Table 2.19: FAFCAS Component Weight and Coordinate Data

Component	Weight (lbs)	X (in.)	Wx (in.lbs)	Y (in.)	Wy (in.lbs)	Z(in.)	Wz (in.lbs)
Wing	10000	292	2920000	0	0	100	1000000
Horizontal Stab.	1910	622	1188020	0	0	100	191000
Vertical Stab.	1690	609	1029210	0	0	140	236600
Fuselage	11600	378	4384800	0	0	100	1160000
GAU-8	2014	48	96672	0	0	76	153064
WE	47400	203	9622200	0	0	58	2749200
Pilot	250	190	47500	0	0	108	27000
WE+Pilot	47650	203	9666200	0	0	58	2767664
Fuel	23000	292	6716000	0	0	100	2300000
WE+Fuel+Pilot	70650	232	16382202	0	0	72	5067664
Ammo	2000	247	494000	0	0	100	200000
Bombs	24000	292	7008000	0	0	100	2400000
WTO	96650	347	33506400	0	0	108	10416860

2.8.2. Landing Gear Design

As the FAFCAS will be flying at high speeds during cruise, a retractable landing gear will be chosen. A conventional tricycle configuration will be chosen for the landing gears. The nose landing gear will retract into the nose of the plane under the pilot and the main landing gears will be placed aft of the center of gravity and retract into the fuselage. Table 2.20 lists the dimensions of the main and nose gear wheels. Table 2.21 lists the dimensions of the main and nose gear struts. When designing the landing gears, the aircraft has to meet two geometric criteria. The two criteria are the tip over criteria and the ground clearance criteria. In Roskam Part II Chapter 9 for tricycle landing gears, the author states the main landing gear must be behind the most aft c.g. with a 15 degree angle relation between the two points to meet the tip over criteria. In Roskam Part II, the author visualizes this which can be seen in Figure 2.8a. To meet the ground clearance criteria, the angle between the ground and the lowest part of the main wing must be at least 5 degrees. Roskam’s visualization of this can be seen in Figure 2.8b.

Table 2.20: Dimensions of Wheels

Landing Gear	Nose Landing Gear	Main Landing Gear
Number of Wheels	2	1
Diameter (in.)	20	42
Width (in.)	6.5	13

Pressure	120 PSI	150 PSI
----------	---------	---------

Table 2.21: Dimension of Landing Gear Struts

Strut	Nose Landing Gear Strut	Main Landing Gear Strut
Length (in.)	42	31
Width (in.)	5	8

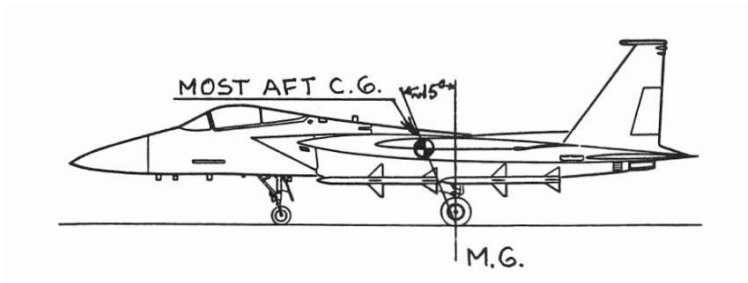


Figure 2.8a: Roskam Definition of Tip Over Criteria

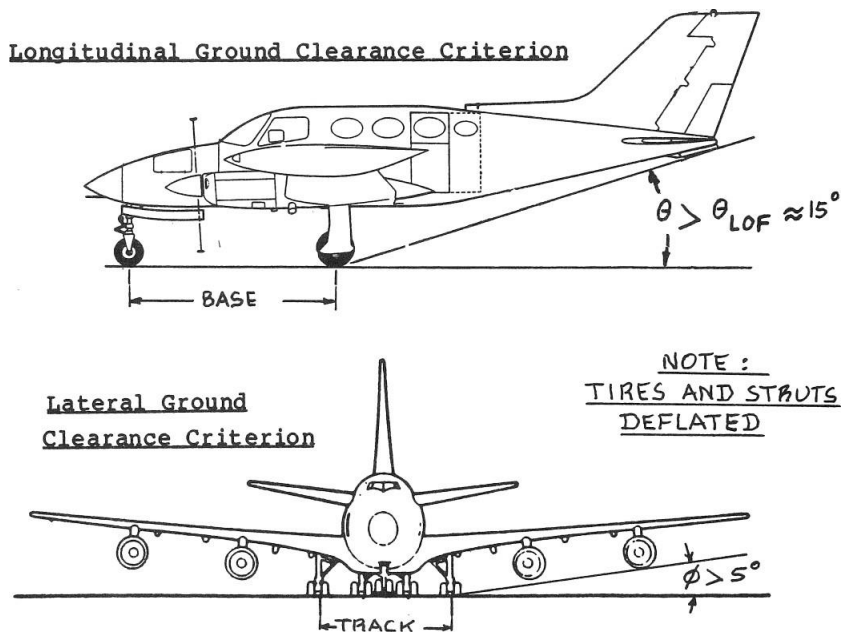


Figure 2.8b: Roskam Definition of Ground Clearance Criteria

Preliminary Landing Gear Arrangement:

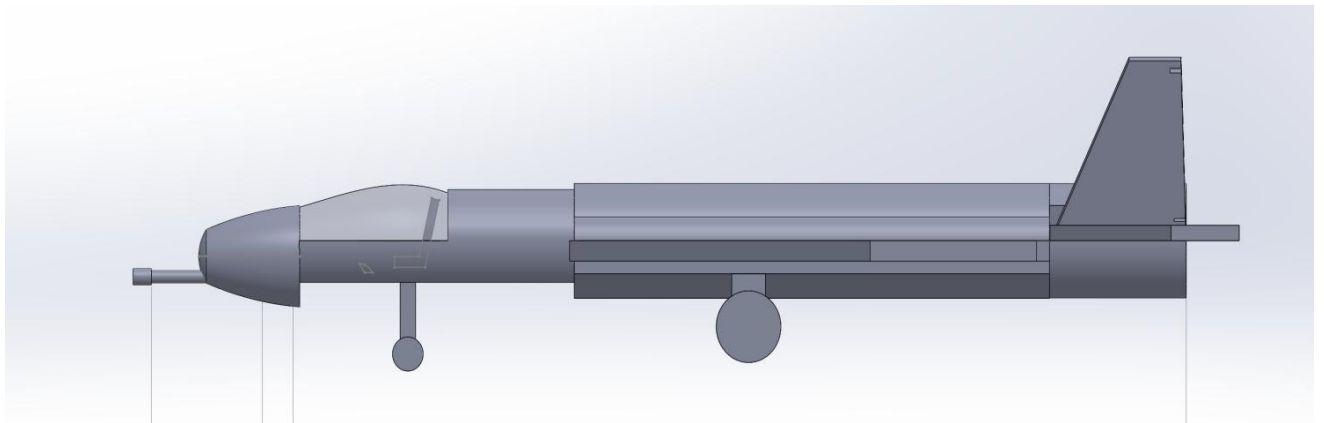
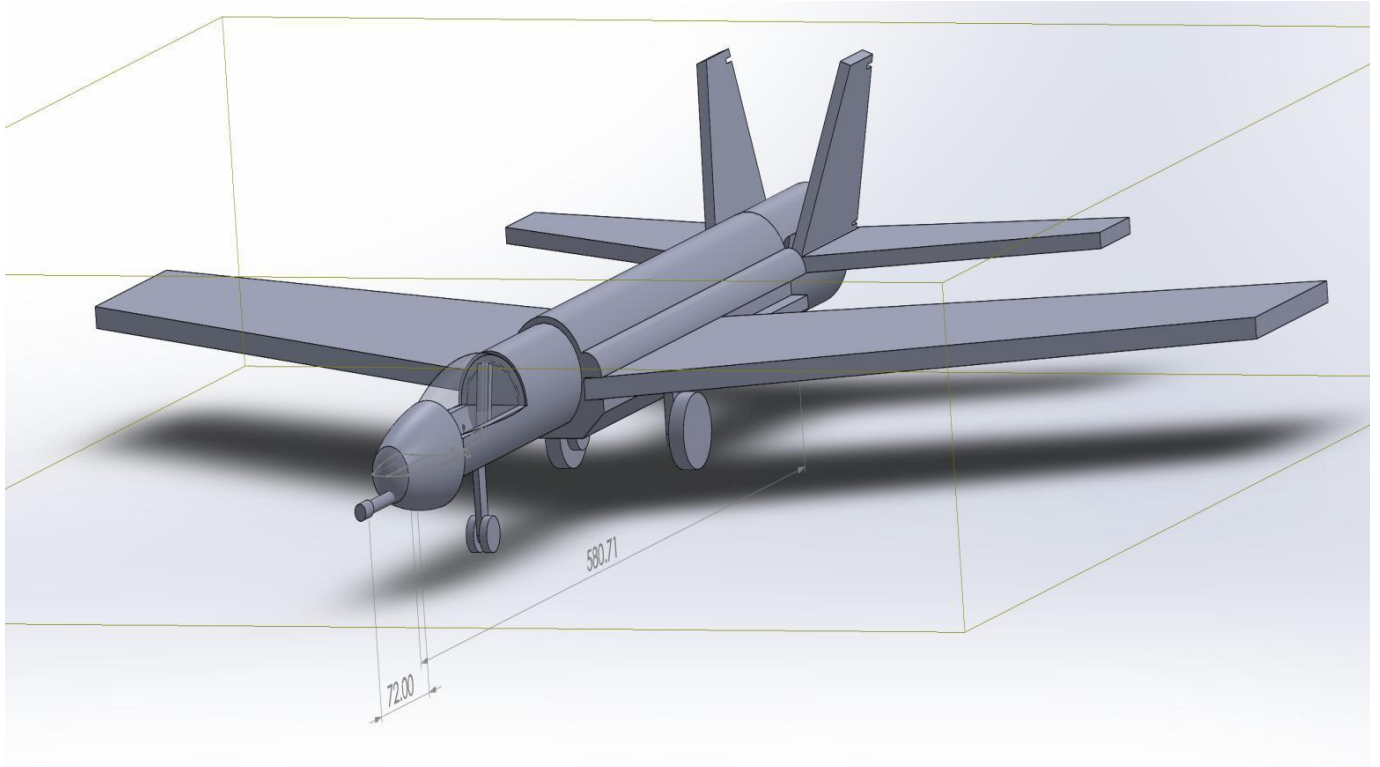


Figure 2.8c: Landing Gears Deployed

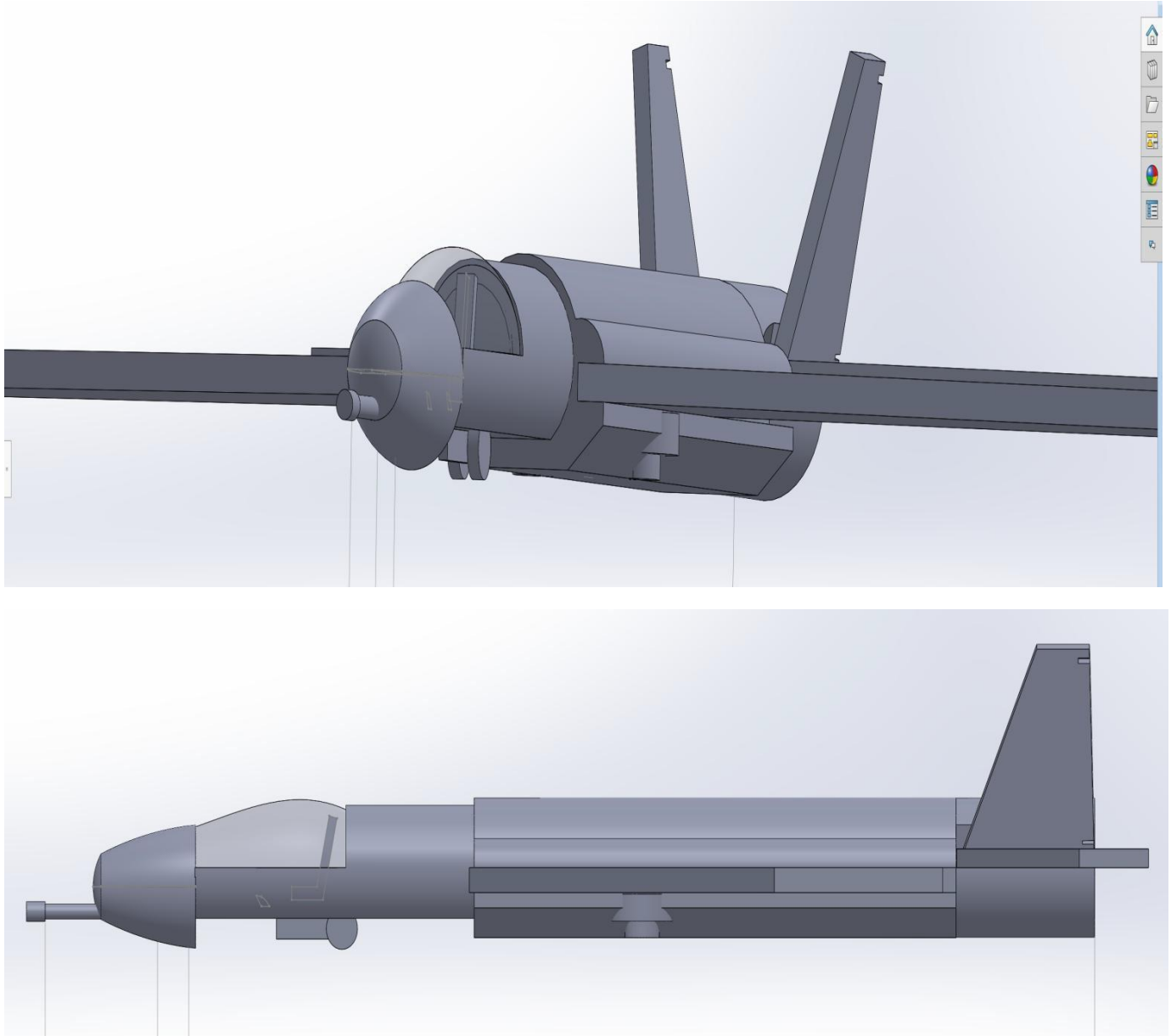


Figure 2.8d: Landing Gears Retracted

For tricycle landing gear configuration, the most aft center of gravity and the main landing gear has a relation of 15 degrees. From Table 2.19, the most aft center of gravity is $x=347$ inches. To fulfill the 15 degrees tip over criteria with a main landing gear strut length of 31 inches and a wheel diameter of 42 inches, the main landing gear was placed at $x=367$ inches.

Ground Clearance:

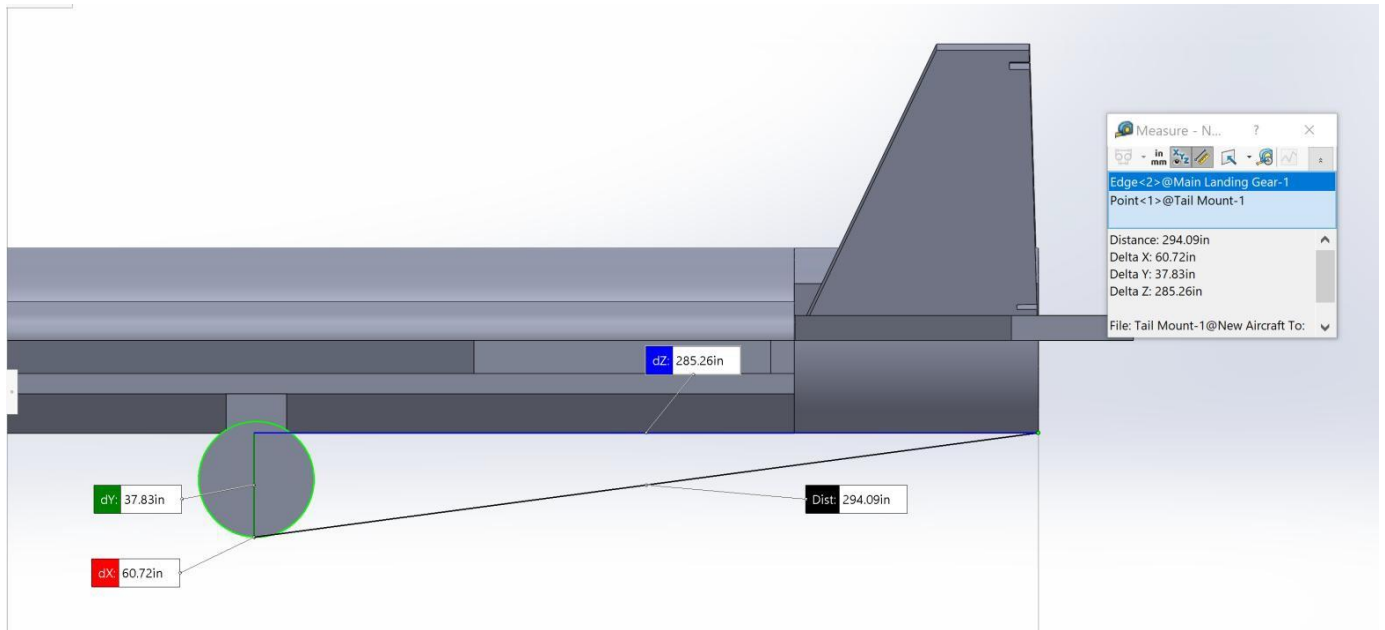


Figure 2.8e: Longitudinal Ground Clearance Criterion

From Figure 2.8e, the angle for the longitudinal ground clearance criterion is around 8 degrees, which is less than the recommended 15 degrees. The struts will need to be made longer or the back of the fuselage will need to be tapered off.

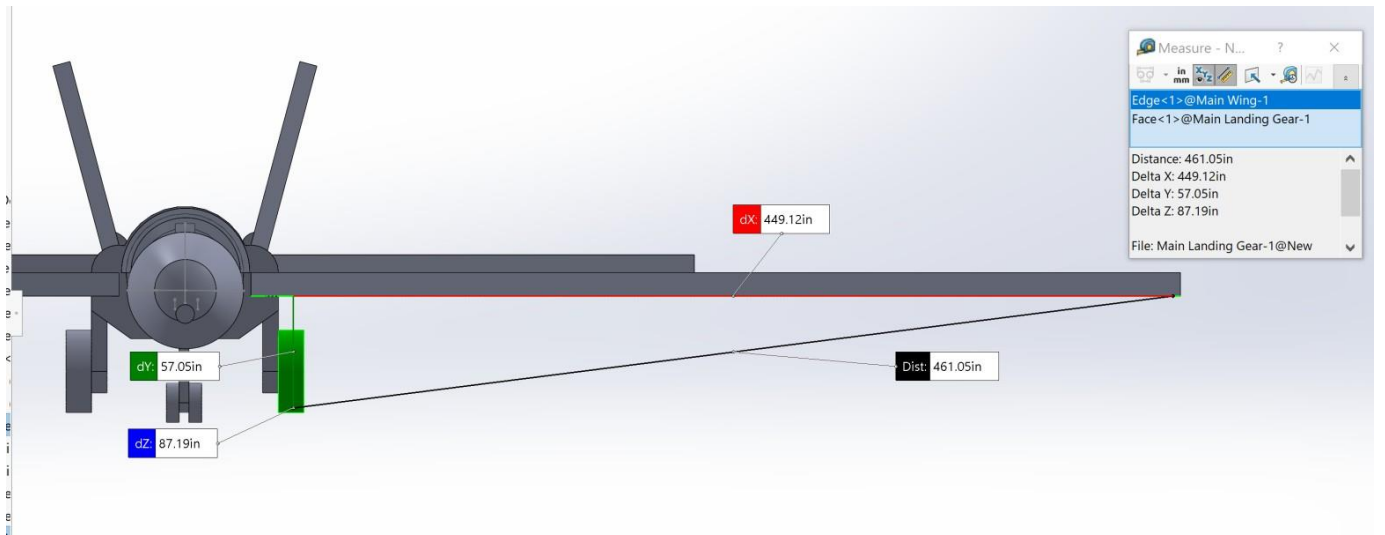


Figure 2.8f: Lateral Ground Clearance Criterion

From Figure 2.8f, the angle for the lateral ground clearance criterion is around 13 degrees, which is more than the 5 degrees recommended by Roskam. Thus this meets the lateral ground clearance criterion.

Maximum Static Load per Strut:

From Figure 2.8c and satisfying the tip-over criteria, the strut distances to center of gravity are:

- $L_m = 20$ inches
- $L_n = 157$ inches
- $N_s = 2$
- $W_{to} = 96650$ lbs.

The resulting gear loads are:

- $P_n = 10,921$ lbs
- $P_m = 42865$ lbs
- $P_n/W_{to} = 0.11$
- $2P_m/W_{to} = 0.89$

From Roskam’s landing wheel data in Part II Chapter 9, the wheel dimensions are acceptable with these gear load ratios.

2.8.3. Updated Estimation of the Center of Gravity Location for the FAFCAS

With the landing gears designed, the component weight and center of gravity tables can be updated.

Table 2.22: FAFCAS Component Weight and Mission Weights

Wing (lbs)	10000
Empennage (lbs)	3600
Fuselage (lbs)	11600
Engine Section 1 (lbs)	300
Landing Gear (lbs)	5000
Engine Section 2 (lbs)	4164
Engine (lbs)	2886
GAU-8 Gun Actual Weight (lbs)	2014
Fix Equipment-Gun (lbs)	7836
Empty Weight (lbs)	47400
Pilot (lbs)	250
Payload (lbs)	26000
Fuel (lbs)	23000
Takeoff Gross Weight (lbs)	96650

With the main landing gear attached, the center of gravity was moved too far away to meet the tip over criterion. When L_m was changed to $X = 280$ inches from 367 in. the tip over criterion is met. Table 2.23 lists the new center of gravity and weights of the components.

Table 2.23: Updated FAFCAS Component Weight and Coordinate Data

Component	Weight (lbs)	X (in.)	Wx (in.lbs)	Y (in.)	Wy (in.lbs)	Z(in.)	Wz (in.)
Wing	10000	292	2920000	0	0	100	1000000
Horizontal Stab.	1910	622	1188020	0	0	100	191000
Vertical Stab.	1690	609	1029210	0	0	140	236600
Fuselage	11600	378	4384800	0	0	100	1160000
GAU-8	2014	48	96672	0	0	76	153064
N.G.	550	190	104500	0	0	24	13200
M.G.	4450	280	1246000	0	0	24	106800
WE	47400	231	10969202	0	0	60	2860664
Pilot	250	190	47500	0	0	108	27000
WE+Pilot	47650	231	11016702	0	0	61	2887664
Fuel	23000	292	6716000	0	0	100	2300000
WE+Fuel+Pilot	70650	251	17732702	0	0	73	5187664
Ammo	2000	247	494000	0	0	100	200000
Bombs	24000	292	7008000	0	0	100	2400000
WTO	96650	261	25234702	0	0	81	7787664

2.8.4. CG Locations for Various Loading Scenarios

The updated centers of gravity of the FAFCAS for different configurations are listed in Table 2.24. The weight c.g. excursion diagram can be seen in Figure 2.8g.

Table 2.24: C.G. for Different Configurations

	X(in.)	Y(in.)	Z(in.)
WE	231	0	60
WE+Pilot	231	0	61
WE+Fuel+Pilot	251	0	73
WTO	261	0	81

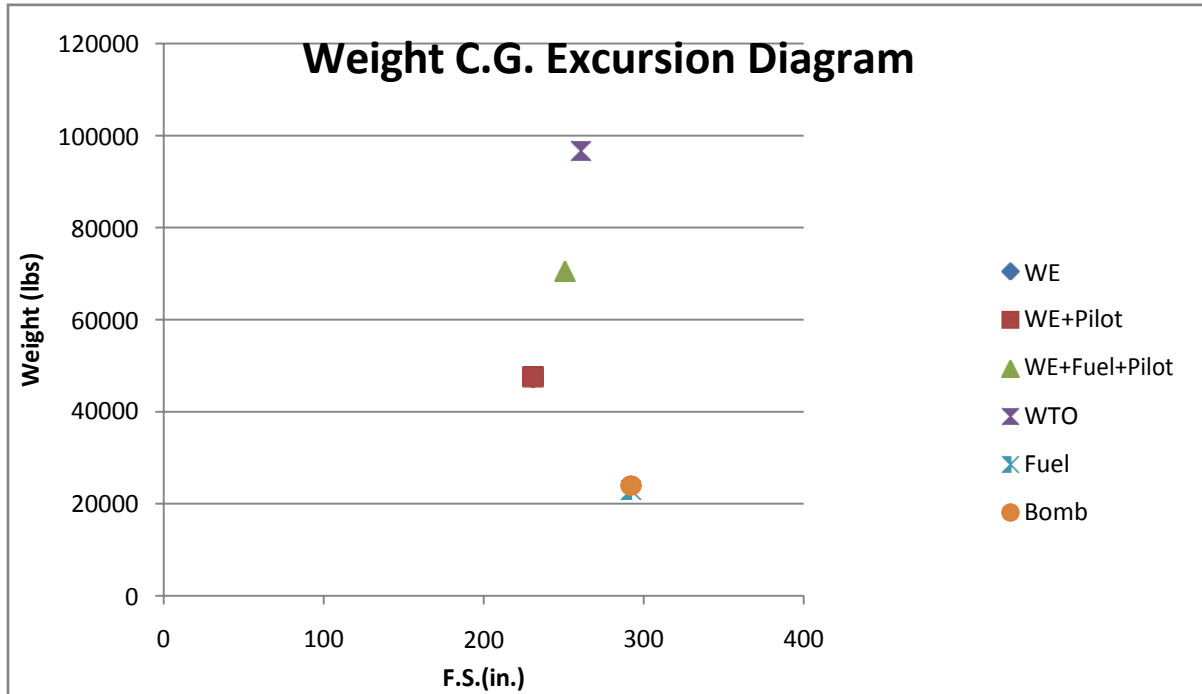


Figure 2.8g: C.G. Excursion Diagram

2.8.5. Discussion of Landing Gear Design and Weight Balance

The initial main landing gear position was too far away after the centers of gravity were designed. Thus they were moved to meet the tip over criterion. From Figure 2.8e, the angle for the longitudinal ground clearance criterion is around 8 degrees, which is less than the recommended 15 degrees. The struts will need to be made longer or the back of the fuselage will need to be tapered off. From the landing gear design, it can be seen the landing gears can be stowed away in the fuselage if doors and panels are attached. Although the data in table 2.23 states to place the landing gear at around 280 inches to meet 15% tip over criterion, in the model it looks to be too close to the front of the aircraft. Thus a middle ground will be chosen between the original X=367 and X=280 inches.

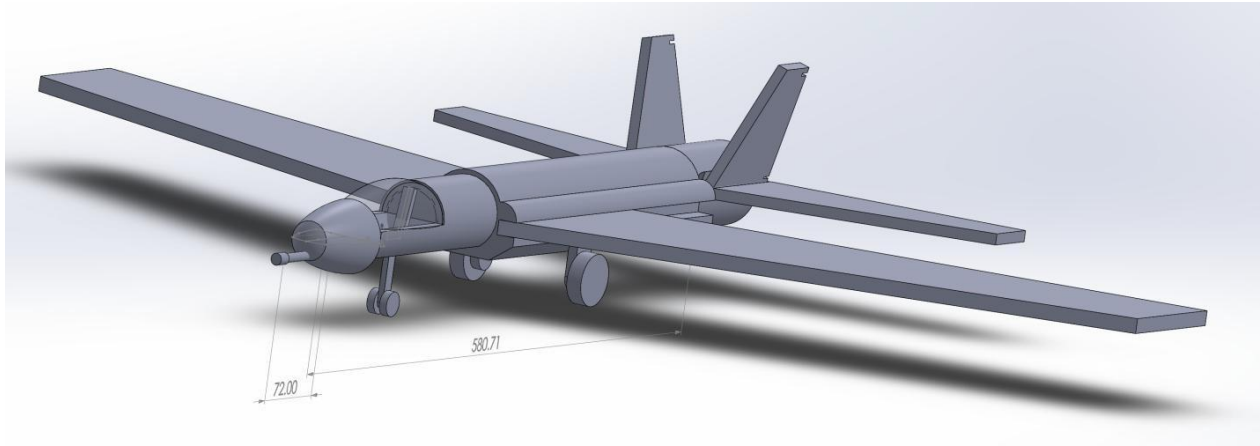


Figure 2.8h: Updated FAFCAS

2.9. Stability & Control Analysis/ Weight & Balance-Stability & Control Check

With the FAFCAS's fuselage, wing, empennage, and landing gear designed the proposed configuration must now be determined if it has satisfactory control and stability characteristics. Military aircraft design allows for some instability in order for the aircraft to have more maneuverability. The configuration will undergo a static longitudinal stability, static directional stability, and minimum control speed with one engine out analysis to determine if this design is controllable and stable.

2.9.1. Static Longitudinal Stability

In Roskam Part II Chapter 11, the author provides a step by step method to determine if the configuration has sufficient stability and control. Appendix 2I contains the process of verifying the FAFCAS stability and control. To determine the longitudinal stability, the horizontal stabilizer area will be varied to determine its effect on the aft center of gravity and aft aerodynamic center. The horizontal tail area is varied from 82 ft² to 200 ft². An empennage weight to area ratio of 4.875 psf was chosen based off of contemporary fighter aircraft data provided by Roskam. This ratio was used to determine the weight of the horizontal and vertical stabilizer which is then used to determine the aft center of gravity. The horizontal empennage was chosen to have 2.58 psf and vertical empennage to have 2.29 psf.

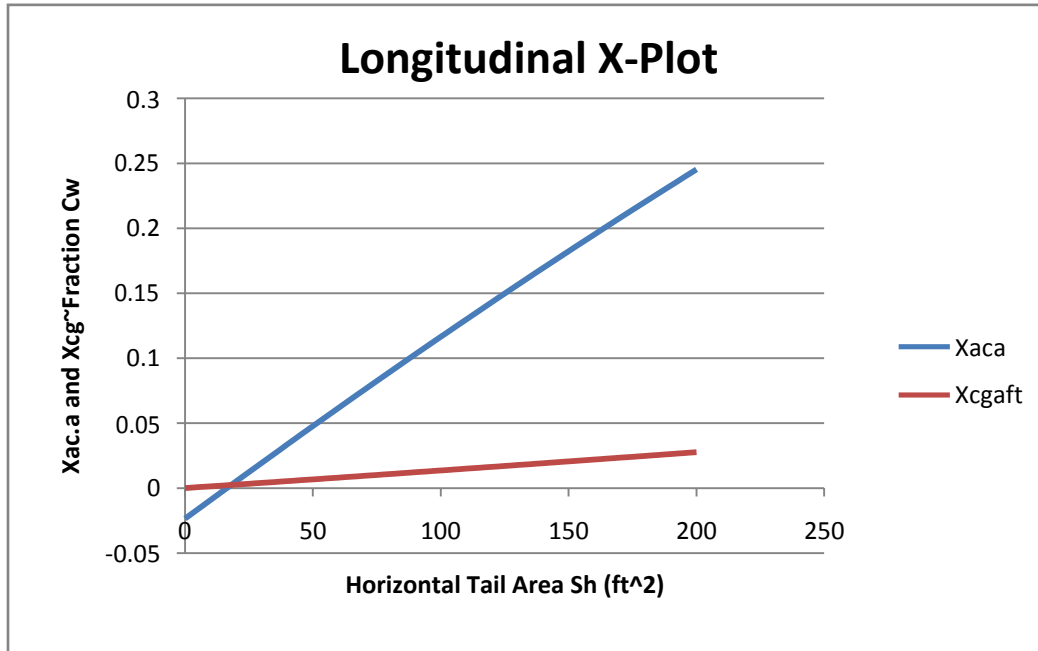


Figure 2.9a: FAFCAS Longitudinal X-Plot

In this design process, the aircraft has to be designed either as inherently stable or de-facto stable. Inherently stable is defined by Roskam as the aircraft not relying on a feedback augmentation system for stability. De-facto stability is defined as requiring feedback augmentation for stability. The FAFCAS design is chosen to be de-facto stable due to the need for maneuverability and the design can't have the plane be too stable. Following the design process leads to a longitudinal x-plot. Figure 2.9a lists the longitudinal x-plot of the FAFCAS. From Figure 2.1 a ΔSM of 0.053 will be chosen with a corresponding horizontal tail area of 100 ft². Cl_{α} of .07 and a $Cl_{\alpha h}$ of .065 are chosen. The total airplane lift curve slope, CL_{α} , was computed to be 0.074 deg⁻¹. The elevator control power derivative, $Cm_{\delta e}$, was computed to be -.0047 deg⁻¹. The resulting feedback gain K_{α} is 0.834. This is acceptable as it does not exceed 5 deg/deg. The horizontal tail area of 100ft² chosen from the X-plot is larger than the original tail area of 82ft².

2.9.2. Static Directional Stability

To determine the directional stability, the vertical stabilizer area will be varied and then directional stability plotted on a directional X-Plot. Figure 2.9b lists the directional stability X-Plot of the vertical stabilizer.

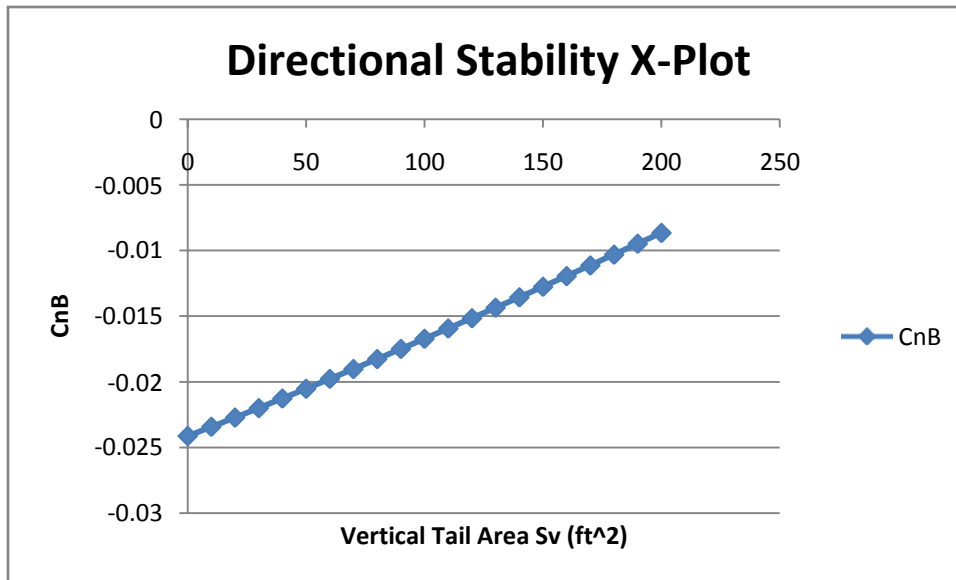


Figure 2.9b: FAFCAS Directional X-Plot

From Figure 2.9b, it can be seen that the FAFCAS is directionally unstable for vertical tail areas up to 200 ft². The desired Cn β level is 0.001. Thus the sideslip feedback system must compensate for this instability. The rudder control derivative of the FAFCAS, Cn δ_r , was computed for vertical tail areas up to 200 ft². The Cn δ_r was then used to calculate the required sideslip to rudder feedback gain, k β . At a vertical tail area of 190 ft², the calculated Cn δ_r is -0.00228 deg⁻¹ and the resulting k β is 4.6 deg/deg. This is less than 5 deg/deg and thus acceptable.

2.9.3. Minimum Control Speed with One Engine Inoperative

The takeoff thrust of the FAFCAS calculated in the performance constraint was determined to be 29,000 lbs. The lateral thrust moment arm, Y_t , was determined to be 6.185 ft as can be seen in Figure 2.9c. The resulting critical engine-out yawing moment, N_{crit} , is around 179,400 lbs*ft. The FAFCAS will use two Pratt & Whitney F100-PW-220 engines, which are low bypass ratio engines. The drag induced yawing moment due to the inoperative engine, N_D , is 33,870 lb*ft. The maximum allowable speed with one engine inoperative is 120 knots. The resulting rudder deflection required to hold the engine out condition, δ_r , with a vertical tail area of 190 ft² is 22.6 degrees. This is an acceptable amount of rudder deflection.

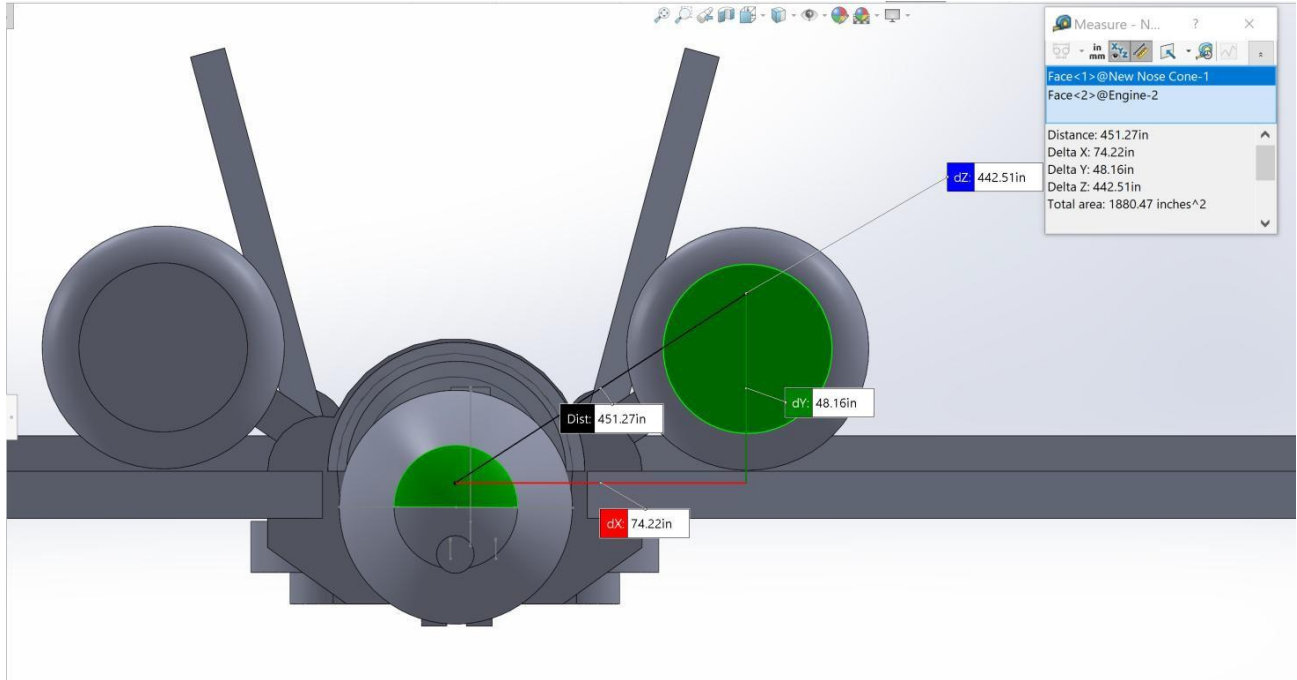


Figure 2.9c: Lateral Thrust Moment Arm, Y_t , of the FAFCAS.

2.9.4. Discussion of Stability and Control Analysis

The vertical tail area was originally 73ft^2 . This was determined from the static directional stability analysis to be inadequate to control the FAFCAS. The vertical tail area was thus increased to 190ft^2 . The original horizontal tail area was 82ft^2 but this was also not large enough to give longitudinal stability to the FAFCAS and was thus increased to 100ft^2 . With these two new empennage areas the new takeoff weight is 93,740 lbs with a center of gravity at $X=250$ inches. The original FAFCAS takeoff weight was 96,650 lbs with the center of gravity at $X=261$ inches. The takeoff weight has decreased due to the original calculation of the empennage weight did not account for there being two vertical and horizontal stabilizers. The center of gravity has also moved forward 11 inches. As this is not a significant change in the center of gravity, the landing gear will remain the same. In Figure 2.9c, the engines are placed in such a position as any further out and the moment arm will be too large and the rudder deflection required will be too large if one engine were to be inoperable.

The changes in the empennage sizes show the significance of the longitudinal and directional stability analysis. The resized empennages led to a new center of gravity position and a different takeoff weight. The stability analysis also determined that the vertical stabilizer will need to have a larger rudder deflection in order to keep the FAFCAS operational with one engine out. The engines being placed on top and aft of the fuselage was determined back in the mission requirement as this was the safest place to place the engines during close air support missions. But due to this the canted vertical stabilizers are between the engines. The flow of the engines might disturb the flow of air passing through the vertical stabilizers.

2.10. Drag Polar Estimation

An airplane's drag is composed of multiple types of drag combined together. There are zero lift drag, low speed drag, compressibility drag, and also drag from different equipment sticking out of the aircraft. A preliminary drag polar will be computed by using the wetted area of the FAFCAS and then compared to the drag polar determined back in the performance constraint analysis.

2.10.1. Airplane Zero Lift Drag

To determine the wetted area of the FAFCAS, the airplane is broken up into segments. The segments are the fuselage, wings, empennage, and nacelles. The calculation of the wetted area can be seen in Appendix 2J. The wetted area of each segment and the total wetted are listed in Table 2.25.

Table 2.25: Wetted Area of FAFCAS

Wing Swet,planform	2*974 ft ²
Horizontal Empennage Swet,planform	2*205 ft ²
Vertical Empennage Swet,planform	2*393 ft ²
Fuselage Swet	812 ft ²
Fan Cowl Swet	2*133 ft ²
Gas Gen. Swet	2*31 ft ²
Total Wetted Area	4284 ft ²

From Roskam's expected equivalent parasite drag, f , chart for wetted area in Part I, with a wetted area of 4284 ft² the expected f will be 15 ft².

The resulting C_{Do} using a wing area of 1040 ft² is 0.0144.

2.10.2. Low Speed Drag Increments

The drag contributions from the flaps and landing gears during takeoff and landing have to be considered for the total drag. See Appendix 2J for the low speed drag increments calculation. Table 2.26 lists the drag increase due to the flaps and landing gear plus the flaps efficiency factor. Table 2.27 lists the drag for different configurations at low speeds.

Table 2.26: Flaps and Landing Gear Drag Contribution

Component	ΔC_{Do}	e
Clean	0	0.8
Takeoff Flaps	0.02	0.75
Landing Flaps	0.075	0.7
Landing Gear	0.025	n/a

Table 2.27: Drag under Different Low Speed Configurations

Clean	$C_D=0.0144+0.066*C_L^2$
Takeoff w/ Landing Gear Up	$C_D=0.0344+0.0707*C_L^2$
Takeoff w/ Landing Gear Down	$C_D=0.0594+0.0707*C_L^2$
Landing w/ Landing Gear Up	$C_D=0.0894+0.0758*C_L^2$
Landing w/ Landing Gear Down	$C_D=0.114+0.0758*C_L^2$

2.10.3. Compressibility Drag

Due to the FAFCAS will be flying at Mach 0.84 at cruise, which is less than Mach 0.9, Roskam's compressibility drag behavior chart in Part II can be used. For Mach 0.84 a zero lift drag rise of 0.0009 is predicted. For Mach 0.84 with clean configuration, the resulting drag is:

$$C_D=0.0153+0.066*C_L^2 \quad (\text{Mach 0.84 with Clean Configuration})$$

2.10.4. Area Ruling

Area ruling is important in the design of the aircraft as it is approaching Mach 1. The flow acting on the aircraft can accelerate into supersonic speeds before the aircraft actually hits Mach 1, which can form local shockwaves on the aircraft and increase the drag. Thus the area distribution of the FAFCAS should be smooth across the length of the aircraft. Figure 2.10a displays the top view of the FAFCAS. The cross sectional area of the FAFCAS over its length is shown in Figure 2.10b.

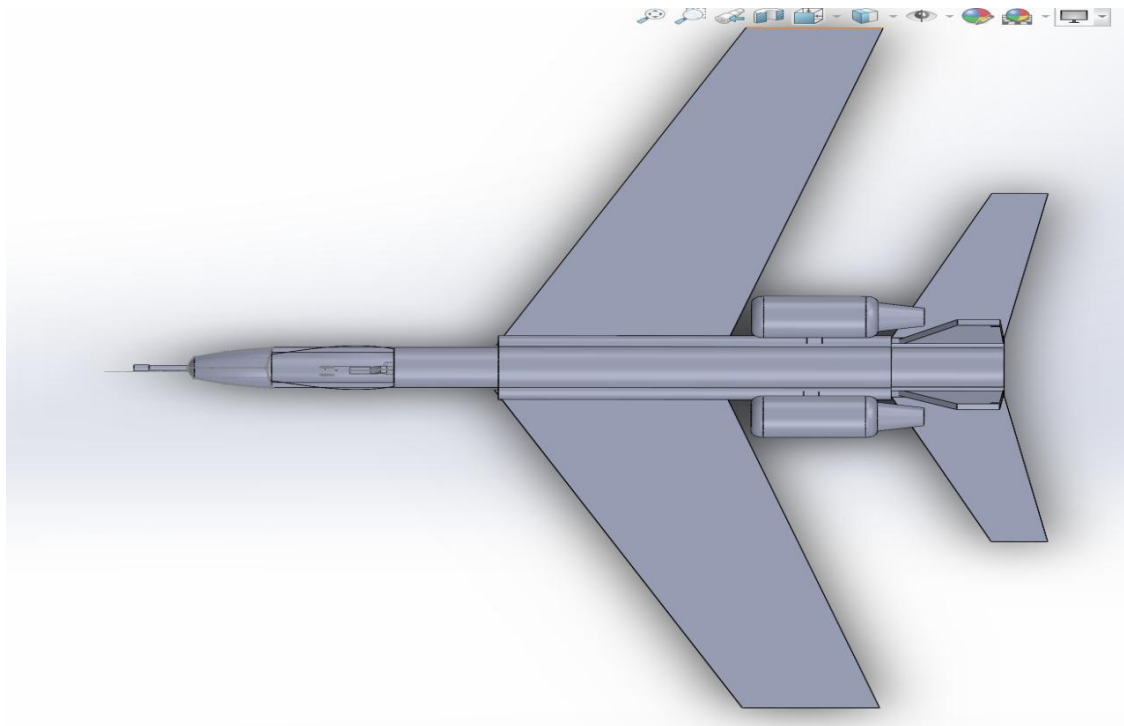


Figure 2.10a: Top View of FAFCAS

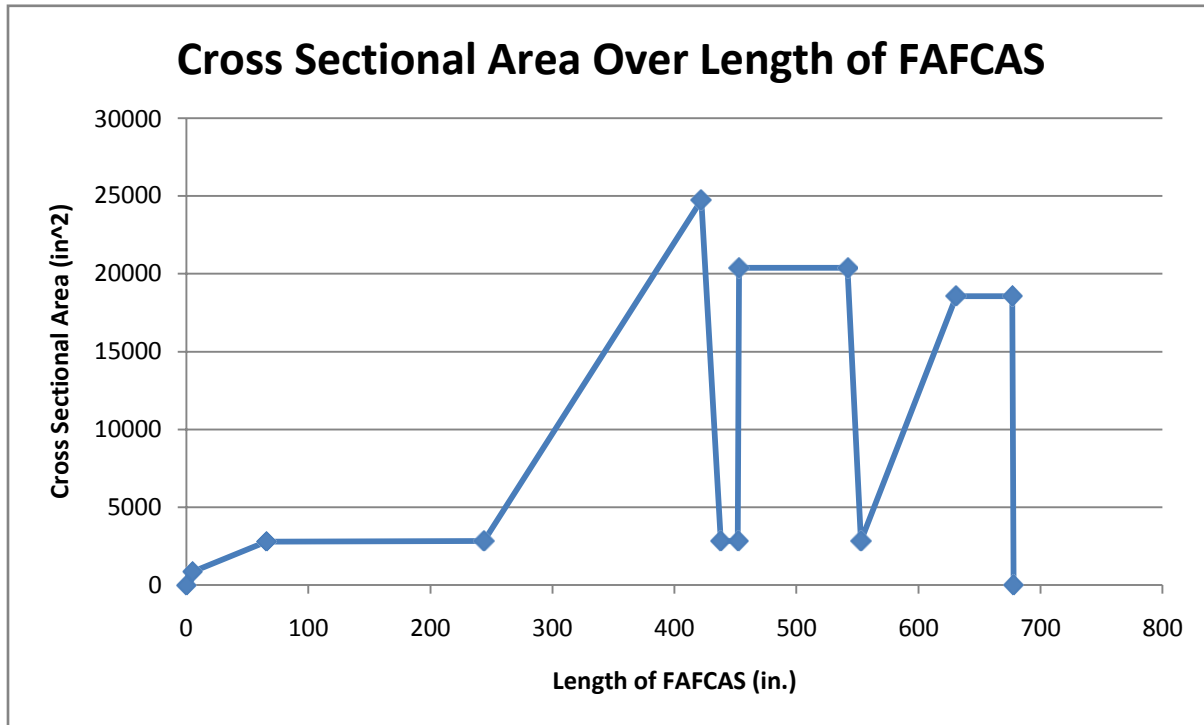


Figure 2.10b: Cross Sectional Area of FAFCAS

2.10.5 Airplane Drag Polars

Using the drag equations for low speed takeoff and landing configurations in §2.10.2 and cruise in §2.10.3, the plots of the drag polars are listed in Figure 2.10c. Appendix 2K contains the calculation for the drag polar equations.

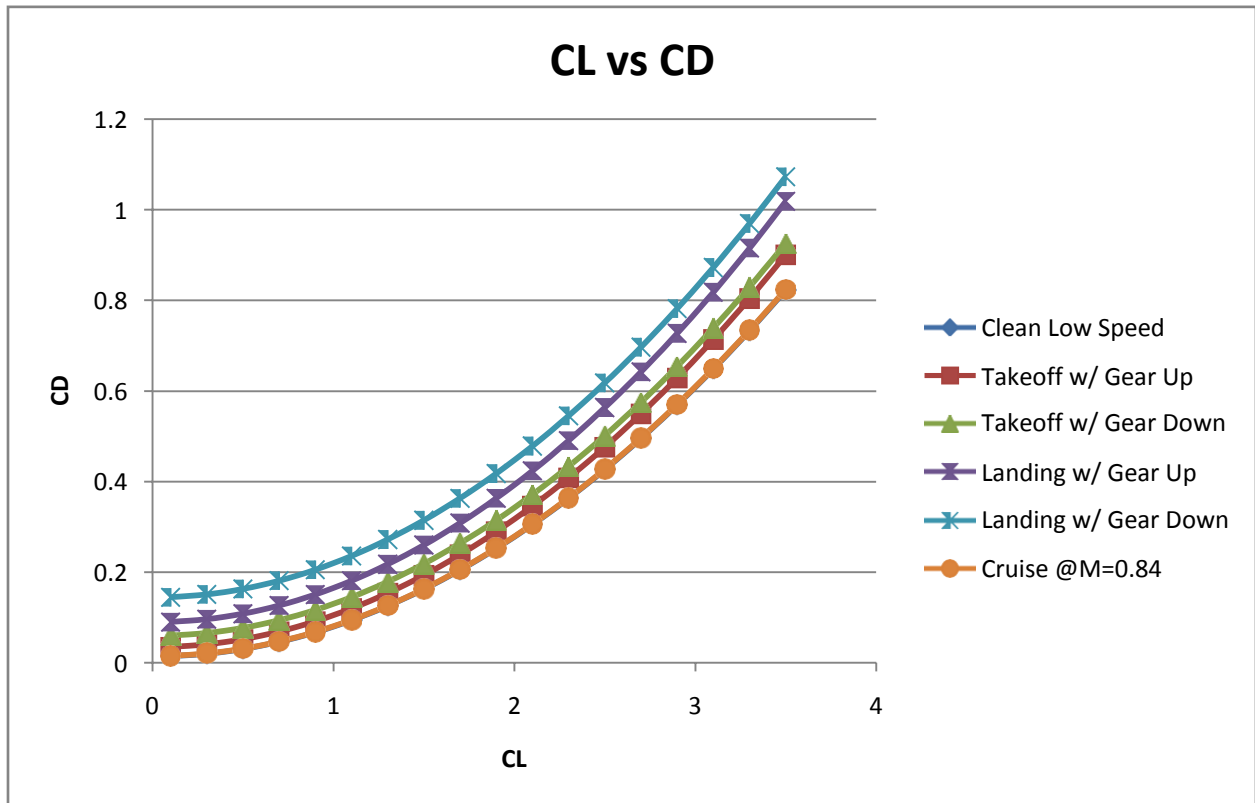


Figure 2.10c: Drag Polars of FAFCAS in Six Configurations

2.10.6. Discussion of Drag Polar

From Figure 3.22C in Roskam Part I, the predicted wetted area for a takeoff weight of 93,740 lbs is around 6000 ft². The calculated total wetted area is smaller than Roskam's prediction. This is likely due to the small diameter of the fuselage as compared to the weight class it is in. For weights of 90,000 lbs or more the planes Roskam uses to predict the wetted area are large cargo transport jets that have much higher diameter. The difference in fuselage diameter between a fighter and a transport plane leads to the discrepancy between the calculated and predicted wetted area. The low speed drag equations for takeoff and landing are similar to the ones predicted back in the performance constraint analysis. To get these similar equations, higher drag increments from the flaps and landing gears and higher efficiency factor were chosen due to the large landing gears that will be required for the heavy airplane and also the large flaps due to the large deflection needed. As can be seen in Figure 2.10b, the cross sectional area of the FAFCAS is smooth throughout the fuselage until it hits the wing, the engine, and the empennages. These jumps in area are undesirable as this can lead to flow acceleration to supersonic, which creates local shock waves on the body. These shock waves will increase the drag of the aircraft.

The drag polar equations for the low speed configurations are similar to the ones determined in the performance constraint by choosing assuming higher drag contributions by the

high lift devices and landing gears. Thus the weight sensitivities can still be used for this current version of the FAFCAS. The wetted area is smaller than the one predicted by Roskam as this is due to the weight class of this aircraft is usually in the transport airplane category and not a fighter jet. To reduce the drag at transonic speeds, the area of the fuselage at the wings, empennage, and nacelles should be reduced to create a smoother area distribution curve.

2.11. Class I Design Method Conclusion

With the drag polar, stability, and control verified for the FAFCAS design, the class I design process is complete. Figure 2.11a displays the current model of the FAFCAS configuration. From the weight and performance constraint analysis, it can be seen that the original mission specifications in Table 2.3 could not be met. Some parameters such as loiter time and climb rate had to be sacrificed for the design to be validated. The updated Class I design method aircraft specifications can be seen in Table 2.28. A summary of the different aircraft components can be seen in Table 2.29- Table 2.

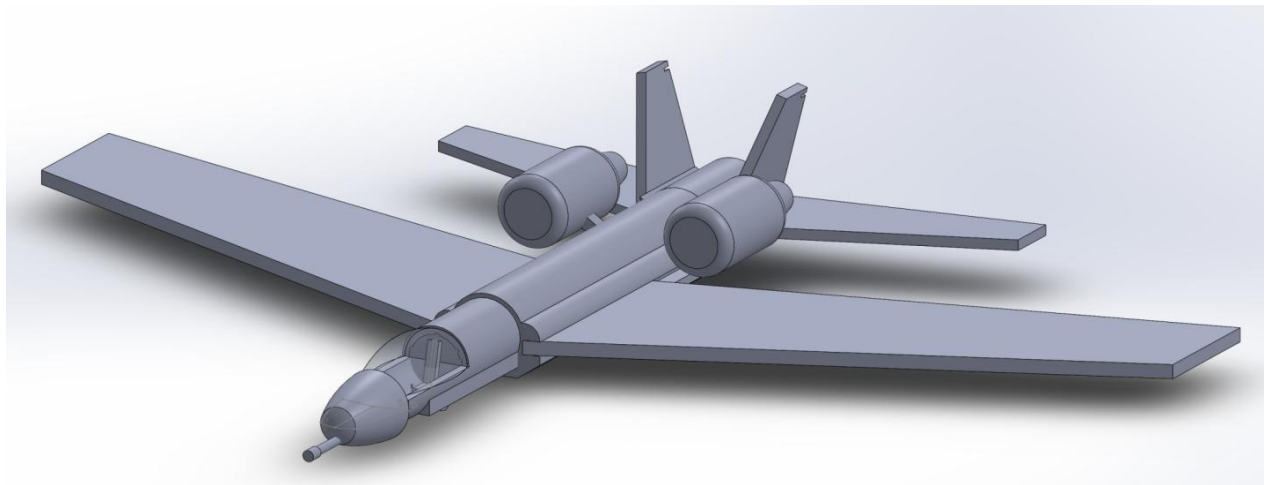


Figure 2.11a: Class I Design Method FAFCAS

Table 2.28: FAFCAS Specifications

Payload Capacity	13,000 lbs (2000 lbs of ammunition/22 x500 lbs bombs)
Takeoff and Landing Field Length	1 km
Loiter Time	50min
Range	1000km
Cruise Ceiling	12km
Cruise Speed	480 knots
Stall Speed	120 knots
Weight takeoff with Payload	96,650 lbs
Weight takeoff without stores	83,650 lbs
Weight empty	47,400 lbs

Weight fuel	23,000 lbs
Fuselage Length	53.5 ft

Table 2.29: Main Wing Specification

Wing Area	1040 ft ²
Wing Span	79 ft
Wing Speed	20 degrees
Taper Ratio	0.45
Fowler Flap Deflection at Landing	40 degrees
Fowler Flap Deflection at Takeoff	25 degrees

Table 2.30: Empennage Specification

	Horizontal Stabilizer	Vertical Stabilizer
Wing Area	100 ft ²	190 ft ²
Elevator Area	82 ft ²	N/A
Rudder Area	N/A	14.6 ft ²
AR	4	1
Taper Ratio	0.5	0.4
Sweep Angle	20 degrees	25 degrees
Thickness Ratio	.1	.135
Dihedral Angle	0 degrees	80 degrees

Table 2.31: Landing Gear Specifications

Landing Gear	Nose Landing Gear	Main Landing Gear
Number of Wheels	2	1
Diameter (in.)	20	42
Width (in.)	6.5	13
Pressure	120 PSI	150 PSI
Strut Length (in.)	42	31
Strut Width (in.)	5	8

3.1. Summary of Class I FAFCAS Design

In Chapter 2, a Class I design process was followed to do a preliminary design of the FAFCAS. In Table 3.1a to Table 3.1d a summary of the FAFCAS parameters are tabulated. In Roskam's airplane design method, the Class I process determined if the design is feasible. In

Chapter 2 the preliminary design was deemed feasible and in the weight range of a heavy fighter. Class II design methods are then used to fine-tune the design and get a realistic layout of the airplane configuration

Table 3.1a: FAFCAS Specifications

Payload Capacity	13,000 lbs (2000 lbs of ammunition/22 x500 lbs bombs)
Takeoff and Landing Field Length	1 km
Loiter Time	50min
Range	1000km
Cruise Ceiling	12km
Cruise Speed	480 knots
Stall Speed	120 knots
Weight takeoff with Payload	96,650 lbs
Weight takeoff without stores	83,650 lbs
Weight empty	47,400 lbs
Weight fuel	23,000 lbs
Fuselage Length	53.5 ft

Table 3.1b: Main Wing Specification

Wing Area	1040 ft ²
Wing Span	79 ft
Wing Speed	20 degrees
Taper Ratio	0.45
Fowler Flap Deflection at Landing	40 degrees
Fowler Flap Deflection at Takeoff	25 degrees

Table 3.1c: Empennage Specification

	Horizontal Stabilizer	Vertical Stabilizer
Wing Area	100 ft ²	190 ft ²
Elevator Area	82 ft ²	N/A
Rudder Area	N/A	14.6 ft ²
AR	4	1
Taper Ratio	0.5	0.4
Sweep Angle	20 degrees	25 degrees
Thickness Ratio	.1	.135
Dihedral Angle	0 degrees	80 degrees

Table 3.1d: Landing Gear Specifications

Landing Gear	Nose Landing Gear	Main Landing Gear
Number of Wheels	2	1
Diameter (in.)	20	42
Width (in.)	6.5	13
Pressure	120 PSI	150 PSI
Strut Length (in.)	42 (3.5 ft)	31 (2.58 ft)
Strut Width (in.)	5 (.417 ft)	8 (.667 ft)

3.1.1. Introduction of Class II Design Method

In Roskam's Class II design method, a step by step process is followed to fine-tune the aircraft like Class I design but considerably more complex. The summary of the Class II design sequence are as follows:

1. Class II Landing Gear Tires and Struts Sizing
2. Construct a V-N Diagram
3. Class II Component Weight Estimation
4. Class II Weight Balance
5. Class II Stability and Control Analysis
6. Class II Drag Polar Calculation
7. Compute the Thrust Characteristics of Propulsion System
8. List Airplane Performance Requirements
9. Calculate Critical Performance Capabilities
10. Finalize the Three-view Airplane Geometry
11. Finalize the Inboard Profile
12. Determine Manufacturing Breakdown, Maintenance Requirements, and Cost Analysis.

This second design sequence is important as it makes the preliminary design into a realistic design and also allows for more iteration in the design. Another important aspect of the final configuration design is that it locks in 90% of the life cycle cost of the airplane (Roskam Part II). This means that the preliminary design will be what determines majority of the cost of the airplane.

In this chapter, the first three steps of the Class II Design sequence will be conducted. The landing gear tires and the struts will be sized using Class II methods. The resulting geometries will be compared with the landing gear parameters in Table 3.1d. The next step is to create a V-N diagram for the FAFCAS to determine the design limits, ultimate load factors, and corresponding speeds. These will be used as inputs during the Class II component weight estimation. The resulting component weight estimation will provide a new empty weight that will be compared with the empty weight determined in Chapter 2.

3.2. Class II Landing Gear Design

In reference 4, Roskam provides the design process to do a Class II sizing of the landing gear tires and the struts. In Chapter 2, it was determined the FAFCAS will use a tricycle landing gear configuration with the initial landing gear specifications listed in Table 3.4. Preliminary landing gear loads were also calculated and are as follows:

- Main Landing Gear Strut Load (P_m) = 42,865 lbs.
- Nose Landing Gear Strut Load (P_n) = 10,925 lbs.

The parameters calculated in Chapter 2 will be used to size the tires for both the main landing gears and the nose landing gears. In addition the shock absorber components of the landing gear will be sized.

3.2.1. Landing Gear Tire Sizing

In Chapter 2, it was determined that the FAFCAS will use a retractable tricycle landing gear configuration due to it allowing the aircraft to have good visibility, good steering characteristics with the nose landing gear, and stability against ground loops. Stability against ground loops means the centrifugal force of the landing gears is stabilizing the aircraft. The nose landing gear will consist of two wheels and the two main landing gears will have one wheel each. In reference 4, Roskam states that there is a limit to landing gear loads depending on what type of surface the tires will be interacting with. This limit is applied so the tires do not cause damage to the surface of the runway. A method called Load Classification Number method (LCN) is used to determine the max allowable tire pressure. The landing gears have to be designed so they don't exceed the runways LCN number to avoid damaged. In Figure 3.2a, the effect of tire pressure and tire load on LCN is provided by Roskam. Using this figure, LCN number of 39, and an equivalent single wheel load of 43,000 lbs for the main landing gear and 11,000 lbs for the nose landing gear, the allowable tire inflation pressure are as follows:

- Main Landing Gear Allowable Inflation Pressure = 85 psi.
- Nose Landing Gear Allowable Inflation Pressure = 140 psi.

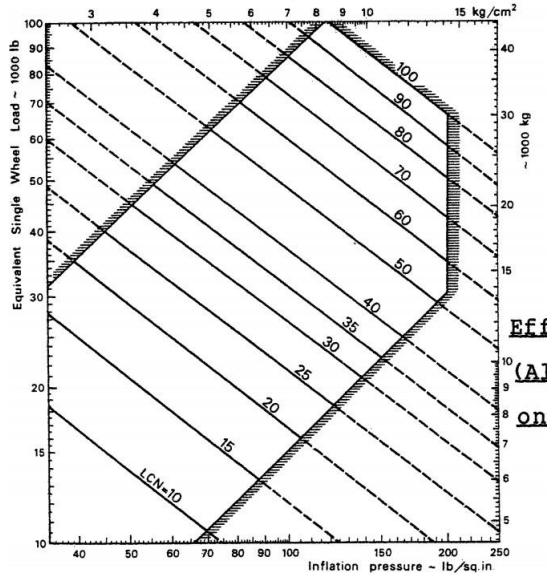


Figure 3.2a: Effect of Tire Pressure and Wheel Load on LCN Number.

The next step in the tire sizing is to determine the maximum tire velocity. From the calculations in Appendix 3A, the resulting tire velocity is $V_{tire / max} = 167 \text{ mp [?]}$. The tires are then chosen that matches this speed and inflation pressure.

In reference 4, Roskam provides a database for tires to choose the correct tires for the design aircraft. The database also contains the geometries for each tire, with the definitions of the tire geometry shown in Figure 3.2b.

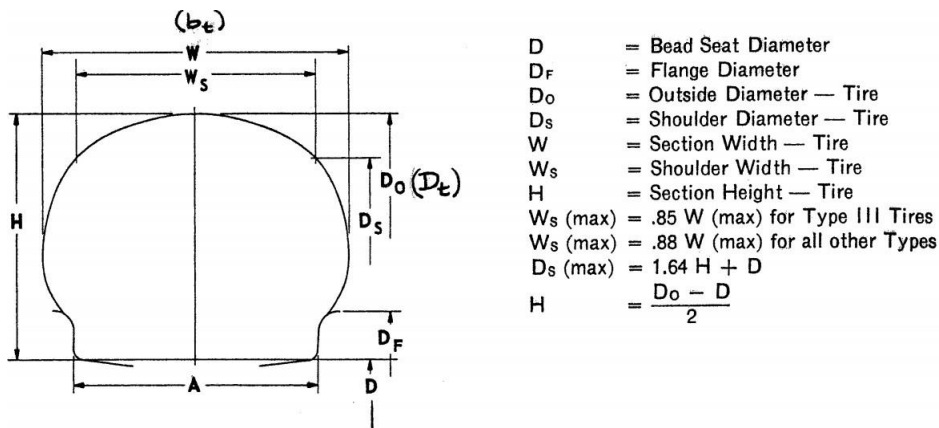


Figure 3.2b: Landing Gear Tire Geometry Definitions.

Before choosing the tires, the landing gear strut loads in §3.2 are increased by 25% to allow for future airplane design growth. The adjusted static loads are as follows:

- $P_{m,max} = 53,580 \text{ lbs 1 tire}$
- $P_{n,max} = 6,825 \text{ lbs 1 tire}$

The tires chosen for each landing gear with the above inputs are tabulated in Table 3.2a.

Table 3.2a: Landing Gear Tire Characteristics

Landing Gear	Do	W	D	Ply Rating	Static Load	Inflation Pressure	Speed Rating	Bead Ledge Diameter	Bump Capability	Qualification
Main L.G.	25in.	25in.	28in.	30	55,000 lbs	85 psi	160mph	28in.	10.1	MIL
Nose L.G.	15.5in.	15.5in.	20in.	20	29,900 lbs	135 psi	160 mph	20in.	5.2	MIL

3.2.2. Strut Design

The two components in the landing gears that absorb the shock of the aircraft during landing are the wheels and the struts. Using the takeoff weight calculated in Chapter 2 and a touchdown speed of 10 ft/s, the max kinetic energy, E_T , the landing gears have to absorb is 30,015 lbs. The calculations for the strut design can be seen in Appendix 3B. For each landing gear strut several design parameters have to be calculated which are; maximum allowable tire deflection (S_t), stroke of the shock absorber (S_s), and the diameter of the shock absorber strut (D_s). Assumptions of the energy absorption efficiency of the tires and the shock absorbers are made before calculations. The tires are assumed to have an energy absorption efficiency of 47%, and the oleo pneumatic shock absorbers assumed to have 80% energy absorption efficiency. A landing gear load factor of 7 is suggested by Roskam in reference 4. Table 3.2b tabulated the resulting landing gear shock absorber properties.

Table 3.2b: Landing Gear Shock Absorber Characteristics

Landing Gear	S_t	S_s	D_s
Nose Gear	.645 ft	.4196 ft	.5675 ft
Main Gear	1.04 ft	.644 ft	.6197 ft

3.2.3. Discussion of Class II Landing Gear Sizing

From this step of the Class II design, the landing gear tire and strut dimensions are obtained. A visualization of the landing gear dimensions is provided by Roskam which can be seen in Figure 3.2c.

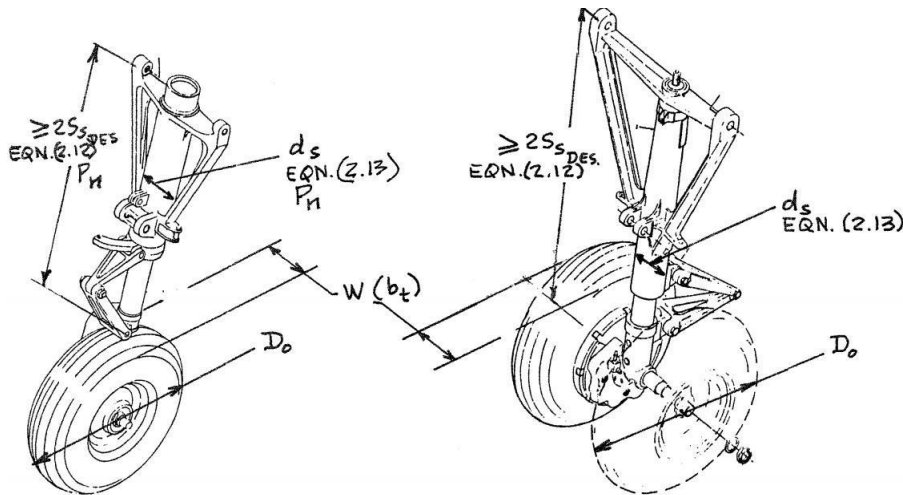


Figure 3.2c: Summary of Nose Landing Gear Dimensions (Left), Main Landing Gear Dimensions (Right).

Comparing the preliminary Class I Landing Gear properties in Table 3.1d and the results of the Class II Landing Gear properties in Table 3.2a and Table 3.2b, there is some differences that can be observed.

In the Class I design, the nose landing gear had a tire pressure of 120 psi. In the Class II design, this tire pressure was increased to 135 psi. This is likely due to the 25% increase to the static load required by this design process. The tire dimensions were also updated from a 20in.x6.5in tire to a 15.5in.x15.5in. From the tire database in reference 4, the 20in.x6.5in tire would not be able to support the load and speed determined from the Class II calculations. The struts of the nose landing gear were also updated from a rectangular shape strut to a more realistic tubular shape. In Figure 3.2c, the strut length is the shock absorber stroke length doubled. This resulting length of 0.8392 ft is much shorter than the original Class I nose strut length of 3.5 ft. The Class II diameter of the strut of 0.5676 ft is comparable with the strut width of 0.417 ft from Class I design.

For the main landing gear, the Class I tire pressure of 150 psi is much higher than the Class II tire pressure of 85 psi. The Class I tire dimensions of 42in.x13in is also bigger than the Class II tire dimensions of 25in.x25in. This shows that the tire was made larger than necessary in the Class I design method. The main landing gear struts were also longer and wider than needed in the Class I design by comparing with the strut values in the Class II design.

3.3. V-N Diagram

The next step of the Class II design is to construct a V-N diagram for the FAFCAS. The load factors and design speed limits shown by the V-N diagram will assist with the Class II weight estimations. Appendix 3C contains the calculations done to obtain the V-N diagram. In reference

5, Roskam provides limit load factors for various military airplanes. For USAF fighters, the following limit load factors are used:

- $n_{lim, positive} = 8.67$
- $n_{lim, negative} = -3.0$

Before the V-N diagram can be constructed, various aircraft speeds have to be obtained which are; maximum level speed, maximum dive speed, and design maneuver speed. Table 3.3a tabulates the speed for the V-N Diagram.

Table 3.3a: Design Speeds

V_H	480 knots
V_L	600 knots
V_A	380 knots

The resulting V-N diagram for the FAFCAS can be seen in Figure 3.3a.

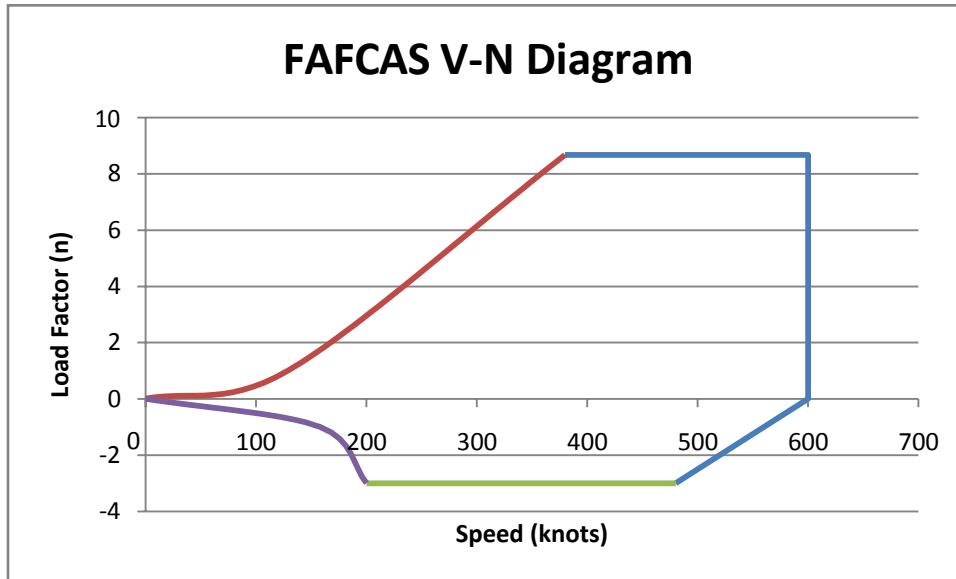


Figure 3.3a: FAFCAS V-N Diagram

For the aircraft to fly safely, it must operate within the envelope shown in the V-N diagram. The load factor and speed limits in Figure 3.3a will be used to estimate the aircraft component weights.

3.4. Class II Weight Estimation

In Chapter 2, preliminary weight estimation was conducted to estimate the component weights and calculate the resulting empty weight. The summary of the Class I weight estimations can be seen in Table 3.4a.

Table 3.4a: Class I FAFCAS Component Weight and Mission Weights

Wing (lbs)	10000
Empennage (lbs)	3600
Fuselage (lbs)	11600
Engine Section 1 (lbs)	300
Landing Gear (lbs)	5000
Engine Section 2 (lbs)	4164
Engine (lbs)	2886
GAU-8 Gun Actual Weight (lbs)	2014
Fix Equipment-Gun (lbs)	7836
Empty Weight (lbs)	47400
Pilot (lbs)	250
Payload (lbs)	26000
Fuel (lbs)	23000
Takeoff Gross Weight (lbs)	96650

Reference 5 provides four different methods to do Class II weight estimation. There is a Cessna method, USAF method, General Dynamics method, and Torenbeek method. Roskam advises to use the General Dynamics (GD) method to do weight estimation for fighters.

The total weight of the aircraft is the takeoff weight. This takeoff weight is broken down to the following:

- W_E = Empty Weight
- W_F = Fuel Weight
- W_{PL} = Payload Weight
- W_{crew} = Crew Weight

The fuel weight, payload weight, and crew weight are carried over from Chapter 2 as they remain fixed. The empty weight is broken down further as follows:

- W_{Struct} = Structure Weight
- W_{pwr} = Power Plant Weight
- W_{feq} = Fixed Equipment Weight

The structure, power plant, and fixed equipment weights are then broken down further into individual components. The GD method provides equations to calculate the weights of each component. The calculations for the weight estimation can be seen in Appendix 3D.

3.4.1. Class II Structure Weight Estimation

The structure weight is broken down into the following components:

- W_w = Wing Weight (with Fowler Flaps)
- $W_{H.Tail}$ = Horizontal Tail Weight
- $W_{V.Tail}$ = Vertical Tail Weight
- W_f = Fuselage Weight
- W_{eg} = Engine Section Weight
- $W_{L.G.}$ = Landing Gear Weight

The resulting structure component weights are tabulated in Table 3.4b.

Table 3.4b: Class II Structure Weight Breakdown

W_w	13,507 lbs
$W_{H.Tail}$	403 lbs
$W_{V.Tail}$	342 lbs
W_f	7697 lbs
W_{eg}	300 lbs
$W_{L.G.}$	2894 lbs

3.4.2. Class II Power Plant Weight Estimation

The power plant weight is broken down into the following components:

- W_{eng} = Engine Weight
- W_{ai} = Air Induction System Weight
- W_{fs} = Fuel System Weight
- W_p = Propulsion System Weight

The air induction system consists of a duct support structure and the subsonic part of the structure. The fuel system assumes the aircraft uses a self sealing bladder with components for inflight-refueling. The propulsion system contains the weight of the engine controls, engine starting system, and oil systems. The resulting power plant component weights are tabulated in Table 3.4c.

Table 3.4c: Class II Power Plant Weight Breakdown

W_{eng}	2886 lbs
-----------	----------

W_{ai}	2180 lbs
W_{fs}	1075 lbs
W_p	1388 lbs

3.4.3. Class II Fixed Equipment Weight Estimation

The fixed equipment weight is broken down into the following components:

- W_{fcs} = Flight Control System Weight
- W_{els} = Electrical System Weight
- W_{api} = Air Condition, Pressurization, and De-Icing System Weight
- W_{arm} = Armament Weight
- W_{fur} = Furnishing Weight
- W_{ox} = Oxygen Systems Weight
- W_{aux} = Auxiliary Gear Weight

The armament weight consists of the cannon and the targeting systems for the weapons. The furnishings are the ejection seat and miscellaneous emergency equipment. The resulting fixed equipment component weights are tabulated in Table 3.4d.

Table 3.4d: Class II Fixed Equipment Weight Breakdown

W_{fcs}	1965 lbs
W_{els}	648 lbs
W_{api}	254 lbs
W_{arm}	2566 lbs
W_{fur}	252 lbs
W_{ox}	17 lbs
W_{aux}	200 lbs

3.4.4. Discussion of Class II Weight Estimations

The summary of the weight breakdown with the resulting empty weight can be seen in Table 3.4e.

Table 3.4e: Summary of Class II Weight Estimation

W_w	13,507 lbs
$W_{H.Tail}$	403 lbs
$W_{V.Tail}$	342 lbs
W_f	7697 lbs
W_{eg}	300 lbs
$W_{L.G.}$	2894 lbs

W_{Struct}	25,143 lbs
W_{eng}	2886 lbs
W_{ai}	2180 lbs
W_{fs}	1075 lbs
W_p	1388 lbs
W_{pwr}	7528 lbs
W_{fcs}	1965 lbs
W_{els}	648 lbs
W_{api}	254 lbs
W_{arm}	2566 lbs
W_{fur}	252 lbs
W_{ox}	17 lbs
W_{aux}	200 lbs
W_{feq}	5902 lbs
W_E	38,573 lbs

The resulting empty weight from the Class II weight estimation is 38,573 lbs vs. 47,400 lbs in Class I weight estimation. This is an 18.6% difference in empty weight. One reason there is such a large difference is the two methods used to estimate component weights from Class I and Class II. In Class I design method, four different fighter aircrafts were compared and their component weight to gross weight ratios tabulated. These ratios were averaged for each component and used for the FAFCAS. Most of the aircraft in Roskam's database are from the 1950's to 1970's. The manufacturing methods and materials used for those aircraft's components are not as advanced as present day, with less composite materials and bulkier electronics. This would account for the much heavier empty weight of the Class I weight estimations.

The component weight breakdown in Class II was also much more complex than in Class I. Class I weight estimation was broken down into nine components meanwhile Class II weight estimation had 17 components. The GD method to calculate component weight didn't rely on a database of aircrafts. Instead the GD method used aircraft geometry and takeoff weight from the design aircraft itself. Thus the Class II method avoids using weight patterns from aircrafts that do not share the same mission statement as the design aircraft.

From the Class II weight estimation, most of the components have had their weights updated and in addition the empty weight has been reduced considerably. Thus the component's center of gravity will have shifted as compared with the Class I weight and balance in Chapter 2. In Chapter 4 of the report, a Class II weight balance will be conducted with the new component weights to find the updated center of gravity, moments, and product of inertia.

4.1 Summary of Class I and Class II Component Weight Estimation

In Chapter 2, a Class I method was used to estimate the airplane component weights and airplane inertias. In Class I design method, the component weights are estimated as a function of takeoff weight. The percentages are obtained from data of existing airplanes with similar mission profiles. In the FAFCAS Class I weight estimation, four different fighter aircrafts were compared and their component weight to gross weight ratios tabulated. These ratios were averaged for each component and used for the FAFCAS. In Chapter 3, Class II component weight estimation was conducted using the General Dynamics (GD) method based off of aircraft geometry and takeoff weight from the design aircraft itself. The resulting empty weight from the Class II weight estimation is 38,573 lbs vs. 47,400 lbs in Class I weight estimation. Table 4.1a tabulates the Class I component weight breakdown. Table 4.1b lists the more complex component breakdown and their corresponding weights.

Table 4.1a: Class I FAFCAS Component Weight and Mission Weights

Wing (lbs)	10000
Empennage (lbs)	3600
Fuselage (lbs)	11600
Engine Section 1 (lbs)	300
Landing Gear (lbs)	5000
Engine Section 2 (lbs)	4164
Engine (lbs)	2886
GAU-8 Gun Actual Weight (lbs)	2014
Fix Equipment-Gun (lbs)	7836
Empty Weight (lbs)	47400
Pilot (lbs)	250
Payload (lbs)	26000
Fuel (lbs)	23000
Takeoff Gross Weight (lbs)	96650

Table 4.1b: Summary of Class II Weight Estimation

W_w	13,507 lbs
$W_{H.Tail}$	403 lbs
$W_{V.Tail}$	342 lbs
W_f	7697 lbs
W_{eg}	300 lbs
$W_{L.G.}$	2894 lbs
W_{Struct}	25,143 lbs
W_{eng}	2886 lbs
W_{ai}	2180 lbs
W_{fs}	1075 lbs

W_p	1388 lbs
W_{pwr}	7528 lbs
W_{fcs}	1965 lbs
W_{els}	648 lbs
W_{api}	254 lbs
W_{arm}	2566 lbs
W_{fur}	252 lbs
W_{ox}	17 lbs
W_{aux}	200 lbs
W_{feq}	5902 lbs
W_E	38,573 lbs

Where:

- W_w = Wing Weight (with Fowler Flaps)
- $W_{H.Tail}$ = Horizontal Tail Weight
- $W_{V.Tail}$ = Vertical Tail Weight
- W_f = Fuselage Weight
- W_{eg} = Engine Section Weight
- $W_{L.G.}$ = Landing Gear Weight
- W_{eng} = Engine Weight
- W_{ai} = Air Induction System Weight
- W_{fs} = Fuel System Weight
- W_p = Propulsion System Weight
- W_{fcs} = Flight Control System Weight
- W_{els} = Electrical System Weight
- W_{api} = Air Condition, Pressurization, and De-Icing System Weight
- W_{arm} = Armament Weight
- W_{fur} = Furnishings Weight

- W_{ox} = Oxygen Systems Weight
- W_{aux} = Auxiliary Gear Weight
- W_{Struct} = Structure Weight
- W_{pwr} = Power Plant Weight
- W_{feq} = Fixed Equipment Weight

4.2. Class II Weight and Balance Analysis

From the Class II weight estimation, most of the components have had their weights updated and in addition the empty weight has been reduced considerably. Thus the component's center of gravity will have shifted as compared with the Class I weight and balance in Chapter 2. Thus a Class II weight balance will be conducted with the new component weights to find the updated center of gravity, moments, and product of inertia. If any of the component's geometry are updated as a result of the weight and balance analysis, the design will have to be tested again for longitudinal stability and if it has any "tip-over" problems as in Chapter 2.

4.2.1 Class II Aircraft Component Center of Gravity Location

With the initial Class II component weight breakdown obtained in §4.1, each of the component's center of gravity then must be obtained. In Reference 5, Roskam provides guidelines to locating the center of gravity locations for the structural, power plant, and fixed components of the aircraft. The reference plane was recommended by Roskam as left and below the aircraft as much as possible to avoid negative signs on the numbers. Thus the reference point was placed 100 inches under the middle of the fuselage with the length axis starting at the gun barrel tip. A visual representation of the reference frame by Roskam can be seen in Figure 4.2a. The calculations for the center of gravity location can be seen in Appendix 4A.

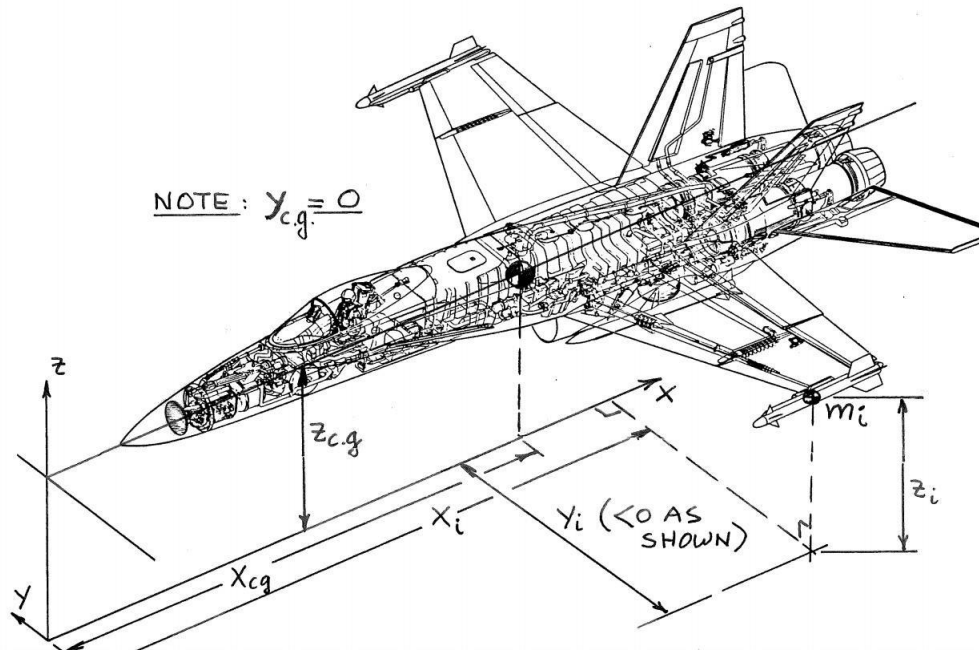


Figure 4.2a: Definition of Reference Frame Coordinates.

4.2.1.1 Structural Component C.G. Location

The structural components for the aircraft are broken down into the wing, horizontal tail, vertical tail, fuselage, engine section, and the main/ nose landing gears. The recommended spots for each of the components are as follows:

- The wing CG was recommended to be at 70% of the distance between the front and rear spar of the wing.
- The horizontal and vertical tail CG was recommended to be at 42% of the distance from the chord to the leading edge of the wing.
- The fuselage CG is at around the half the length of the fuselage.
- Engine section CG located at 40% of the nacelle length from the nacelle nose.
- Nose Landing Gear CG near the pilot.
- Main Landing Gear CG at around halfway the length of the aircraft

The initial CG locations in the x axis for the structural components are listed in Table 4.2a.

Table 4.2a: Class II Structural Component CG Location in the X-Axis

Structural Component	CG Location in the X-Axis (in.)
Wing	398
Horizontal Tail	633
Vertical Tail	637
Fuselage	365
Engine Section	490

Main Landing Gear	195
Nose Landing Gear	380

4.2.1.2. Power Plant Component C.G. Location

The power plant components are broken down into the engine, air induction system, fuel system, and propulsion system. The guidelines for choosing the CG for each of the components are as follows:

- Engine CG at half the length of the engine.
- Fuel system CG in the fuselage, away from landing gear struts, away from the engines, and away from the wingtips.
- Propulsion and Air induction CG placed near the engine.

The multiple guidelines for the fuel system CG placement is so it avoids potential areas where a structural damage can ignite the fuel lines. The initial CG locations in the x axis for the power plant components are listed in Table 4.2b.

Table 4.2b: Class II Power Plant Component CG Location in the X-Axis

Power Plant Component	CG Location in the X-Axis (in.)
Engine	544
Air Induction System	540
Fuel System	250
Propulsion System	540

4.2.1.3. Fixed Equipment C.G. Location

The fixed equipment components are broken down into the flight control system, electrical system, air-conditioning/Pressurization/De-icing system, armament systems, furnishings, oxygen systems, and auxiliary equipment. The guidelines for choosing the CG for each of the components are as follows:

- The irreversible flight control systems (FCS) will use mechanical signaling to control the hydraulic actuators. The actuators will be placed next to the empennages. Thus flight control system CG will be near the tail of the aircraft.
- Electrical system consists of the auxiliary power unit (APU) and should be placed at the bottom of the tail.
- The air-conditioning/Pressurization/De-icing (API) system CG location should be near the engine.
- The armament and targeting systems CG location will be near the cockpit.
- The furnishing consists of the escape system and thus the CG will be placed near the pilot.

- The auxiliary equipment CG will be placed near the nose of the aircraft.

The electrical system CG has to be placed at the bottom of the tail of the aircraft to avoid lightning strike from damaging the APU. The API system CG is near the engine so it is close to the engine to get the bleed air to function. Mechanical signaling is used for the hydraulic actuators so the FAFCAS can still use manual reversion on the flight surfaces in case there is damage to the hydraulic systems. The initial CG locations in the x axis for the fixed equipment components are listed in Table 4.2c.

Table 4.2c: Class II Fixed Equipment Component CG Location in the X-Axis

Fixed Equipment Component	CG Location in the X-Axis (in.)
FCS	635
ELS	630
API	550
Armament Systems	180
Furnishings	192
Oxygen Systems	550
Auxiliary Systems	270

4.2.2. Effect of Moving Components on Overall C.G.

With all the CG located for each component, the CG of the overall aircraft can be calculated. Equation 4.2a displays the equation used to determine the aircraft CG. See Appendix 4B for the calculations of the aircraft CG.

$$x_{cg} = \frac{W_i x_i}{W_E} \quad (\text{Eqn. 4.2a})$$

With the initial Class II component CGs in Tables 4.2a-4.2c and component weights in Table 4.1b, the aircraft CG (x_{cg}) of the FAFCAS is calculated to be at 411 inches. A problem can already be seen with this CG location, as the aircraft CG is aft of the main landing gear CG. This will cause a tip over problem in the aircraft. In Roskam Part II Chapter 9 for tricycle landing gears, the author states the main landing gear must be behind the most aft CG with a 15 degree angle relation between the two points to meet the tip over criteria. To meet the 15 degree angle relation and have the main landing gear located behind the aircraft CG, the main landing gear is moved to $x = 417.5$ in. This will lead to a marginal shift in the aircraft CG to $x_{cg} = 413$ in.

As can be seen in the aircraft CG shift when the main landing gear was moved, each component moved has an overall effect on the aircraft CG. The rate x_{cg} moves when a component is shifted can be calculated with Equation 4.2b.

$$\frac{\partial x_{cg}}{\partial x_i} = \frac{W_i}{W_E} \quad (\text{Eqn. 4.2b})$$

Table 4.2d displays how much the aircraft CG when each of the components is moved.

Table 4.2d: Rate Aircraft CG Moves for Each Component Shifted.

Component	Rate x_{cg} moves when component is moved
Wing	0.349741067
Horizontal Tail	0.011952356
Vertical Tail	0.008529259
Fuselage	0.19930088
Engine Section	0.007767996
Main Landing Gear	0.049948213
Nose Landing Gear	0.024987053
Engine	0.07472812
Air Induction System	0.056447437
Fuel System	0.027835318
Propulsion System	0.035939927
FCS	0.050880373
ELS	0.016778871
API	0.006576903
Armament Systems	0.066442258
Furnishings	0.006525117
Oxygen Systems	0.000440186
Auxiliary Systems	0.005178664

As can be seen in Table 4.2d, the moving the wing has the highest effect in shifting the aircraft CG.

4.2.3. Class II Weight & Balance- Stability and Control Check

With the configuration of the airplane changed due to the new component weights and center of gravity location, the longitudinal stability of the aircraft has to be checked. To determine the longitudinal stability, the horizontal stabilizer area will be varied to determine its effect on the aft center of gravity (x_{cg}) and aft aerodynamic center ($x_{ac,aft}$). Equation 4.2c displays the function for the aft center of gravity divided by the mean geometric chord (c). Equation 4.2d displays the function for the aft aerodynamic center. Appendix 4C displays the calculations to verify the stability.

$$\bar{x}_{cg} = \frac{x_{cg} - x_{LE}}{c} \quad (\text{Eqn. 4.2c})$$

$$\bar{x}_{ac,aft} = \frac{C1 + C2(x_{ac,LE})}{1 + C2} \quad (\text{Eqn. 4.2d})$$

C1 and C2 are terms consisting of lift curve slopes and aerodynamic centers, which are derived back in Chapter 2 Appendix. Using the two functions, a longitudinal X-plot is made to determine the horizontal tail area required for de-facto stability. De-facto stability is defined as requiring

feedback augmentation for stability. The FAFCAS design is chosen to be de-facto stable due to the need for maneuverability and the design can't have the plane be too stable. Figure 4.2b displays the longitudinal X-plot after the Class II weight and balance analysis.

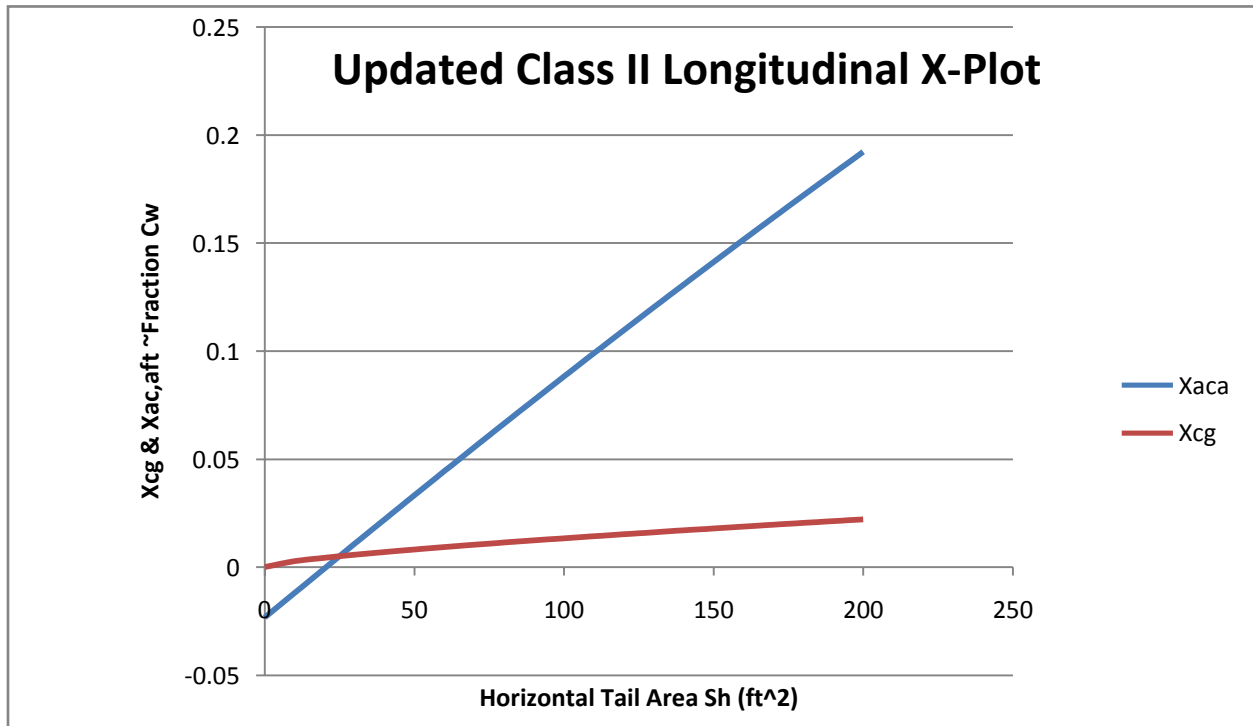


Figure 4.2b: Class II Longitudinal X-Plot

From Figure 4.2b a ΔSM of 0.054 will be chosen with a corresponding horizontal tail area of 130 ft². The resulting feedback gain $K\alpha$ is 0.865, which is acceptable as it doesn't exceed 5 degree/degree. The horizontal tail area of 130ft² chosen from the X-plot is larger than the original tail area of 100ft². The updated component weight and CG location can be seen in Table 4.2e.

Table 4.2e: Updated Class II Component Weight and CG Location

Component	Component Weight (lbs)	CG Location on X-axis (in.)	CG Location on Y-axis (in.)	CG Location on Z-axis (in.)
Wing	13,507	398	0	100
Horizontal Tail	461.6	624.77	0	100
Vertical Tail	329.4	637	0	140
Fuselage	7697	365	0	100
Engine Section	300	490	0	123.08
Main Landing Gear	1929	417.5	0	68.272
Nose Landing Gear	965	195	0	70.97
Engine	2886	544	0	123.08

Air Induction System	2180	540	0	100
Fuel System	1075	250	0	100
Propulsion System	1388	540	0	100
FCS	1965	635	0	100
ELS	648	630	0	76
API	254	550	0	100
Armament Systems	2566	180	0	100
Furnishings	252	192	0	100
Oxygen Systems	17	550	0	100
Auxiliary Systems	200	270	0	100
FAFCAS Empty Weight	38,620	413	0	100

The resulting empty weight of the FAFCAS has increased from 38,573 lbs to 38,620 lbs.

4.2.4. Estimating Airplane Inertias

Using the updated component weights and CG locations, the airplane's inertias can be calculated. In reference 5, Roskam provides equations for the moments and products of inertia which can be seen in Figure 4.2c. The calculations can be seen in Appendix 4D.

$$I_{xx} = \sum_{i=1}^{i=n} m_i ((y_i - y_{cg})^2 + (z_i - z_{cg})^2)$$

$$I_{yy} = \sum_{i=1}^{i=n} m_i ((z_i - z_{cg})^2 + (x_i - x_{cg})^2)$$

$$I_{zz} = \sum_{i=1}^{i=n} m_i ((x_i - x_{cg})^2 + (y_i - y_{cg})^2)$$

$$I_{xy} = \sum_{i=1}^{i=n} m_i (x_i - x_{cg})(y_i - y_{cg})$$

$$I_{yz} = \sum_{i=1}^{i=n} m_i (y_i - y_{cg})(z_i - z_{cg})$$

$$I_{zx} = \sum_{i=1}^{i=n} m_i (z_i - z_{cg})(x_i - x_{cg})$$

Figure 4.2c: Class II Roskam Aircraft Inertia Equations

For symmetrical aircraft the value of I_{xy} and I_{yz} are zero. The resulting inertia values are tabulated in Table 4.2f.

Table 4.2f: Class II Aircraft Inertia

I_{xx}	5352530.522 lbs*in ²
I_{yy}	530711485.8 lbs*in ²
I_{zz}	525358955.3 lbs*in ²
I_{xy}	0 lbs*in ²
I_{yz}	0 lbs*in ²
I_{zx}	14671231.07 lbs*in ²

4.3. Discussion of Class II Weight and Balance Analysis

With the Class II weight and balance analysis conducted, the configuration of the FAFCAS has been updated. The aircraft components have become much lighter than as they were in Class I weight estimation. The CG location has also been moved drastically, from 231 inches in Class I methods to 431 inches in Class II methods. The main landing gear positions have also been shifted in order to meet the tip-over criterion and be aft of the updated aircraft CG. With the enlarged horizontal tail area, the weight has increased from 403 lbs to 462 lbs with the horizontal tail CG shifted from 633 inches to 625 inches. But as can be seen on Table 4.2d, the horizontal tail component does not affect the overall aircraft CG much, with only a 0.22 inch shift in x_{cg} with the enlarged horizontal tail.

The next part of the Class II design after the calculation of the aircraft inertias is the Class II Stability and Control analysis using the updated design. This will finalize the sizing of the control surfaces and may require iteration in the weight balance depending if the weight and drag changes drastically.

5.1 Class II Stability and Control

In this chapter a Class II Stability and Control analysis will be conducted on the updated aircraft configuration resulting from the Class II Weight and Balance analysis in Chapter 4. Roskam's definition of good flying qualities is as follows:

- The airplane has sufficient control power to maintain steady state, straight line flight.
- The airplane can be safely maneuvered from one steady state flight condition to another.
- Cockpit control force level is acceptable under all expected conditions.
- The airplane can be trimmed in certain flight conditions.

The statements above provide a qualitative definition of airworthiness for the aircraft. The quantitative definition for military aircraft airworthiness is found in the military aircraft design regulation MIL-F-8785C. This regulation provided by Roskam contains the military specification and flying qualities of piloted airplanes.

Due to the enlarged horizontal stabilizer and change in center of gravity location, the aircraft's longitudinal controllability and trim has to be analyzed for each flying condition listed in regulation MIL-F-8785C.

5.2 Development of Trim Diagram

To analyze the aircraft's longitudinal controllability and trim, a trim diagram has to be constructed. The procedure to construct the trim diagram is as follows:

1. Determine the most forward and aft center of gravity location for the aircraft.
2. The flight conditions the aircraft will be exposed to under regulation MIL-F-8785C has to be tabulated.
3. Construct the airplane lift vs. α curve.
4. Construct the airplane pitching moment coefficient vs. airplane lift coefficient curve.

5.2.1 MIL-F-8785C Flight Conditions

Under the military regulation MIL-F-8785C, to determine if the aircraft has good longitudinal flying qualities the aircraft has to be tested for twenty design and test conditions. For each test condition the following parameters have to be obtained:

- Critical C.G. loading location (Forward, aft, or reference).
- Initial and end load factor.
- Initial and end point altitude and speed.

Table XVIII in Roskam Part VII defines each longitudinal flight conditions. Using these definitions the flight conditions and its respective parameters are tabulated in Table 5.2a. The most forward C.G. location is 34.42 ft and the most aft position is 36.92 ft. Conditions that doesn't have a critical loading use the reference C.G. location at 35.66 ft.

Table 5.2a: Longitudinal Flying Conditions

Title	CG Loading (ft)	Min Load Factor	Max Load Factor	Initial Altitude (ft)	End Altitude (ft)	Initial Speed (kts)	End Speed (kts)
Longitudinal Static Stability	36.9	1	1	0	43000	100	480
Relaxation in Transonic Flight	36.9	1	1	0	43000	100	480
Elevator Control Force Variations during Rapid Speed Changes	35.66	1	1	0	43000	100	480
Phugoid Stability	34.42	1	1	0	43000	100	480
Flight-Path Stability	35.66	1	1	0	43000	100	95
Short Period Frequency and acceleration sensitivity	34.42	1	1	0	43000	100	480

Short Period Damping	36.9	1	1	0	43000	100	480
Residual Oscillations	35.66	1	1	0	43000	100	480
Control Feel and Stability in Maneuvering Flight	36.9	-3	8.67	0	43000	100	480
Control Forces in Maneuvering Flight	36.9	-1	8.67	0	43000	100	480
Control Motions in Maneuvering Flight	34.42	-1	8.67	0	43000	100	480
Longitudinal Pilot-Induced Oscillations	35.66	-3	8.67	0	43000	100	480
Dynamic Control forces in Maneuvering Flight	34.42	1	1	0	43000	100	480
Control Feel	36.9	1	1	0	43000	100	480
Longitudinal Control in Unaccelerated Flight	34.42	1	1	0	43000	100	480
Longitudinal Control in Maneuvering Flight	34.42	1	1	0	43000	100	480
Longitudinal Control in Takeoff	35.66	1	1	1000	1000	100	100
Longitudinal Control Force and Travel in Takeoff	34.42	1	1	0	1000	0	480
Longitudinal Control in Landing	34.42	1	1	0	1000	100	480
Longitudinal Control Forces in Dives	34.42	1	8.67	2000	43000	100	480

5.2.2 Airplane Lift vs. α Curve

To construct the airplane lift vs. α curve the following four parameters have to be calculated:

- α_{0l} - Airfoil zero-lift angle of attack
- $C_{L\alpha}$ - Airfoil lift curve slope
- α^* - Airfoil linear range angle of attack
- α_{clmax} - Airfoil angle of attack for maximum lift

In Roskam Part VI, the author provides experimental low speed data for various NACA airfoils. Appendix 5A contains the calculation for the airplane lift vs. α curve using Roskam's low speed data. The effect of the elevator deflection on the airplane lift coefficient vs. α curve is then calculated for a +10 degree deflection and -10 degree deflection. Roskam illustrates the effect of elevator deflection of the airplane lift which can be seen Figure 5.2a.

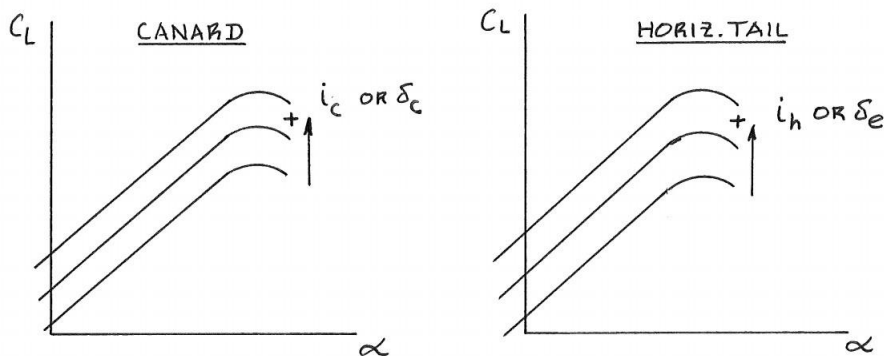


Figure 5.2a: Effect of Control Surface Deflection on Airplane Lift.

The resulting airplane lift coefficient vs. α curve for an elevator deflection of +10, 0, and -10 degrees is displayed in Figure 5.2b.

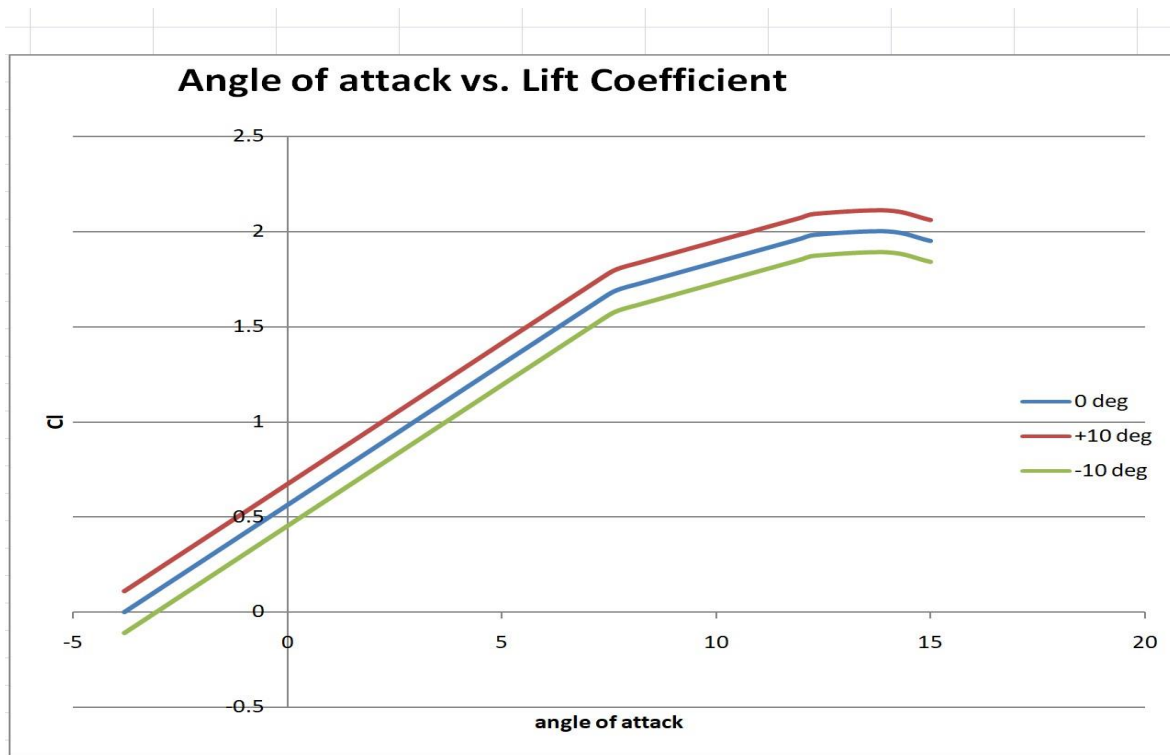


Figure 5.2b: Airplane Lift Coefficient vs. α Curve for Various Elevator Deflections.

5.2.3 Airplane Pitching Moment Coefficient vs. Airplane Lift Coefficient Curve

To construct the airplane pitching moment coefficient vs. airplane lift coefficient curve the following parameters have to be obtained:

- C_{m0} - Airplane zero-lift pitching moment coefficient
- $\frac{dC_m}{dC_l}$ - Airplane pitching moment variation with lift coefficient
- C_{Lmax} - Max lift coefficient
- α_{A^*} - Airplane linear range of angle of attack

After these parameters are obtained, the aircraft has to be determined if it has stable or unstable pitch break. Pitch break is the $C_m - C_L$ behavior at the aft and forward C.G. location. In Roskam Part III, the author provides an example of stable and unstable pitch break behavior in a trim diagram which can be seen in Figure 5.2c.

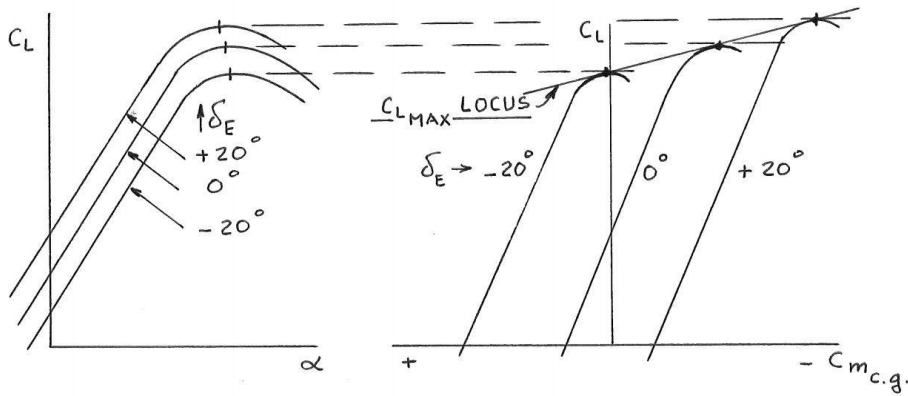


Figure 5.8a Stable Pitch Break Behavior

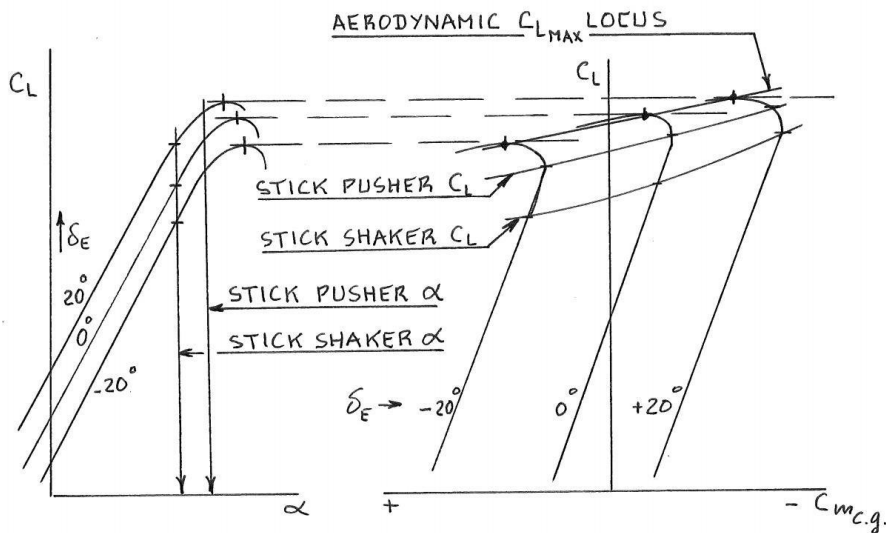


Figure 5.8b Unstable Pitch Break Behavior

Figure 5.2c: Illustration of Stable and Unstable Pitch Break Behavior

Unstable pitch breaks are acceptable on military aircraft if it does incur significant performance penalties. Appendix 5B contains the calculation for the airplane pitching moment coefficient vs. airplane lift coefficient parameters. An unstable pitch break is chosen for this aircraft. The effect of the elevator deflection on the airplane pitching moment coefficient vs. airplane lift coefficient curve is then calculated for a +10 degree deflection and -10 degree deflection. Roskam illustrates the effect of elevator deflection on the airplane pitching moment which can be seen in Figure 5.2d.

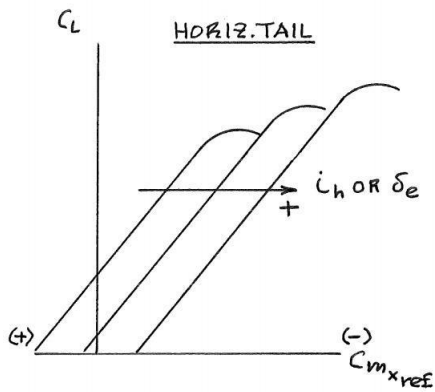


Figure 5.2d: Effect of Control Surface Deflection on Airplane Lift

The resulting airplane pitching moment coefficient vs. airplane lift coefficient curve for an elevator deflection of +10, 0, and -10 degrees is displayed in Figure 5.2e.

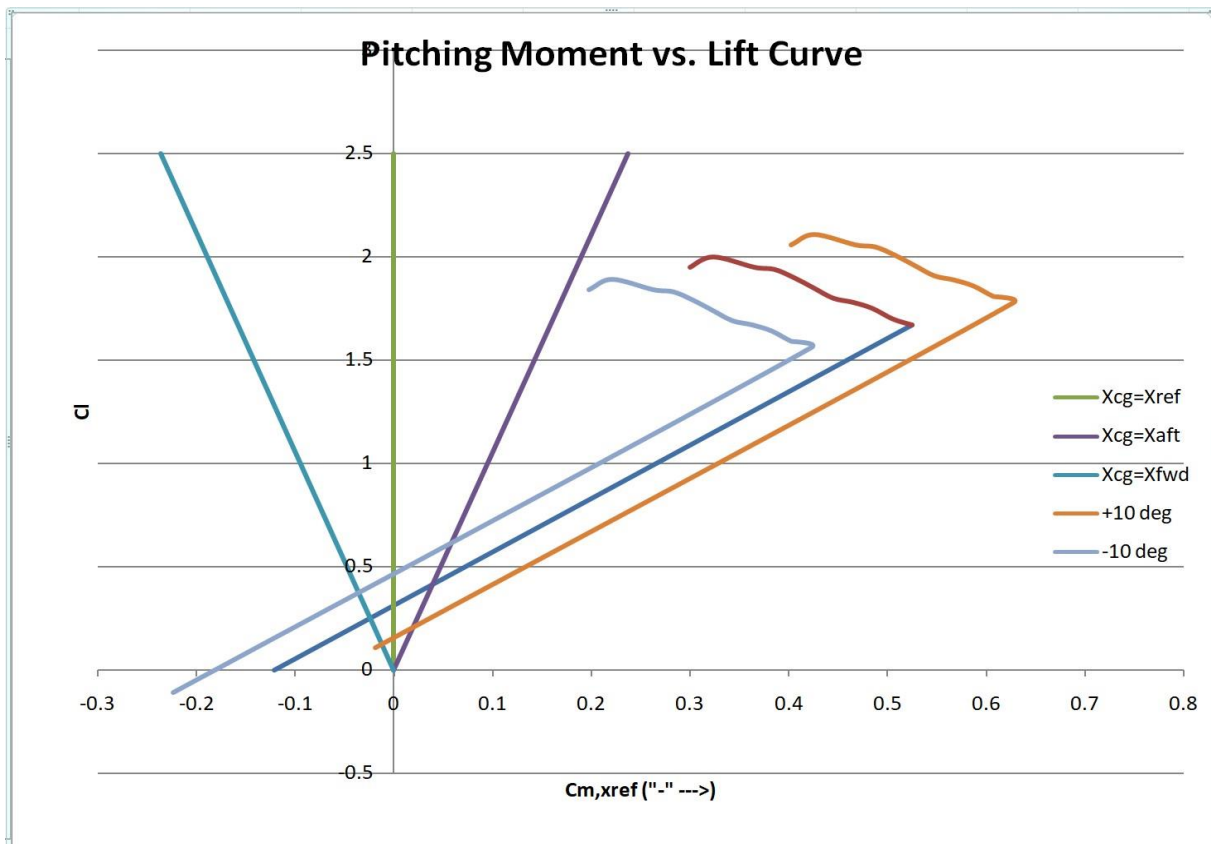


Figure 5.2e: Airplane Pitching Moment Coefficient vs. Airplane Lift Coefficient Curve for Various Elevator Deflections

5.3. Airplane Trim Diagram and Longitudinal Controllability and Trim

With the flight conditions tabulated in Table 5.2a and the airplane lift coefficient vs. α curve and airplane pitching moment coefficient vs. airplane lift coefficient curve constructed in Figure 5.2b and Figure 5.2e respectively, the trim diagram can now be put together. Using the parameters in Table 5.2a, the Mach #, dynamic pressure and resulting lift coefficient is calculated for each flight condition. The resulting parameters are tabulated in Table 5.2b.

Table 5.2b: Mach #, Dynamic Pressure, and Lift Coefficient for Each Flight Condition

Title	Mach # Initial	Mach # End	Dynamic Pressure Initial	Dynamic Pressure End	C_L Initial	C_L End
Longitudinal Static Stability	0.151218254	0.8370963	0.235236993	1.054108456	1.094919	0.244344
Relaxation in Transonic Flight	0.151218254	0.8370963	0.235236993	1.054108456	1.094919	0.244344
Elevator Control Force Variations during Rapid Speed Changes	0.151218254	0.8370963	0.235236993	1.054108456	1.094919	0.244344
Phugoid Stability	0.151218254	0.8370963	0.235236993	1.054108456	1.094919	0.244344
Flight-Path Stability	0.151218254	0.1656753	0.235236993	0.282366234	1.094919	0.912168
Short Period Frequency and acceleration sensitivity	0.151218254	0.8370963	0.235236993	1.054108456	1.094919	0.244344
Short Period Damping	0.151218254	0.8370963	0.235236993	1.054108456	1.094919	0.244344
Residual Oscillations	0.151218254	0.8370963	0.235236993	1.054108456	1.094919	0.244344
Control Feel and Stability in Maneuvering Flight	0.151218254	0.8370963	0.235236993	1.054108456	1.094919	0.244344
Control Forces in Maneuvering Flight	0.151218254	0.8370963	0.235236993	1.054108456	1.094919	0.244344
Control	0.151218254	0.8370963	0.235236993	1.054108456	1.094919	0.244344

Motions in Maneuvering Flight						
Longitudinal Pilot-Induced Oscillations	0.151218254	0.8370963	0.235236993	1.054108456	1.094919	0.244344
Dynamic Control forces in Maneuvering Flight	0.151218254	0.8370963	0.235236993	1.054108456	1.094919	0.244344
Control Feel	0.151218254	0.8370963	0.235236993	1.054108456	1.094919	0.244344
Longitudinal Control in Unaccelerated Flight	0.151218254	0.8370963	0.235236993	1.054108456	1.094919	0.244344
Longitudinal Control in Maneuvering Flight	0.151218254	0.8370963	0.235236993	1.054108456	1.094919	0.244344
Longitudinal Control in Takeoff	0.151745791	0.1517458	0.228886245	0.228886245	1.125299	1.125299
Longitudinal Control Force and Travel in Takeoff	0	0.7283798	0	5.273539086	#DIV/0!	0.048841
Longitudinal Control in Landing	0.151218254	0.7283798	0.235236993	5.273539086	1.094919	0.048841
Longitudinal Control Forces in Dives	0.152264005	0.8370963	0.222337698	1.054108456	1.158442	0.244344

The next step is to place both the airplane lift coefficient vs. α curve and airplane pitching moment coefficient vs. airplane lift coefficient curve adjacent to each other. A horizontal line is drawn across the α_{stall} point on each of the curves in Figure 5.2b. These horizontal lines are then drawn onto the airplane lift coefficient vs. α curve in Figure 5.2e. This is illustrated in Figure 5.3a. By connecting the points where the horizontal lines intersects the pitching moment curves and the $C_m = 0$ lines, the trim triangle can be formed on the pitching moment curve. The lift coefficients tabulated in Table 5.2b are then placed on the $C_m = 0$ lines that match their corresponding C.G. location. The finalized trim diagram with the flight condition points can be seen in Figure 5.3b. The points O, A, and B are the corners of the trim triangle. The sides of the

triangle are formed by the aft and forward $C_m = 0$ lines and the line formed by the intersection of the horizontal α_{stall} on the pitching moment curves.

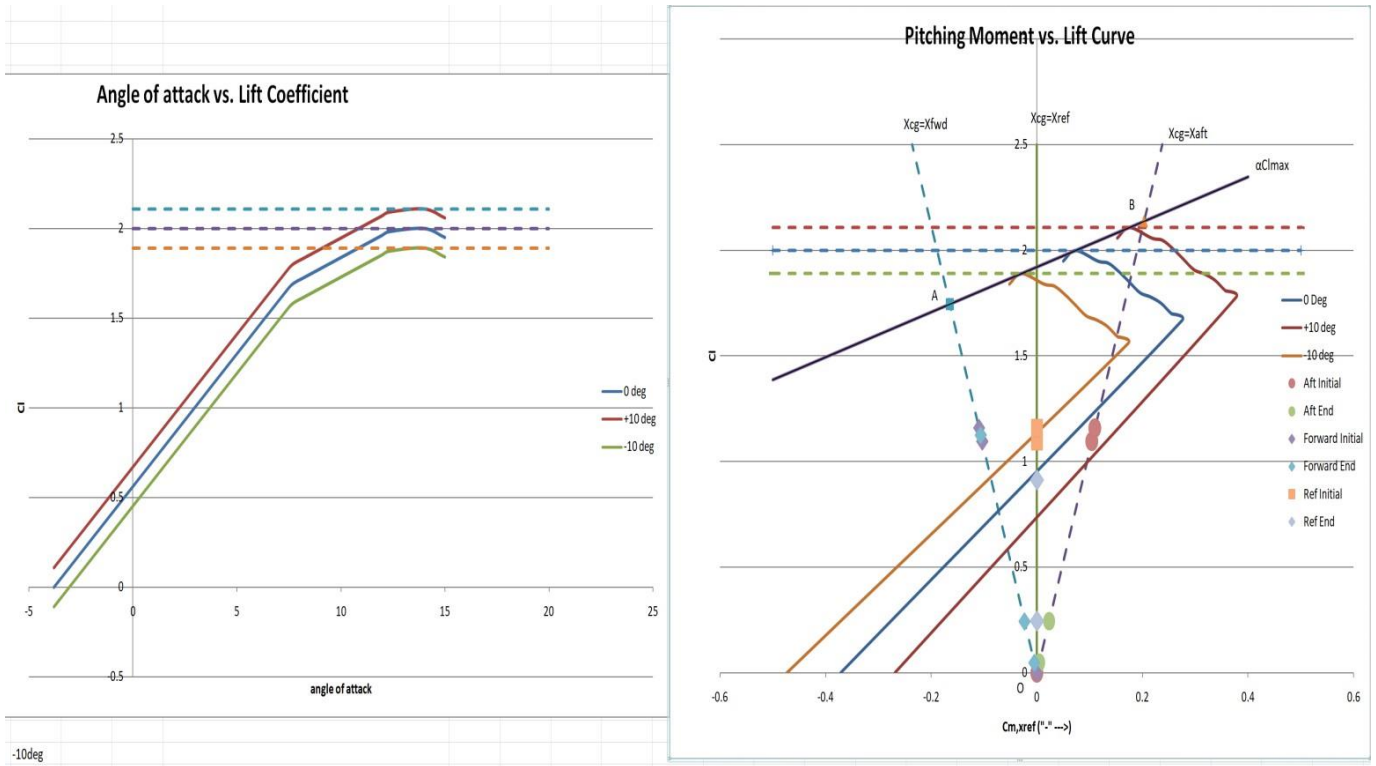


Figure 5.3a: Construction of Final Trim Diagram

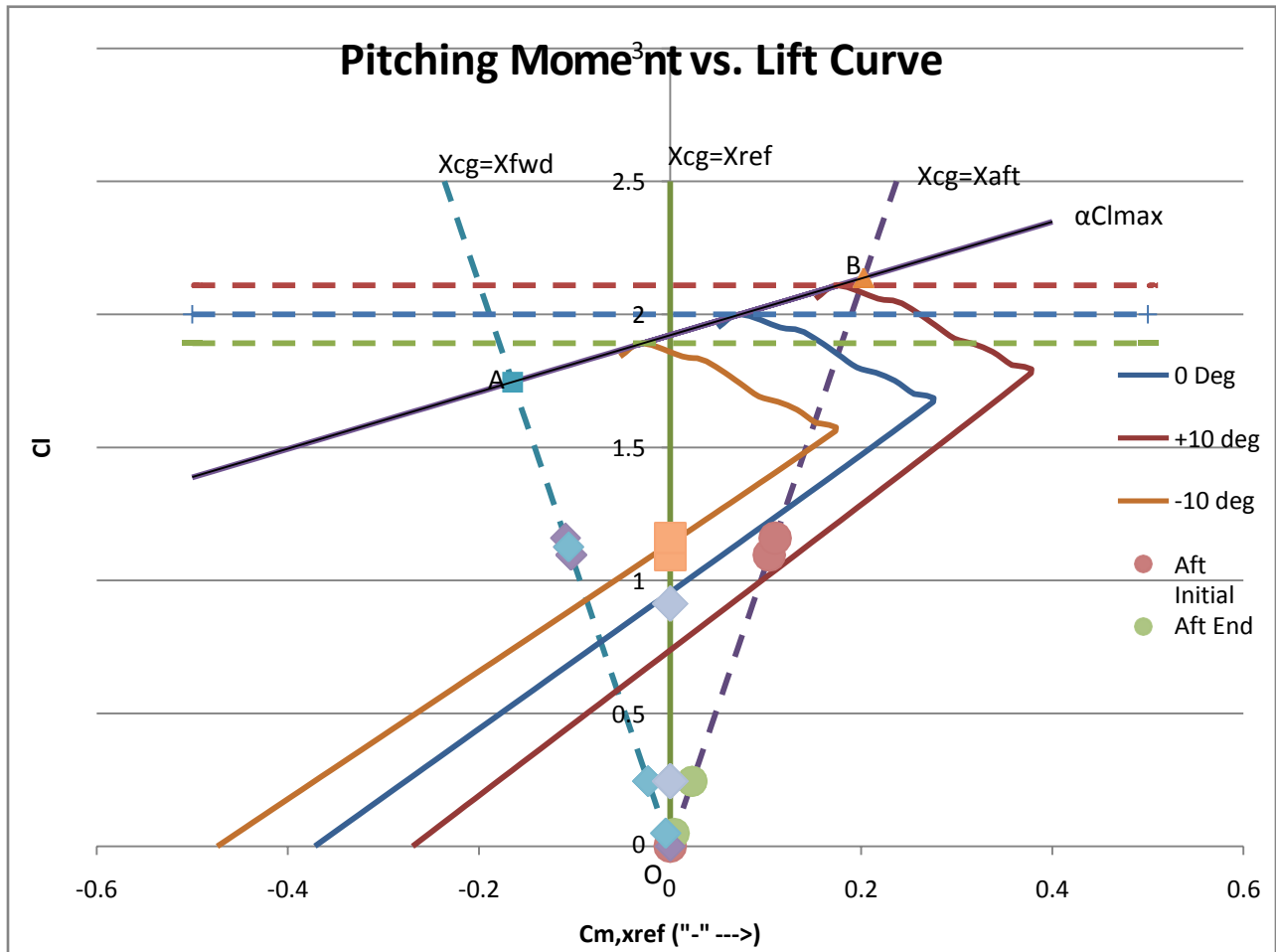


Figure 5.3b: Trim Triangle OAB with Flight Condition Points.

5.4 Results of Class II Longitudinal Control and Trim Analysis

With the trim triangle constructed and flight conditions inputted into the triangle, the FAFCAS longitudinal control and trim can be analyzed. To determine if the aircraft has good longitudinal flying qualities, the lift coefficient at the initial and end point of the flight conditions are plotted into the trim triangle as can be seen in Figure 5.3b. The line connecting point A and B is the airplane stall line. For each flight condition, the lift coefficients are plotted into the trim triangle and observed if it is above the stall line. As can be seen in Figure 5.3b, none of the flight condition points are above the stall line in both the most aft or most forward C.G. loading. Some flight conditions edge closer to stall than others such as during longitudinal control forces in dives. With all the points under the stall line the aircraft is considered to have good longitudinal flying qualities as defined by the military aircraft regulation MIL-F-8785C. As no controllability issues were observed from this analysis, no significant changes have to be made in the configuration of the FAFCAS.

6.1 Cost Estimation of the FAFCAS

In Chapters 1 to 5, the preliminary design and configuration of the FAFCAS was constructed. In this chapter, the life cycle cost of this design will be estimated using the method provided by Roskam Part VIII. Life cycle cost is the cost of the entire airplane program, from the planning phase to the operating phase. The life cycle cost is broken into the following components:

- C_{RDTE} - Research, development, test and evaluation cost.
- C_{ACQ} - Acquisition cost.
- C_{OPS} - Operating cost.

With the calculation of the life cycle cost, the preliminary cost estimate of the FAFCAS program can be obtained.

6.1.1 Research, Development, Test and Evaluation Cost

In this section of the airplane program, the following phases occur:

- Planning and Conceptual Design
- Preliminary Design and System Integration
- Detail Design and Development

The previous chapters of the airplane design cover these phases. The research, development, tests and evaluation cost is broken down into the following cost components:

- C_{AEDr} - Airframe engineering & design cost.
- C_{DSTr} - Development support & test cost.
- C_{FTAr} - Flight test airplanes cost.
- C_{FTORr} - Flight test operations cost.
- C_{TSFr} - Test & simulation facilities cost.
- C_{PROr} - Profit over flight test airplane.
- C_{FINr} - Cost to finance the flight test airplane.

The summation of all these components equates to C_{RDTE} . The calculations for this cost can be found in Appendix 6A. The assumptions for the calculations are that there will be ten test airplanes made, two static test air frames, and will have a fairly complex design. The cost breakdown of C_{RDTE} is tabulated in Table 6.1a. In addition, C_{FTAr} have multiple components to its cost which is tabulated in Table 6.1b. The cost of the research, development, tests and evaluation phase computes to around \$1,991,100,000.

Table 6.1a: Research, Development, Test and Evaluation Cost Breakdown

Cost Component	Cost
C_{AEDr}	\$223,950,722

C_{DSTr}	\$90,923,259
C_{FTAr}	\$814,389,458
C_{FTORr}	\$65,396,979
C_{TSFr}	\$398,220,140
C_{PROr}	\$199,110,070
C_{FINr}	\$199,110,070
C_{RDTE}	\$1,991,100,698

Table 6.1b: Flight Test Airplanes Cost Breakdown

Engines & Avionics	\$89,857,784
Manufacturer Labor Cost	\$350,008,988
Material Cost	\$35,854,252.1
Tooling Cost	\$293,167,266
Quality Control Cost	\$45,501,168.4

6.1.2 Acquisition Cost

The acquisition cost of the FAFCAS program consists of the manufacturing cost, C_{MAN} , and the manufacturer's profit, C_{PRO} . The manufacturing cost is broken down into the following cost components:

- C_{AEDm} - Airframe engineering and design cost of production aircraft
- C_{APCm} - Airplane program production cost.
- C_{FTOm} - Cost of flight test operations for production airplanes
- C_{FINm} - Manufacturing program financing cost.

The summation of these costs equate to C_{MAN} . The calculations for this cost can be seen in Appendix 6B. The assumptions for this calculation are that 750 airplanes will be manufactured, with ten being the test airplanes. The cost breakdown of C_{MAN} is tabulated in Table 6.2a. The cost component C_{APCm} has a cost breakdown of its own, which is tabulated in Table 6.2b.

Table 6.2a: Manufacturing Cost Breakdown

Cost Component	Cost
C_{AEDm}	\$269,551,006
C_{APCm}	\$5,051,817,529
C_{FTOm}	\$118,400,000
C_{FINm}	\$604,418,726
C_{MAN}	\$6,044,187,262

Table 6.2b: Airplane Program Production Cost

Cost Component	Cost
Engines & Avionics Cost	\$89,857,784
Cost of the Interiors	\$0
Manufacturer Cost of Production Planes	\$3,012,096,216
Materials Cost for Production Planes	\$1,059,587,245
Tooling Cost for Production Planes	\$498,703,776
Quality Control Cost for Production Planes	\$391,572,508

C_{PRO} is calculated in terms of C_{MAN} , which equates to $C_{PRO} = \$604,418,726$. With both C_{PRO} and C_{MAN} calculated, the acquisition cost can be found. Table 6.2c displays the acquisition cost and its components.

Table 6.2c: Acquisition Cost of FAFCAS Program

C_{MAN}	\$6,044,187,262
C_{PRO}	\$604,418,726
C_{ACQ}	~\$6,648,606,000

6.1.3 Operation Cost

The operating cost is the cost incurred while operating the airplane. The operation cost consists of the following:

- C_{POL} - Airplane program fuel, oil, and lubrication cost.
- $C_{PERSDIR}$ - Program cost of direct personnel.
- $C_{PERSIND}$ - Program cost of indirect personnel.
- C_{CONMAT} - Program cost of consumable materials used in conjunction with maintenance.
- C_{SPARES} - Program cost of spares.
- C_{DEPOT} - Program cost associated with depots.
- C_{MISC} - Program miscellaneous cost.

In Roskam Part VIII, the author provides operation costs of various military aircrafts used by the U.S. Air Force. As the FAFCAS will perform a similar role to the A-10, the operation cost of the A-10 will be used for the calculation of the FAFCAS operation cost. The operation cost will be estimated to be \$22,755,000,000.

6.2 Life Cycle Cost of the FAFCAS Program

Using the cost components computed in §6.1.1- §6.1.3, the life cycle cost of the FAFCAS can be computed. The cost breakdown of the life cycle cost, LCC , is tabulated in Table 6.3a.

Table 6.3a: Life Cycle Cost Breakdown of the FAFCAS

C_{RDTE}	\$1,991,100,698
C_{ACQ}	\$6,648,606,000
C_{OPS}	\$22,755,000,000
L_{CC}	\$31,394,706,686

The resulting life cycle cost for the FAFCAS program is around \$31,394,700,000. Assuming there will be 750 airplanes manufactured, the resulting unit cost for each FAFCAS will be around \$42,425,000. From Ref. 9, the most comparable existing aircraft, the A-10 Thunderbolt II, has a unit cost of \$18.8 million. From this preliminary cost estimation of the FAFCAS program, it can be seen that the FAFCAS is more expensive than the A-10 per unit-wise.

7.1 Conclusion of Class I and II Preliminary Design

With the life cycle cost calculated in Chapter 6, the Class I and II preliminary design process of the FAFCAS program is completed. By the conclusion of the Class II phase of the design process, several changes were made to the Class I FAFCAS configuration. The empty weight was decreased by 8780 lbs from Class I to II due to the refined component weight calculations. The horizontal stabilizer wing area was also increased from Class I to II to satisfy the Class II weight and balance analysis. The landing gears also had an updated design as summarized in §3.2.3. In Chapter 5, the Class II stability and control analysis determined the configuration change still allowed for good longitudinal flying qualities.

Several issues were made apparent though as the design process was underway. From the Class I performance constraint analysis in §2.4, the aircraft loiter time and climb rate could not meet the mission specifications in Table 2.3. The high takeoff weight also puts this design within the ranges of a heavy fighter. As the FAFCAS is intended to replace the A-10 Thunderbolt II in the USAF, an aircraft specifications comparison is made between the two. Table 7.1a-7.1d displays the updated FAFCAS specifications. Ref. 9 contains the A-10 characteristics, which is tabulated in Table 7.1e.

Table 7.1a: FAFCAS Class II Specifications

Payload Capacity	13,000 lbs (2000 lbs of ammunition/11 x1000 lbs bombs)
Takeoff and Landing Field Length	3280 ft (1 km)
Loiter Time	50min
Range	620 miles (1000km)
Cruise Ceiling	39400 ft (12km)
Cruise Speed	480 knots
Stall Speed	120 knots
Weight takeoff with Payload	87,870 lbs
Weight takeoff without stores	74,870 lbs

Weight empty	38,620 lbs
Weight fuel	23,000 lbs
Fuselage Length	53.5 ft
Thrust/Weight	0.3
Wing Loading	93 psf

Table 7.1b: Class II Main Wing Specification

Wing Area	1040 ft ²
Wing Span	79 ft
Wing Speed	20 degrees
Taper Ratio	0.45
Fowler Flap Deflection at Landing	40 degrees
Fowler Flap Deflection at Takeoff	25 degrees

Table 7.1c: Class II Empennage Specification

	Horizontal Stabilizer	Vertical Stabilizer
Wing Area	130 ft ²	190 ft ²
Elevator Area	82 ft ²	N/A
Rudder Area	N/A	14.6 ft ²
AR	4	1
Taper Ratio	0.5	0.4
Sweep Angle	20 degrees	25 degrees
Thickness Ratio	.1	.135
Dihedral Angle	0 degrees	80 degrees

Table 7.1d: Class II Landing Gear Specifications

Landing Gear			St			Ss			Ds	
Nose Gear			.645 ft			.4196 ft			.5675 ft	
Main Gear			1.04 ft			.644 ft			.6197 ft	
Landing Gear	Do	W	D	Ply Rating	Static Load	Inflation Pressure	Speed Rating	Bead Ledge Diameter	Bump Capability	Qualification
Main L.G.	25in.	25in.	28in.	30	55,000 lbs	85 psi	160mph	28in.	10.1	MIL
Nose L.G.	15.5in.	15.5in.	20in.	20	29,900 lbs	135 psi	160 mph	20in.	5.2	MIL

Table 7.1e: A-10 Thunderbolt II Specifications

	General Characteristics
Length	53 ft, 4 in.

Height	14ft, 8 in.
Wingspan	57 ft, 6in.
Wing Area	506 ft ²
	Performance
Engine Thrust	9,065 lbs each engine
Max Speed	381 knots
Stall Speed	120 knots
Ceiling	45,000 ft
Range	800 miles
Maximum Takeoff Weight	51,000 lbs
Thrust/Weight	0.36
Wing Loading	99 psf
	Armament
	16,000 lbs of mixed ordnance (11 hard points)

By comparing the Tables 7.1a-7.1d and Table 7.1e, the similarities and differences in the aircrafts can be seen. The FAFCAS and the A-10 both have 11 hard points to mount ordnance, similar thrust/weight ratio, stall speed, and wing loading. In terms of aircraft size and weight, there are multiple differences between the two aircrafts. The FAFCAS is 36,870 lbs heavier than the A-10 at max weight takeoff configuration. The FAFCAS main wing has a wing area twice as big as the A-10 and 22 ft longer wing span. In the performance aspect, the FAFCAS has higher max speed than the A-10 but lower cruise ceiling, range, and time to climb. Both aircrafts have similar takeoff/landing distance and loiter time.

In summary, the FAFCAS has multiple aspects in which it is inferior to the A-10 but also has some advantages. The FAFCAS is larger and heavier than the A-10. This means the FAFCAS will be limited to air fields that can maintain large bombers or transport aircraft. It is also unable to climb as fast, fly as far and high as the A-10. The FAFCAS unit cost is also higher than the A-10. The FAFCAS is able to fly faster than the A-10 and can carry more cannon ammunition. Thus if the FAFCAS is stationed close to the frontlines, the FAFCAS can provide close air support faster than the A-10 with its higher max speed. In this situation, the FAFCAS disadvantage in range and ceiling can be mitigated. The FAFCAS will also be able to fire at more targets than the A-10 due to the higher ammunition count but unable to drop heavier ordnance as the A-10. The unit cost estimation can also be decreased as currently the life cycle cost calculations uses data from the 1990s provided by Roskam. With more up to date data, the unit cost of the FAFCAS can decrease.

In conclusion, the preliminary configuration design of the FAFCAS program is completed using Roskam's Class I and II design methods. The mission specifications originally required an aircraft with similar or better performance than the A-10 Thunderbolt II but as seen above, not all requirements were met. As most of the performances are similar to the A-10 and

the design is considered stable, the FAFCAS design can be a potential replacement to the aging A-10 Thunderbolt II.

References:

1. Roskam, J., "Airplane Design: Part I, Preliminary Sizing of Airplanes." Roskam Aviation and Engineering Corporation, Rt 4, Box 274, Ottawa, Kansas, 66067. Length: 207 pages. References: 19.
2. Roskam, J., "Airplane Design: Part II, Preliminary Configuration Design and Integration of the Propulsion System." Roskam Aviation and Engineering Corporation, Rt 4, Box 274, Ottawa, Kansas, 66067. Length: 310 pages. References: 53.
3. Roskam, J., "Airplane Design: Part III, Layout Design of the Cockpit, Fuselage, Wing, and Empennage." Roskam Aviation and Engineering Corporation, Rt 4, Box 274, Ottawa, Kansas, 66067. Length: 454 pages. References: 82.
4. Roskam, J., "Airplane Design: Part IV, Layout of Landing Gear and Systems." Roskam Aviation and Engineering Corporation, Rt 4, Box 274, Ottawa, Kansas, 66067. Length: 432 pages.
5. Roskam, J., "Airplane Design: Part V, Component Weight Estimation." Roskam Aviation and Engineering Corporation, Rt 4, Box 274, Ottawa, Kansas, 66067. Length: 209 pages. References: 19.
6. Roskam, J., "Airplane Design: Part VI, Preliminary Calculation of Aerodynamic, Thrust and Power Characteristics." Roskam Aviation and Engineering Corporation, Rt 4, Box 274, Ottawa, Kansas, 66067. Length: 550 pages. References: 58.
7. Roskam, J., "Airplane Design: Part VII, Determination of Stability, Control and Performance Characteristics: FAR and Military Requirements." Roskam Aviation and Engineering Corporation, Rt 4, Box 274, Ottawa, Kansas, 66067. Length: 348 pages. References: 30.
8. Roskam, J., "Airplane Design: Part VIII, Airplane Cost Estimation: Design, Development, Manufacturing and Operating." Roskam Aviation and Engineering Corporation, Rt 4, Box 274, Ottawa, Kansas, 66067. Length: 368 pages. References: 61.
9. Strouble, Dennis D. and Jacques, David R., "A-10 Thunderbolt II (Warthog) Systems Engineering Case Study", *Air Force Center for Systems Engineering*, <http://www.dtic.mil/dtic/tr/fulltext/u2/a530838.pdf>. [October 2007]
For this review, the authors conducted a case study of the A-10 Thunderbolt II that the design aircraft is trying to replace. In this report, the mission specifications for the A-10 were based on the U.S. military's experience in past wars. Other potential prototypes for the close air support aircraft were explored. The case study also described the history of the design process from concept to completion. Length: 103 pages. References: 129.
10. "F-35 Joint Strike Fighter (JSF) Lightning II Specifications," *Global Security*, <http://www.globalsecurity.org/military/systems/aircraft/f-35-specs.html>. [14 April 2016]

- For this review, the author lists the specifications and some performance parameters for the F-35 Lightning II. The A, B, and C models were listed in this document. These parameters were averaged with other military aircraft to be used in the design aircraft's preliminary sizing. Length: 1 page.
11. "Fighter-bomber Su-34 Details," *Ministry of Defense of Russia*, <http://structure.mil.ru/structure/forces/air/weapons/aviation/more.htm?id=10332831@mo rfMilitaryModel>. [Retrieved 3 September 2017]

For this review, the author lists the specifications and performance parameters for the Su-34 fighter bomber. The takeoff weight and the range listed on this reference were used as a basis of performance for a heavier fighter aircraft. The parameters were averaged with other military aircraft to be used in the design aircraft's preliminary sizing. Length: 1 page.
 12. Pike, John, "AV-8B Harrier," *FAS Military Analysis Network*, <https://fas.org/man/dod-101/sys/ac/av-8.html>. [2 November 2016]

For this review, the author lists the specifications and performance parameters for the AV-8B Harrier. Wing geometry and takeoff weight for different configurations were listed by the author. The parameters were averaged with other military aircraft to be used in the design aircraft's preliminary sizing. Length: 1 page. References: 7.
 13. "Su-25K Aircraft Performance," *Sukhoi*, <http://www.sukhoi.org/eng/planes/military/su25k/lth/>. [Retrieved 3 September 2017]

For this review, the author lists the specifications and performance parameters for the Su-25K. This aircraft has similar mission specifications to the A-10. The parameters were averaged with other military aircraft to be used in the design aircraft's preliminary sizing. Length: 1 page.
 14. "Su-32 Aircraft Performance," *Sukhoi*, <http://www.sukhoi.org/eng/planes/military/su32/lth/>. [Retrieved 3 September 2017]

For this review, the author lists the specifications and performance parameters for the Su-32 fighter bomber. The parameters were averaged with other military aircraft to be used in the design aircraft's preliminary sizing. Length: 1 page.
 15. Aalbers, Willem, "History of the Fairchild-Republic A-10 Thunderbolt II, Part Two," *SimHQ*, http://www.simhq.com/_air/air_052a.html. [11 May 2011]

For this review, the author discusses the various subsystems of the A-10 Thunderbolt II and its performances. The load factors and turn radius for different load factors and flap angles are listed. These parameters are used as reference for the design aircraft. Length: 1 page. References: 7.
 16. "F/A-18 Hornet Strike Fighter," *United States Navy Fact File*, http://www.navy.mil/navydata/fact_display.asp?cid=1100&tid=1200&ct=1. [Retrieved 25 September 2017]

- For this review, the author lists the specifications and performance parameters for the F/A-18 Hornet Strike Fighter. The parameters were averaged with other military aircraft to be used in the design aircraft's preliminary sizing. Length: 1 page.
17. "Boeing F-15 Strike Eagle," *Boeing*, <http://www.boeing.com/defense/f-15-eagle/>. [Retrieved 25 September 2017]
- For this review, the author lists the specifications and performance parameters for the different variations of the F-15 Eagle. The parameters were averaged with other military aircraft to be used in the design aircraft's preliminary sizing. Length: 1 page.
18. Struett, Ryan C., "Empennage Sizing and Aircraft Stability using Matlab," *California Polytechnic State University, San Luis Obispo*, <http://digitalcommons.calpoly.edu/cgi/viewcontent.cgi?article=1074&context=aerosp> [Retrieved 30 November 2017] Length: 37 pages. References: 6.
19. "Pratt & Whitney Engines F100-PW-220/F100-PW-220E Turbofan Engine," *PowerWeb*, <http://www.fi-powerweb.com/Engine/PW-F100.html>
- For this review, the author lists the specifications of the Pratt & Whitney F100 engines. The differences between different versions of the F100 engines are also discussed. Length: 1 page. References: 4.
20. "MIL-C-005011B (USAF)/ Military Specification Charts: Standard Aircraft Characteristics and Performance, Piloted Aircraft (Fixed Wing)," Department of Defense, Wright-Patterson AFB, OH 45433, 21 June 1977.
- For this review, the author defines and discusses the MIL-C-005011B (USAF) military aircraft certification. This certification lists the design standards for fixed wing military aircraft to be considered a safe design. Minimum takeoff and landing distances are listed for a safe military design. Example mission profiles are also provided by this document. Length: 109 pages. References: 12.
21. "MIL-STD-3013A/ Glossary of Definitions, Ground Rules, and Mission Profiles to Define Air Vehicle Performance Capability," Department of Defense Standard Practice, 9 Sept. 2008.
- For this review, the author defines the MIL-STD-3013A fixed wing military aircraft certification. This certification is the most up to date version for the fixed wing aircraft. The document provides the definitions of aircraft maneuvers and missions. Rules and criteria are listed for each aircraft maneuver that has to be met for a safe design. Length: 120 pages. References: 12.
22. "Tornado Multi-Role Combat Aircraft [MRCA]," *Global Security*, <https://www.globalsecurity.org/military/world/europe/tornado-specs.html>. [Retrieved 3 September 2017]
- For this review, the author lists the specifications and performance parameters for the different variations of the Tornado aircraft. The parameters were averaged with other military aircraft to be used in the design aircraft's preliminary sizing. Length: 1 page.

23. Bingham, Gene J. and Noonan, Kevin W., "NASA TM X-2623 Low-Speed Aerodynamic Characteristics of NACA 6716 and NACA 4416 Airfoils with 35-Percent-Chord Single-Slotted Flaps," *Nasa Technical Memorandum*, U.S. Army Air Mobility R&D Laboratory, Hampton, Va., 23665.
<https://ntrs.nasa.gov/archive/nasa/casi.ntrs.nasa.gov/19740013521.pdf>.
For this review, the author provides the lift and pitching coefficients of the NACA 6715 and NACA 4416 airfoils. The data is tabulated and graphed for different pitch angles. Length: 50 pages. References: 7.
24. Mizokami, Kyle, "One of These Three Light Attack Planes Could Help Replace the A-10," *Popular Mechanics*,
<https://www.popularmechanics.com/military/aviation/a26515/three-planes-oax-help-replace-the-a-10/> [Retrieved 28 June 2018]
25. Jackson, Paul (ed.). *Jane's All the World's Aircraft 2010–2011*. Surrey: Jane's. p. 37. [ISBN 9780710629166](#).
26. "Scorpion Jet Features, Specifications". *Scorpion jet*. Textron AirLand. <http://scorpion.txtav.com/en/scorpion-jet-features#specs>. [Retrieved 30 June 2018]
27. "AT-6 Wolverine Light Attack," *Beechcraft*. Textron Aviation. <http://defense.txtav.com/en/at-6> [Retrieved 30 June 2018]
28. Torenbeek, Egbert. *Synthesis of Subsonic Airplane Design*. Springer Science. ISBN 978-94-017-3202-4